A continental record of the Carnian Pluvial Episode (CPE) from the Mercia Mudstone Group (UK): palynology and climatic implications

VIKTÓRIA BARANYI[1*], CHARLOTTE S. MILLER[1,2], ALASTAIR RUFFELL[3], MARK W. HOUNSLOW[4] & WOLFRAM M. KÜRSCHNER[1]

[1]*Department of Geosciences, University of Oslo, POB 1047 Blindern, 0316 Oslo, Norway*

[2]*MARUM – Center for Marine Environmental Sciences and Faculty of Geosciences, University of Bremen,* Leobener Str. 8*, 28359, Bremen, Germany*

[3]*School of the Natural and Built Environment, The Queen's University, Belfast, BT7 1NN, N. Ireland*

[4]*Lancaster Environment Centre, Lancaster University, Bailrigg, Lancaster LA1 4YQ, UK*

*Correspondence: viktoria.baranyi@geo.uio.no

Abbreviated title: Continental record of the CPE in the UK

Abstract

The generally arid Late Triassic climate was interrupted by a wet phase during the mid Carnian termed Carnian Pluvial Episode (CPE). Quantitative palynological data from the Mercia Mudstone Group in the Wessex Basin (UK), reveals vegetation changes and palaeoclimate trends. Palynostratigraphy and bulk organic carbon isotope data enable

correlation to other Carnian successions. The palynostratigraphy indicates that the Dunscombe Mudstone is Julian and the lowest part of the overlying Branscombe Mudstone Formation is Tuvalian.. The *Aulisporites* acme characterizing the CPE in Tethyan successions and the Germanic Basin, is missing in the UK. The quantitative palynological record suggests the predominance of xerophyte floral elements with a few horizons of increased hygrophytes. A humidity signal is not seen due to the dry climate in central Pangea. Secondly, the signal might be masked by the overrepresentation of xerophyte regional pollen and the predominance of xerophyte hinterland flora. The bias towards regional pollen rain is enhanced by the potential increase in continental runoff related to seasonally humid conditions and differences in pollen production rates and transport mechanisms. The vegetation of British CPE successions suggests a more complex climate history during the Carnian indicating that the CPE is not recognized by the same changes everywhere.

Supplementary material: Detailed lithological log of the Strangman`s Cove (Devon) outcrop with the description of the MMG lithostratigraphical units, description of the laboratory techniques, seven photoplates with selected spores and pollen grains, a list of all identified palynomorphs, Excel sheets with the palynological and palynofacies counts, bulk organic carbon isotope ratios and TOC values of the Strangman`s Cove outcrop are available at https://doi.org/xxxx

49

During the Late Triassic the continental interior of Pangea was characterized by predominantly arid climates in low-mid latitudes with strong seasonality and a monsoonal regime (Kutzbach & Gallimore 1989; Parrish 1993; Sellwood & Valdes 2006; Preto *et al.* 2010). In central Pangea (Preto *et al.* 2010), the depositional setting of the Mid- to Late Triassic Mercia Mudstone Group (MMG) in the Wessex Basin (SW England, UK) was marked by playa lake deposits with red beds and local evaporites similar to the Keuper Group of the Southern Permian (or Germanic) Basin (Bachman *et al.* 2010; Hounslow *et al.* 2012). During the Carnian, the depositional style of the Mercia Mudstone Group changed significantly, marked by short-lived lacustrine interval and more pronounced fluvial influence (Simms & Ruffell 1989, 1990; Porter & Gallois 2008; Hounslow & Ruffell 2006; Ruffell *et al.* 2016). In the Wessex Basin, this transition is manifested by the lithological change from gypsiferous red mudstone to a green-grey mudstones with locally sandy beds: termed the Dunscombe Mudstone Formation (Porter & Gallois 2008; Ruffell et al. 2016). This facies change is also expressed in the Keuper Group in the Germanic Basin, where red playa lake deposits were temporarily interrupted by sandy fluvial channel and overbank deposits of the Schilfsandtstein (Stuttgart Formation) during the late Julian (e.g., Bachmann *et al.* 2010; Kozur & Bachmann 2010; Shukla *et al.* 2010). The lithological shift seen at the base of the Dunscombe Mudstone Formation and in the Schilfsandstein may be coincident with a climate change towards more humid conditions known as the Carnian Pluvial Episode (CPE, Ruffell *et al.* 2016), which in other localities, appears to have commenced in the early Carnian, close to the early to late Julian boundary (Dal Corso *et al*. 2015; Mueller *et al.* 2016a, b). The global nature of the CPE has been debated, but evidence from successions in Europe (e.g., Schlager & Schöllnberger 1974; Simms & Ruffell 1989, 1990), the Middle East (Bialik *et al.* 2013), Iberia and eastern North America (Arche & López-Gómez 2014) and also Asia (Hornung *et al.* 2007 a, b; Nakada *et al.* 2014; Sun *et al.* 2016), suggest that the CPE wet

conditions had global extent (Ogg 2015; Ruffell *et al.* 2016). Previously Visscher *et al.* (1994) had rejected the presence of a wetter climatic phase during the Carnian based on palynological evidence from the Schilfsandstein explaining the facies change by the establishment of a large river system in an overall dry floodplain, but with locally wet environments near the river banks; with the present-day Nile Valley as an analogue. Despite differing local interpretations, major environmental change is evident from the switching in lithology occurring in both continental and marine Carnian successions. The CPE was probably accompanied by sea level changes, global warming (Trotter *et al.* 2015; Sun *et al.* 2016) increased continental weathering (Rostási *et al.* 2011), demise of carbonate platforms (Keim *et al.* 2006; Breda *et al.* 2009; Lukeneder *et al.* 2012; Arche & López-Gómez 2014) and deepening of the carbonate compensation depth in the oceans (Rigo *et al*. 2007; Lukeneder *et al.* 2012; Nakada *et al.* 2014). At low palaeolatitudes enhanced terrigenous input appears to have lasted from the late Julian (Julian 2) to the early Tuvalian (Roghi *et al.* 2010, Rostási *et al.* 2011). The CPE is characterized by wet-dry cycles and multiple humid pulses; before the climate returned to persistent aridity in the late Carnian or Norian (Preto *et al.* 2010; Lukeneder *et al.* 2012; Bialik *et al.* 2013; Mueller *et al.* 2016b; López-Gómez *et al.* 2017). At high latitudes (in the Boreal Realm, e.g Svalbard) higher temperatures, increased humidity and the local development of coals represent the equivalent of the CPE (Mueller et al. 2016a).

In the marine realm the onset of the CPE in the mid Julian is associated with a negative carbon isotope excursion in the marine realm suggesting the injection of a significant amount of ^{13}C-depleted CO_2 into the atmosphere (Dal Corso *et al.* 2012, 2015). The first evidence of a negative carbon isotope excursionin the CPE from a terrestrial realm has been provided by the Wiscombe Park-1 Borehole succession in the MMG from the Wessex Basin (Miller *et al.* 2017). There, the initial carbon isotope excursion (labelled IIE) in both total organic carbon

100 and plant leaf waxes (Miller *et al.* 2017), is followed by four other negative C-isotope
101 excursions. Miller et al. (2017) recognised *ca.* 413 ka eccentricity cycles from the Dunscombe
102 Mudstone Formation suggesting the establishment of a duration for the isotope excursions,
103 lasting for *ca.* 1.09 Ma ;comparable to previous estimates of 0.8–1.2 Ma from marine units in
104 China (Zhang *et al.* 2015). The release of isotopically lighter CO_2 into the atmosphere caused
105 the intensification of Pangean monsoon activity and is the most likely responsible for the
106 increase in rainfall (Parrish 1993). The origin of ^{13}C-depleted CO_2 and the carbon isotope
107 excursion may be linked to enhanced volcanic activity and associated feedbacks (warming,
108 dissociation of methane clathrates, reduction in marine primary productivity) (Simms *et al.*
109 1995; Hornung *et al.* 2007a, b). The emplacement of the Wrangellia Large Igneous Province
110 basalts is considered the most likely trigger of the CPE (Furin *et al.* 2006, Dal Corso *et al.*
111 2012) although Greene *et al.* (2010) and Xu *et al.* (2014) showed that the Wrangellia
112 eruptions started earlier than the Carnian. There is evidence for regionally widespread
113 contemporaneous exhalative, acidic volcanic activity from the Anatolian Terrane in Greece
114 and Turkey (Huglu-Pindos Series: Moix *et al.* [2008, 2013]), Apennines (Furin *et al.* 2006)
115 and Iberia (e.g., Arche & López-Gómez 2014), but the extent of this volcanic activity is less
116 voluminous compared to the Wrangellia LIP.
117 Changes in plant communities are good proxies for terrestrial climate, therefore palaeobotany
118 and palynology have been widely utilized in understanding the climate change during the Late
119 Triassic (e.g., Reitz 1985; Visscher *et al.* 1994; Roghi 2004, Pott *et al.* 2008; Roghi *et al.*
120 2010; Bonis & Kürschner 2012; Mueller *et al.* 2016a, b). Palynology of sediments from the
121 CPE typically show a shift towards hygrophyte vegetation with increased abundance of ferns,
122 equisetaleans and cycadaleans (Roghi 2004; Hochuli & Vigran 2010; Roghi *et al.* 2010;
123 Mueller *et al.* 2016a, b). Particularly distinctive is the widely distributed *Aulisporites*
124 *astigmosus* assemblage typical of the late Julian in the western Tethys (Roghi *et al.* 2010).

125 *Aulisporites astigmosus* is a hygrophyte vegetation element and its widespread distribution
126 during the Carnian is a crucial argument for the global scale of a wet phase (Roghi *et al.*
127 2010). However, the palaeoclimatic significance of the *Aulisporites* acme during the Carnian
128 is controversial (Visscher *et al.* 1994) and some recent studies indicate that it may be
129 diachronous (Mueller *et al.* 2016a).
130 Here we provide quantitative palynological data from four terrestrial successions of the
131 Dunscombe Mudstone Formation from the UK and interpret the vegetation changes and
132 palaeoclimate trends. The palynological data are further integrated with organic carbon
133 isotope stratigraphy and are compared to other Carnian successions in Europe, in order to
134 evaluate regional differences.
135 **Geological setting**
136 Thick (up to 1 km, usually *ca.* 450 m) packages of fluvial-lacustrine sediments of the Mercia
137 Mudstone Group accumulated in SW England during the Mid-Late Triassic, in fault-bounded
138 basins that were formed during the syn-rift phase of crustal extension as a consequence of
139 Pangean rifting and thermal relaxation (Ruffell & Shelton 1999; Howard *et al.* 2008; McKie
140 & Williams 2009; Hounslow et al. 2012; Fig. 1). In the Wessex Basin, the Mercia Mudstone
141 Group comprises *ca.* 450 m of predominantly red mudstones and local evaporites that indicate
142 deposition in a low-relief sabkha environment in a hot desert (Gallois & Porter 2006;
143 Hounslow & Ruffell 2006; Hounslow *et al.* 2012; Fig. 1). The MMG in central and southern
144 England has been nationally rationalised into the Sidmouth Mudstone Formation, Arden
145 Sandstone Formation, Branscombe Mudstone Formation and the Blue Anchor Formation
146 (Howard *et al.* 2008 (Fig. 1, detailed description of each unit can be found in the
147 Supplementary Data). In the Wessex Basin, Dunscombe Mudstone Formation distinguishes a
148 variation of the mid parts of the MMG with predominantly green, grey to purple mudstone
149 unit between the red mudstones of the under-and overlying Sidmouth and Branscombe

Mudstone formations (Porter & Gallois 2008). In the coastal sections in Devon, the Arden Sandstone Fm of Howard et al. (2008) occupies only the mid 24 m of the Dunscombe Mudstone Fm (Warrington 2004), so we prefer to use the formation designations defined used by Gallois (2001), Gallois & Porter (2006) and Porter & Gallois (2008), which better represent the local lithological change. The Dunscombe Mudstone Formation consists of a 25 to 43 m-thick laterally variable succession of green, purple and grey laminated mudstones interbedded in the lower part with thin (typically, 5 cm to 30 cm) calcareous siltstone/sandstone beds. Breccia beds, caused by gypsum/anhydrite and halite collapse are also present (Gallois 2003; Gallois & Porter 2006; Porter & Gallois 2008). Palaeosols, bioturbated horizons, hardgrounds and lag deposits are evidence of condensation and minor hiatuses through the DMF (Gallois & Porter 2006). The DMF represents a fluvial–lacustrine succession with shallow freshwater lakes fed by shallow distributary channels in low-relief topography (Gallois & Porter 2006; Porter & Gallois 2008). On the Devon coast in the lower part of the formation, a lenticular unit of calcareous siltstones and fine-grained sandstones, (the Lincombe Member) is geographically restricted, but evidence of an oxygenated freshwater lake (Gallois & Porter 2006).

The palynomorph assemblages of the Dunscombe Mudstone Fand Arden Sandstone formations were reconnaissance sampled by Clarke (1965), Warrington (1967, 1970, 1971), Fisher (1972), Warrington (1974, 1984), Warrington & Williams (1984), Warrington (1997) and Kousis (2015). The previous studies of the Arden Sandstone Fm have suggested a late Carnian (Tuvalian) age (e.g., Warrington *et al.* 1980; Barclay *et al.* 1997). The only work that has systematically sampled the DMF in the Devon coastal area using the logs of Jeans (1978) is that of Fisher (1985) who recognized an older and a younger Carnian assemblage. In contrast, based on data from the nearby Wiscombe Park-1 Borehole, Miller et al. (2017) assigned a Julian age to the DMF. Kozur (in Gallois & Porter 2006) found the conchostracan

175 *Laxitexella multireticulata* within the Lincombe Member in the coastal sections which is
176 indicative of the early Carnian *L. mucroreticulata* Zone (Kozur & Weems 2010). This species
177 is common in the early Carnian 'Estheria Beds' (in the upper Grabfeld Formation in
178 Germany), but is also reported from the Schilfsandstein in Germany. Hounslow *et al.* (2002)
179 suggested that the Ladinian-Carnian boundary may be in the upper part of the Sidmouth
180 Mudstone Formation and the Carnian-Norian boundary near the boundary between the DMF
181 and overlying Branscombe Mudstone Formation, however, this was based on hitherto
182 unpublished magnetostratigraphic data. The DMF crops out along coastal cliffs between
183 Higher Dunscombe Cliff and Strangman`s Cove and has a wide distribution in the sub-surface
184 of the Wessex Basin (Gallois & Porter 2006; Porter & Gallois 2008) (Fig. 1). The DMF was
185 cored in two boreholes Wiscombe Park 1 and 2 (WP-1 and 2) about 5 km north of the coastal
186 outcrop (Porter & Gallois 2008) (Fig. 1). Further north in Somerset, several lenticular
187 sandstone units of the Arden Sandstone Fm can be found around Taunton, North Curry and
188 Sutton Mallet areas (Fig. 1), similar to the Lincombe Member of the Dunscombe Mudstone
189 Fm. However, the stratigraphic correlation of these arenaceous units remains uncertain
190 (Gallois 2003; Gallois & Porter 2006). On lithostratigraphical and palaeoenvironmental
191 grounds, Howard et al. (2008) argued that the sandstone bodies in Somerset are
192 contemporaneous with the Lincombe Member, but Gallois (2001) suggested they might occur
193 in a higher stratigraphic position within the DMF compared to the Lincombe Member.

194 **Methods**

195 *Palynology*

196 Palynological samples were taken from four locations: the Strangman`s Cove outcrop, the
197 Wiscombe Park-1 Borehole section in Devon and Sutton Mallet and Lipe Hill outcrops in
198 Somerset. Detailed description of the sample locations can be found in the Supplementary
199 Data. A detailed lithological log for the WP-1 and Strangman's Cove sections is provided in

200 the Supplementary Data (Fig. S1) with the exact position of the palynological samples. A total
201 of 104 samples were processed for palynological analysis from the studied sections and cores.
202 The palynological preparation follows standard procedures Wood et al. (1996) and as
203 described in Kuerschner et al. (2007). Details of the preparation technique can be found in the
204 Supplementary Data. The palynological slides and organic residues are stored at the
205 Department of Geosciences, University of Oslo, Norway. In each sample, *ca.* 300 terrestrial
206 palynomorphs (spores and pollen) were determined after scanning 2-4 slides (quantitative
207 analysis). After encountering at least 300 terrestrial taxa all remaining slides were scanned for
208 rare taxa (qualitative analysis). *Lycopodium*, undetermined palynomorphs and aquatic
209 palynomorphs were counted concomitantly but excluded from the palynomorph sum.
210 Identification of the taxa is based on the works of Klaus (1960), Clarke (1965), Schulz (1967),
211 Scheuring (1970, 1978), Fisher (1972), Roghi (2004), Planderová (1972, 1980), Van der Eem
212 (1983), Hochuli & Frank (2000), Mehdi *et al.* (2009), Fijałkowska-Mader *et al.* (2015),
213 Paterson *et al.* (2016). Spore coloration index (SCI) values follow those of Batten (2002).
214 Relative palynomorph abundances were calculated and plotted using the Tilia/TiliaGraph
215 computer program (Grimm, 1991–2001). Palynomorph assemblages at Strangman`s Cove and
216 Lipe Hill were distinguished by stratigraphically constrained cluster analysis using CONISS
217 within Tilia (Grimm 1987). For plotting this diagram, the counted abundance data of all
218 identified taxa were used, but unidentified forms and aquatics were excluded from the cluster
219 analysis. For palynofacies analysis different types of sedimentary organic matter (SOM)
220 particles were distinguished in the samples. Approximately 300 SOM particles were counted
221 in each sample. The subdivision of the different groups and terminology follows Oboh-
222 Ikuenobe & de Villiers (2003). The complete palynofacies and palynomorph raw data set is
223 provided in the Supplementary Data (Table S3-S9).

Palaeoecological affinity of palynomorphs and palynomorph source areas

The classification of dispersed palynomorphs as hygrophyte and xerophytes (Table S1, Supplementary Data) is based on the concept of Visscher & Van der Zwan (1981), taking into consideration the known or supposed ecological preferences of the parent plant. It can be regarded as the first approximation of a climatic signal, yet it should be applied with caution as the exact botanical affinity and ecological needs of many Mesozoic dispersed spore and pollen are uncertain. All spores identified in this study are assigned to the hygrophyte group. The elements of *Alisporites* spp. are considered to be transitional elements in the sense of Visscher & Van der Zwan (1981), but some workers attribute them to a hygrophyte affinity (e.g., Roghi *et al.* 2010; Whiteside *et al.* 2015, Mueller *et al.* 2016a). All other bisaccate pollen, monosaccate pollen and the members of the Circumpolles group are assigned to the xerophyte group (e.g., Hochuli & Vigran 2010; Roghi *et al.* 2010; Mueller *et al.* 2016a, b). *Cycadopites* sp. and *Aulisporites astigmosus* are generally assigned to hygrophyte pollen (Roghi 2004; Roghi *et al.* 2010).

Unlike plant megafossils which represent predominantly local vegetation, the palynological assemblages record plant communities of different habitats, as well as local and regional vegetation types (Jacobson & Bradshaw 1981; Demko *et al.* 1998; Kustatscher *et al.* 2012). Elements of the local pollen rain originate within a distance of *ca*. 20 m from the sampling site in the sense of Jacobson & Bradshaw (1981) (Table S1). Extra local elements grow between 20 m and several hundred metres of the sampling site and regional pollen derives from plants at greater distance (Jacobson & Bradshaw 1981). To assign the dispersed palynomorphs to local or regional elements, the habitat of the parent plant and the transport mechanisms characteristic for palynomorph types have to be considered. These environmental parameters form the basis of the sporomorph ecogroup model (SEG) method of Abbink *et al.* (2004) for assigning the pollen and spores to various habitats. The SEG is an ecological

model which groups dispersed palynomorphs into different habitats based on the known or presumed parent plants (Abbink et al. 2004). The original SEG method was established for Jurassic–Cretaceous assemblages, but several workers have applied the method to Triassic palynomorph assemblages (Ruckwied *et al.* 2008; Götz *et al.* 2009, 2011; Kustatscher *et al*. 2012; Paterson *et al.* 2016). In fully terrestrial settings four SEGs (habitats) are defined: river SEG, dry and wet lowland SEG and upland/hinterland SEG. The upland/hinterland SEG includes upland communities growing on higher terrains, well above groundwater level and is never submerged by water (Abbink et al. 2004). The river SEG reflects riverbank communities that are periodically submerged and subject to erosion, the dry lowland SEG reflects floodplain vegetation that can be occasionally submerged, wet lowland SEG represents marshes and swamps and the hinterland SEG reflects plant communities on well-drained terrains, above groundwater table (Abbink et al. 2004). Due to proximity of habitats to permanently wet environments (river, lake or marsh), the palynomorphs in the river and lowland SEG consists of the local and extra local vegetation elements. The hinterland SEG consists of the elements of the regional pollen flora that can be transported over long-distance (Olivera et al. 2015) (Table S1).

Organic carbon isotope analysis and TOC

A total of 36 samples from the Strangman's Cove outcrop were selected for $\delta^{13}C_{TOC}$ analyses. Details of the analytical technique and the data set (Table S10) can be found in the Supplementary Data.

Results

Palynological assemblages

Only 36 out of 104 processed samples provided palynomorph assemblages. The rest of the samples were barren or the scanned slides contained less than 10 specimens. The

palynomorphs are generally moderately to well preserved, the wall colour varies between pale yellow to golden brown, their SCI index ranges from 2 to 7 depending on wall-thickness variations between the grains (Batten 2002). A total of 81 spore and pollen taxa and 5 aquatic palynomorphs are distinguished. The most important palynomorphs are illustrated in Fig. 4. A list of all identified taxa with full author citation and seven additional photoplates can be found in the Supplementary Data.

Sidmouth Mudstone Formation

Palynological assemblages from the Sidmouth Mudstone Formation are only recorded in core WP-1from depths 111.98 m and 109.11 m (Fig. 2). The assemblages are characterized by the predominance of bisaccate pollen grains with a trilete mark (*Triadispora* group) (up to 45% of the total abundance) along with Circumpolles (up to 22% of the total abundance). The species *Triadispora obscura*, *T. plicata* and *T. aurea* are predominant and the stratigraphically useful *T. verrucata* is present at 111.98 m. Among the Circumpolles group, various species of the genus *Partitisporites* (e.g., *P. novimundanus*, *P. scurrilis*) and *Praecirculina granifer* are common as well as *Duplicisporites granulatus*. *Camerosporites secatus* is present but rare in both samples from the Wiscombe Park Borehole. Alete bisaccates are less common, with only *Alisporites* spp. and *Ovalipollis ovalis* reaching more than 10% of the total spore-pollen flora. Monosaccate pollen grains are represented only by *Vallasporites ignacii*. *Aulisporites astigmosus* and *Cycadopites* sp. are observed in both samples, but they are minor components of the assemblage. During quantitative analysis only a few spore taxa are documented; among them *Aratrisporites* spp. and *Calamospora tener* are more common (2-3% of the total abundance). Other spore taxa were recorded only during the qualitative analysis and then only represented by one or two specimens (e.g., *Thomsonisporis toralis*, *Verrucosisporites morulae*, *Krauselisporites* sp.).

297 **Dunscombe Mudstone Formation**

298 The palynological assemblages from the Dunscombe Mudstone Formation recorded in the
299 Strangman's Cove section and in the WP-1 core (Fig. 2) contain predominantly bisaccate
300 pollen grains and members of the Circumpolles group. *Triadispora* spp. are very frequent
301 throughout the DMF, especially the species *T. obscura*, *T. plicata* and *T. sulcata*. Alete
302 bisaccate pollen grains are represented mainly by *Ovalipollis* spp., *Alisporites* spp.,
303 *Pityosporites* sp. and *Klausipollenites gouldii*. The abundance of *Minutosaccus crenulatus,*
304 *Ellipsovelatisporites plicatus* and *Microcachrydites doubingeri* occasionally increases. Striate
305 bisaccate pollen grains (*Lunatisporites acutus*) are scarce. Among monosaccate pollen grains
306 only *Enzonalasporites vigens* is common. *Patinasporites densus* is recorded first in sample
307 WE017 (within the Lincombe Member) in the Strangman's Cove section and at the top of the
308 WP-1 core, at 56.51m (Fig. 2), but its abundance is low. *Camerosporites secatus*,
309 *Duplicisporites granulatus* and *Praecirculina granifer* are the most abundant members of the
310 Circumpolles group. *Aulisporites astigmosus* is virtually absent in the DMF except for one
311 questionable specimen at 71.41m in core WP-1. The colonial chlorococcalean algae
312 *Plaesiodictyon mosellanum* dominate the palynological samples from the Lincombe Member
313 at Strangman`s Cove (Fig. 2). Cluster analysis helped to distinguish two assemblages
314 (assemblage I and II) at the Strangman`s Cove. Assemblage I and II differ mainly in the
315 increase of *C. secatus* among the Circumpolles and the presence of *Patinaporites densus* in
316 Assemblage II. The boundary between these two assemblages is placed between samples
317 WE017 and WE109 (Fig. 2, Supplementary Data).

318 **Branscombe Mudstone Formation**

319 In the Branscombe Mudstone Formation, only one palynological assemblage (Assemblage III)
320 is encountered from the upper part of the Strangman`s Cove section, in sample WE203 (Fig.
321 2). This sample is characterized by an increase in the abundance of spores (up to 30% of the

total abundance in WE203) compared to the DMF *Calamospora tener, Porcellispora longdonensis, Todisporites major* and *T. rotundiformis* are the most frequent taxa. Among the bisaccate pollen grains, the abundance of genus *Triadispora* decreases in favour of alete bisaccates e.g., *Alisporites* spp., *Klausipollenites gouldii* and *Ovalipollis* spp. The abundance of monossaccate pollen (*Patinasporites densus*, *Enzonalasporites vigens*, *E. manifestus, Pseudoenzonalasporites summus, Vallasporites ignacii*) is higher compared to the DMF and SMF. *Camerosporites secatus* dominates the Circumpolles group. *Partitisporites quadruplices* and cf. *Partitisporites tenebrous* are also recorded in this assemblage, while *P. maljawkinae, P. novimundanus* and *P. scurrilis* are absent. The enigmatic sporomorph *Brodispora striata* is also more frequent here compared to its single occurrence in the DMF.

Somerset Sandstone units

From the Somerset localities (Fig. 1), samples from the Sutton Mallet and Lipe Hill sections yielded palynomorphs, but the samples atKnapp Quarry were barren (Fig. 3). At Lipe Hill two assemblages are distinguished by cluster analysis (Assemblage LH I and II) (Fig. 3). Ten samples from the Lipe Hill section in Somerset provided well-preserved assemblages (Fig. 4). The palynomorph abundance in sample LH-1 is very low, and the proportion of the terrestrial palynomorphs decreases significantly in samples LH-5 and LH-6 as these are especially rich in algae, predominantly *P. mosellanum* (Fig. 3). The terrestrial palynomorphs are characterized by the predominance of the *Triadispora* group (up to 60%), mainly *Triadispora obscura* and *T. plicata*. The Circumpolles group is also common; the proportion of *D. granulatus* is somewhat elevated compared to *C. secatus.* Two palynomorph assemblages are distinguished by cluster analysis, with sample LH-1 as a third group that differs from the other two assemblages by a low total palynomorph count. The two other assemblages differ primarily in the proportion of *Ovalipollis* spp. (LH I 20-30%, LH II ca. 10%) to *Triadispora* spp (LH I *ca.* 40%, LH II up to 60%). Spores are present in all samples but their diversity and

abundance is very low (<5%). In samples LH-1–LH-2, LH-5–LH-6 a few acanthomorph acritarchs (*Micrhystrydium* sp.) are observed. Some of these acritarchs are probably reworked as suggested by a darker wall colour or a damaged vesicle. However, some specimens are well-preserved and show no signs of reworking.

In the Sutton Mallet section (Figs 1 and 3) the palynomorph assemblages predominantly contain bisaccate pollen grains (Fig. 3). *Triadispora* spp. are the most frequent (*ca.* 50-60%). Alete bisaccates are less common and are represented mainly by *Ovalipollis ovalis, O. lunzensis, Alisporites grauvogeli* and *A. grandis*. Spores are more abundant in this locality than in the coastal section and the WP-1 core. *Aratrisporites* spp. is especially frequent; it reaches around 10% of the total abundance in each sample. The only striate bisaccate pollen encountered is *Lunatisporites acutus*. Among the Circumpolles, *Camerosporites secatus* is predominant, while other genera occur only in minor proportions. *Ricciisporites tuberculatus* is recorded in sample SM2 at Sutton Mallet. *Plaesiodictyon mosellanum* is frequent also in the samples from this locality. *Botryococcus* is present but less abundant than *P. mosellanum*. In sample SM4 a few acanthomorph acritarchs (*Micrhystrydium* sp.) are observed. These specimens are well-preserved and show no ambiguous signs of reworking.

Organic carbon isotopes

Bulk organic carbon isotope ratios ($\delta^{13}C_{TOC}$) from WP-1 core (Miller *et al.* 2017) and samples from the Strangman's Cove section allow stratigraphical correlation of these data to be assessed (Fig. 6). The Strangman's Cove Section outcrop contains several negative isotope excursions: the older part of the section shows larger variations but a gradual upwards shift to more negative values, which culminates in the negative isotope excursion in sample WE015. A shift to more positive values occurs near the top of the DMF (Fig. 6).

Discussion

Palynostratigraphy

Palynology provides a powerful tool in the correlation of Late Triassic marine and non-marine successions; however, many assemblages are not dated independently with other fossils (e.g., ammonoids, conodonts) or other geochronological methods (e.g., radiometric dating) (Cirilli 2010). Important taxa often lack well-calibrated stratigraphical ranges and these are often diachronous in different regions (e.g., between Germanic Basin and Alpine realm) (Cirilli 2010).

In the Southern Permian Basins (mainly Germany,Poland and southern North Sea), early Julian assemblages are characterized by *Triadispora verrucata*, *Camerosporites secatus,* *Patinasporites densus* and *Vallasporites ignacii* (e.g., Scheuring 1970, 1978; Orłowska-Zwolińska 1983, 1985; Reitz 1985; Heunisch 1999; Kürschner & Herngreen 2010; Fijałkowska-Mader *et al.* 2015) with an increase in *Aulisporites astigmosus* in the younger part of the Julian. The Tuvalian is characterized by the appearance of *Ricciisporites tuberculatus* and *Classopollis* spp. (Kürschner & Herngreen 2010). The common occurrence of *Granuloperculatipollis rudis* with *Classopollis zwolinskae* and *Chasmatosporites* spp. marks the beginning of the assumed Norian *Granuloperculatipollis rudis* Zone in the Germanic basins (e.g., in the Arnstadt Formation) (Kürschner & Herngreen 2010). However, late Carnian and Norian palynological records with independent marine biostratigraphical control or other geochronological age constrains are still lacking from the Germanic Triassic basins (Cirilli 2010; Kürschner & Herngreen 2010). In the GSSP section for the Carnian, Prati di Stuores/Stuores Wiesen, *Vallasporites ignacii*, *Patinasporites densus*, *Aulisporites astigmosus* and *Camerosporites secatus* all have their first occurrences in the lowermost part of the *Daxatina canadensis* Subzone of the *Trachyceras* Zone (Fig. 5) in the lowermost Carnian (Mietto *et al.* 2012).

The palynological assemblages in Devon and Somerset yielded typical Carnian palynological assemblages with *Camerosporites secatus*, various *Partitisporites* and *Duplicisporites* species, *Enzonalasporites* spp., *Vallasporites ignacii* and *Patinasporites densus*. However, distinct Julian palynomorph assemblages e.g., the *Triadispora verrucata* assemblage and the *Aulisporites astigmosus* acme reported from the Schilfsandstein (Visscher *et al.* 1994) and marine series in the Alps (Roghi *et al.* 2010), are not seen in the British succession.

The common taxa in the uppermost part of the Sidmouth Mudstone Fm (Fig. 2), *Partitisporites* spp., *Camerosporites secatus* and *Praecirculina granifer,* are generally characteristic in Carnian palynological assemblages in the Germanic realm (from the e.g., Lower Gipskeuper, Schilfsandstein and Upper Gipskeuper). Few specimens of *Triadispora verrucata* are recorded in the studied part of the Sidmouth Mudstone Fm, which in contrast is a common species in the early Julian assemblages from the Lower Gipskeuper in the Germanic Basins (e.g., Kürschner & Herngreen 2010; Fijałkowska-Mader et al. 2015) (Fig. 5). This species is frequent in the *Triadispora verrucata* subzone of the *Camerosporites secatus* Zone in NW and central Europe (Kürschner & Herngreen 2010), and in the *verrucata* Subzone of the *longdonensis* Zone in the Polish Keuper (Orłowska-Zwolińska 1983, 1985; Fijałkowska-Mader *et al.* 2015), and in the GTr 12-13 zones of Heunisch (1999) (Fig. 5). The assemblages with abundant *T. verrucata* are usually found in the upper part of the Lower Gipskeuper in the Germanic Basin (Kürschner & Herngreen 2010; Fijałkowska-Mader *et al.* 2015), but the complete range of *T. verrucata* has a longer duration, first appearing in the Grenzdolomit (topmost Erfurt Formation, late Ladinian-earliest Carnian, [e.g., Szulc 2000]) and disappearing around the Carnian/Norian boundary in Germany (Heunisch 1999; Kürschner & Herngreen 2010). The palynological assemblages from the 'Mudstone I' unit of Fisher (1985), which underlies the Dunscombe Mudstone Formation is similar to our assemblage of the Sidmouth Mudstone Fm in the WP-1 core that contains *Camerosporites*

secatus, *Duplicisporites granulatus* and *Ovalipollis ovalis* but lacks *Enzonalasporites vigens*. Fisher (1985) did not identify *Triadispora verrucata* in any of his samples from 'Mudstone I'. He assigned this assemblage to the latest Ladinian (Longobardian)-early Carnian (Cordevolian) based on correlation to the assemblages from the Meridenkalken (Scheuring 1978). The preliminary magnetostratigraphy of the MMG (Hounslow *et al.* 2002) suggests that the Ladinian/Carnian boundary may be placed in the upper part of the SMF. However, characteristic Ladinian taxa from the Germanic Basins such as *Heliosaccus dimorphus* or *Echinitosporites iliacoides* (Kürschner & Herngreen 2010) are absent in `Mudstone I` of Fisher (1985) and in the upper part of the SMF in our study.Hence, the co-occurrence of *Triadispora verrucata* with other characteristic Carnian taxa e.g., *C. secatus*, *Partitisporites* spp., *V.ignacii, A. astigmosus* within the palynoflora from the SMF suggest an early Julian age (Orłowska-Zwolińska 1983, 1985; Heunisch 1999; Kürschner & Herngreen 2010; Fijałkowska-Mader *et al.* 2015). Therefore the Ladinian/Carnian boundary is located lower than the investigated interval according to the palynological results.

Aulisporites astigmosus is a characteristic component of Julian assemblages in the western Tethys (e.g., Roghi *et al.* 2010), as well as in the Schilfsandstein (Visscher *et al.* 1994). An acme of the species is recorded in several late Julian successions in the Dolomites, Julian Alps and Northern Calcareous Alps (Roghi 2004; Roghi *et al.* 2010). Mueller *et al*. (2016b) found an increase in *A. astigmosus* only in the Rheingraben Shales of mid Julian age. In the British successions, the species has been recorded only in the Sidmouth Mudstone Formation represented by a few specimens and one poorly preserved specimen was found in the DMF (WP-1, sample 71.41 m, Fig. 6). The *Aulisporites* acme is often associated with the presence of other Cycadophyte related pollen grains such as *Cycadopites* spp. and lycopsid spores of the *Aratrisporites* group (Roghi *et al.* 2010). A palynoflora with similar composition to that is absent in the British successions. In the WP-1 core *Cycadopites* is extremely rare, and in the

445 Strangman's Cove coastal outcrop only a few specimens of *Cycadopites* sp. are recorded in
446 the interval from sample WE017 in the Lincombe Member, to sample WE214 in the upper
447 part of the DMF (Figs 2 and 6). This interval might reflect an expression of the *Aulisporites*
448 assemblage however, the British successions appear to completely lack an acme of
449 *Aulisporites astigmosus* as seen in the western Tethys or in the Schilfsandstein.
450 The previous study of Fisher (1985) distinguished two palynological assemblages in the DMF
451 in the South Devon Coast: an older and younger palynomorph assemblage with the boundary
452 between the two placed within the Lincombe Member (Fisher 1985; Gallois & Porter 2006).
453 The assemblages were informally termed the "Dunscombe cycle" and "Weston cycle". These
454 "cycles" most likely correspond to the Assemblages I and II from the Strangman`s Cove
455 coastal outcrop respectively. The composition of the "Dunscombe cycle" is similar to the
456 Assemblage I from the Strangman`s Cove (Fig. 2), with a high volume of bisaccate pollen
457 grains, *Praecirculina granifer*, *Enzonalasporits vigens*, *Ovalipollis ovalis,*
458 *Ellipsovelatisporites plicatus* and *Triadispora* spp. Fisher (1985) correlated the older
459 "Dunscombe cycle" to the palynological assemblages of the Gipskeuper and Zones D-E of
460 Scheuring (1970) from the Keuper in Switzerland based on the restricted occurrence of
461 *Protodiploxypinus gracilis* and *Triadispora plicata* in this assemblage and suggested an early
462 Carnian ("Cordevolian" age, now considered early Julian). The "Weston cycle" of Fisher
463 (1985) has a similar palynological composition to Assemblage II in the upper part of the DMF
464 in our study, characterized by an increase in *Camerosporites secatus* and the restricted
465 occurrence of *Patinasporites densus*. Fisher (1985) correlated the "Weston cycle" to the upper
466 part of the Gipskeuper and the Schilfsandstein (Zones F-G of Scheuring 1970) and suggested
467 a Julian-Tuvalian age. The local first occurrence (FO) of *Patinasporites densus* is recorded in
468 the upper part of the WP-1 (at 56.51 m). In the Strangmans`s Cove section, the species is
469 present from *ca.* 20 m above the base of the section (sample WE017, Fig. 2). *Patinasporites*

densus and *Partitisporites maljawkinae* are characteristic for the *densus–maljawkinae* phase of Van der Eem (1983) (Fig. 5) characteristic for the late Julian in the Dolomites. As the last local occurrence of *Partitisporites novimundanus* is recorded in the upper part of the DMF at Strangman's Cove (Figs 3 and 6), the uppermost studied part of the DMF is most likely still Julian according to the recent palynological zonation for NW and central Europe (Kürschner & Herngreen 2010). Characteristic Tuvalian taxa e.g., *Ricciisporites* or *Classopollis* spp. are absent in the studied part of the DMF.

The assemblage from the Branscombe Mudstone Fm is characterized by the presence of *Porcellispora longdonensis*, *Calamospora tener*, *Partitisporites quadruplices* and *Brodispora striata* is more common compared to the single occurrence of the species in the DMF (Strangman`s Cove, sample WE111). *Brodispora striata* is a characteristic element of the Arden Sandstone Formation of the English Midlands (Clarke 1965) (e.g., Warrington 1970, Warrington *et al.* 1980; Fisher 1985; Barclay *et al.* 1997). This formation has been assigned to the Tuvalian substage based on the palynological assemblage with *Duplicisporites* spp., *Camerosporites secatus*, *Haberkornia gudati*, *Vallasporites ignacii*, *Ovalipollis pseudoalatus*, *Ellipsovelatisporites plicatus*, *Ricciisporites umbonatus*, *Patinasporites densus* and *Brodispora striata* (Clarke 1965; Warrington 1970a; Warrington *et al.* 1980; Barclay *et al.* 1997) although many of these taxa are not confined to the Tuvalian (Cirilli 2010; Kürschner & Herngreen 2010). In the Alpine Realm, *B. striata* has been recorded from the Opponitz Formation in the Lunz am See area in Austria (Dunay & Fisher 1978) dated to the uppermost Carnian *Tropites subbulatus* ammonoid Zone suggesting Tuvalian age (Fig. 5). The species *Partitisporites quadruplices* characterizes the Tuvalian in the western Tethys (Visscher & Krystyn 1978; Cirilli & Eshet 1991). *Brodispora striata* and *P. quadruplices* are found together in the Carnitza Formation and Travenanzes Formation in the Dolomites (Roghi 2004), which based on ammonoids is Tuvalian in age (De Zanche *et al.* 2000). According to

the national rationalisation of the Mercia Mudstone Group lithostratigraphy by Howard *et al*. (2008), the DMF includes the equivalent of the Arden Sandstone Formation of the English Midlands there considered to be Tuvalian in age. Our palynological data and the results of Fisher (1985) from the DMF are inconsistent with a Tuvalian age assignment. The studied part of the DMF on the South Devon Coast being Julian in age, with Tuvalian assemblages confined to the overlying Branscombe Mudstone Formation in the upper part of the Strangman's Cove section. The Julian/Tuvalian boundary might be placed in the uppermost part of the DMF or the lowermost part of the Branscombe Mudstone which has not been investigated in this study.

Correlation of the sandstone units from Somerset and the English Midlands

Based on lithostratigraphy and log correlations Howard *et al.* (2008) suggested that the North Curry Sandstones from Somerset are equivalent to the Lincombe Member of the Devon coast and also the Arden Sandstone Formation in the English Midlands. *Brodispora striata* and *Ricciisporites* are frequent elements of the Arden Sandstone Formation (Warrington et al. 1980). *Brodispora* is common only in the Branscombe Mudstone Formation on the Devon coast and *Ricciisporites* was only recorded at Sutton Mallett, in Somerset. The palynological assemblages at Lipe Hill are comparable with Assemblage I at Strangman`s Cove and the "Dunscombe cycle" of Fisher (1985) from the coast, based on the high amount of *Triadispora* spp. especially *T. obscura*, *Ovalipollis* spp., *Praecirculina granifer, Duplicisporites granulatus.* Tthe assemblages at Lipe Hill suggests Julian (probably late Julian) age but it cannot be defined more precisely based on the palynological assemblages only.

The assemblage at the Sutton Mallet section is younger, based on the presence of Ricciisporites tuberculatus in sample SM 2, indicating the Tuvalian. In the Alpine realm this species appears first in the Travenanzes Formation in the Dolomites and in the Carnitza

520 Formation in the Julian Alps in the Tropites dilleri Zone of the Tuvalian (Fig. 5) (Roghi 2004;
521 Roghi et al. 2010).
522
523 *Chemostratigraphy and correlation*
524 In marine successions, $\delta^{13}C_{CARB}$ shows an overall rise of 3‰ in the earliest Carnian
525 ($\delta^{13}C_{CARB}$, +1 ‰– +3 ‰ compared to V-PDB) with a small negative excursion near the
526 Ladinian-Carnian boundary (-1 ‰) (Korte et al. 2005) and a sharp negative excursion at the
527 early-late Julian boundary both in carbonate carbon and organic carbon (Korte et al. 2005;
528 Muttoni et al. 2014; Mueller et al. 2016a, b).
529 The correlation of the negative carbon isotope excursion at the Ladinian-Carnian boundary
530 and the IIE excursion in the WP-1 core is unlikely since palynological evidence does not
531 suggests a Ladinian age for the lowermost part of the DMF or topmost part of the Sidmouth
532 Mudstone Fm. The correlation of the IIE excursion in the WP-1 core to the early-late Julian
533 boundary excursion seems to be more plausible and it can be matched to the Julian 1/2 zonal
534 boundary excursion in the Alpine areas (Dal Corso *et al.* 2012, 2015). The lithostratigraphical
535 and palynological correlation between the Strangmans' Cove section and WP-1 core (Gallois
536 & Porter 2006) is supported by $\delta^{13}C_{TOC}$ wiggle matching in Fig. 6. The third isotope
537 excursion (CIE-3) in WP-1 can be matched with the excursion in sample WE015 in the
538 coastal outcrop. This excursion is located at the base of the Lincombe Member, just below
539 calcareous marker bed C (Gallois 2007; Gallois & Porter 2008) at Strangman`s Cove (Fig. 6).
540 The correlation of this interval between the core and the outcrop is supported by the local first
541 appearance date of *Patinasporites densus*. CIE-4 is located in both sections at calcareous
542 marker bed G (Fig. 6). CIE-5 is just above bed I (Fig. 6) at Strangman's Cove which
543 correlates to the interval between 51 m and 52 m in WP-1 (Gallois & Porter 2006) with the
544 fifth negative carbon isotope excursion (Fig. 6). CIE-2 is located at calcareous marker bed A

545 and the IIE is few metres above the base of the DMF in both sections (Fig. 6). However, the
546 latter two excursions cannot be precisely matched.
547 As the bulk organic matter analysed for its $\delta^{13}C$ composition comprises not only the
548 particulate organic matter and palynomorphs identified here but includes the whole
549 sedimentary organic matter (kerogen), it is not straightforward to directly compare the
550 palynological/palynofacies data with the bulk carbon isotope data. The bulk $\delta^{13}C_{TOC}$ values
551 are more negative in the Strangman's Cove outcrop than in the Wiscombe Park core. These
552 differences may be due to variations in the composition of the organic matter, indeed TOC
553 values, although generally low, do differ between the core and the outcrop (Fig. 6).
554 Unfortunately, Rock-Eval data which may help to quantify the composition of the total
555 sedimentary organic matter are not available.
556 Multiple carbon source contributes to and thus complicate the interpretation of the bulk
557 organic $\delta^{13}C$ signal. Fluctuations in bulk organic $\delta^{13}C$ can be associated with both changes in
558 lithology and changes in environmental conditions (Pancost et al. 1999). Major factors
559 controlling bulk organic $\delta^{13}C$ values include variations in the composition of the organic
560 matter (i.e. aquatic *vs*. terrestrial) and the carbon isotopic composition of atmospheric CO_2
561 during inorganic carbon uptake by plants (e.g. Diefendorf & Freimuth, 2017). Compound
562 specific carbon isotope analysis of plant leaf waxes (*n*-alkanes) can help resolve the multiple
563 isotopic signals that contribute to the bulk organic carbon $\delta^{13}C$ signal. Miller et al. (2017)
564 suggest that the negative carbon isotope excursions recorded simultaneously in both WP-1
565 $\delta^{13}C_{TOC}$ and in plant leaf waxes (*n*-alkanes) represent an injection of light carbon into the
566 atmosphere, resulting in significant global perturbations of the carbon cycle. The good
567 correlation between WP-1 and Strangman's Cove $\delta^{13}C_{TOC}$ may suggest that changes in
568 $\delta^{13}C_{TOC}$ at Strangman's Cove are also likely a result of changes in the carbon isotopic
569 composition of atmospheric CO_2 and not fully related to changes in organic matter source.

570 Nevertheless, climate change often results in vegetation shifts. The amount of carbon isotope
571 fractionation, is heavily controlled by the plant's photosynthetic pathway, which varies
572 depending on plant type (e.g. Diefendorf & Freimuth, 2017; Collister et al. 1994). The
573 negative carbon isotope excursions at Strangman`s Cove (CIE-3, -4 and -5) coincide with
574 higher bisaccate pollen and spore abundances (Supplementary Data), although there is no
575 statistically significant correlation with any of the individual palynomorph groups (R^2 below
576 0.5 for each palynomorph group, see Supplementary Data, Fig. S2). Therefore, we suggest
577 that the observed shifts in bulk carbon isotopes may also be the result of changes in vegetation
578 as well as shifts in the C isotopic composition of atmospheric CO_2. Moreover, precipitation
579 amount (humidity) is a strong factor governing plant carbon isotopic fractionation. Except for
580 in extremely wet environments, the $\delta^{13}C$ of C_3 plants tends to decrease with increasing rainfall
581 (e.g. Kohn 2010). Thus, the increased humidity experienced during the CPE may have also
582 contributed to the observed negative C isotope excursions.
583 *Climatic and palaeoenvironmental implications*
584 In the Southern Permian Basin and western Tethys marine sections, hygrophyte pteridophytic
585 spores and pollen grains with hygrophyte affinity (e.g., *Aulisporites astigmosus*) arose in
586 abundance during the Julian (Roghi *et al.* 2010) (Table S2). However, the pollen record across
587 the Dunscombe Mudstone Fm shows the predominance of xerophyte-related land vegetation
588 during this interval (Figs. 2–4, Figs 7–8, Table S1. Despite the shift in climate, evident from
589 the lithological change into the base of the Dunscombe Mudstone Fm: Porter & Gallois,
590 2008), a clear humid climate signal is missing from the palynological record. There are two
591 different ways to interpret the lack of a clear humid climate signal. Firstly, during the Late
592 Triassic NW Europe was at *ca.* 30ºN in the continental interior of Pangaea within the dry
593 climate belt with low annual precipitation (Fig. 1), likely falling during the Northern
594 Hemisphere-summer period when the main rainfall zone with the ITCZ migrated to the north

595 (Kutzbach & Gallimore 1989; Parrish 1993; Ziegler *et al.* 1994; Sellwood & Valdes 2006;
596 Vollmer *et al*. 2008). Hence, in the Wessex Basin, the lack of an expected increase in
597 hygrophyte floral elements e.g., ferns or the Bennettitalean parent plant of *Aulisporites*
598 (*Williamsonianthus keuperianus*) (Kräusel & Saarschmidt 1966; Balme 1995) might be
599 related to this strongly seasonal precipitation, which during the dry season may have
600 prohibited the development of a permanent extensive wetland vegetation and the preservation
601 of spores and pollen grains. Also, the regional palaeogeography and topography of the studied
602 area such as subdued upland surrounding a low-relief interior basin (Talbot et al 1994) may
603 have caused isolation from other basins and the development of a locally more arid climate
604 than in other region of the Germanic Triassic, even during the CPE. *Aulisporites astigmosus*
605 seems to be extremely rare in the British Carnian palynological assemblages, as it has not
606 been identified in most palynological studies (e.g., Warrington 1970, 1971; Fisher 1972;
607 Warrington 1974, 1984; Warrington & Williams 1984; Fisher 1985; Warrington 1997, 2004).
608 Even though the species is present in some coeval sections of the UK (pers. comm. with G.
609 Warrington 2017), the parent plants might have formed only minor part of the vegetation.
610 Although the acme of *A. astigmosus* is recognized in different depositional settings and at
611 different palaeolatitudes there are locations across Europe, like the UK, where it is absent in
612 the Carnian palynological assemblages.The *A. astigmosus* acme has not been recorded in the
613 Carnian Manuel Formation from Spain (Arche & López-Gómez 2014) (Table S2) and
614 Lindström et al. (2017) do not record any well expressed hygrophyte palynological
615 assemblages from the mid– to late Carnian assemblages of the Danish Basin which may
616 suggest that these areas were probably too dry even during the CPE.
617 Secondly, if the parent plants of *Aulisporites* and other humidity indicators (ferns) were
618 present in the Wessex Basin, the balance between local and regional vegetation elements in
619 the palynological record could have masked a real humid signal. Pollen and spores come from

620 both local and regional sources, and catchments of different sizes can represent vegetation at
621 different spatial scales (Berglund 1973; Jacobson & Bradshaw 1981; Hicks & Hyvärinen
622 1999). In modern lacustrine settings, the contribution of regional pollen increases with larger
623 lake size or catchment area (Jacobson & Bradshaw 1981), which can lead to the
624 underrepresentation of local hygrophyte vegetation growing on the shoreline. This principle,
625 when applied to the Late Triassic vegetation elements of the UK, suggests the regional pollen
626 rain is probably associated with the xerophyte pollen group originating from conifers and
627 upland seed ferns (monosaccates, bisaccates, Circumpolles), while the local and extra local
628 elements were likely the hygrophyte lowland and riparian elements including *Aulisporites*
629 *astigmosus* (Table S1), fern- and lycopsid spores.
630 Such differences between the contribution of local and regional pollen rain has already been
631 discussed by Visscher *et al.* (1994) in the case of the Schilfsandstein. They considered the
632 *Aulisporites*-acme as only a local signal and rejected the possibility of a European-wide
633 humid climatic phase, as the regional pollen was likely characterized by xerophyte pollen
634 during the whole Julian. In contrast to the mainly lacustrine DMF, the Schilfsandstein in
635 Germany is considered a predominantly fluvial-deltaic deposit (Shukla *et al.* 2010; Franz *et*
636 *al.* 2014). The local wet spots on the floodplain probably collected more material from the
637 local and extra local pollen rain resulting in hygrophyte palynological assemblages enriched
638 in *Aulisporites astigmosus* and spores.
639 The Schilfsandstein depositional system probably provided a more favourable habitat for the
640 parent plant of *Aulisporites* (Bennettitalean) which grew in warm and often in deltaic settings
641 (Van Konijnenburg-Van Cittert & Van der Burgh 1989; Vakhrameev 1991).
642 The Lincombe Member in Devon represents a geographically restricted freshwater lake
643 (Porter & Gallois 2008). If this lake was of considerable size (>1km), according to the pollen
644 catchment model of Jacobson & Bradshaw (1981) the size of the lake might explain the

predominance of the regional pollen rain of xerophyte vegetation and the lack of local and extra local pollen rain including spores and pollen from hygrophyte vegetation (e.g., *Aulisporites*) (Fig. 7).Within the Sidmouth Mudstone and Branscombe Mudstone formations , the samples with high spore abundance come from cm-thick greenish-grey intervals within between thicker red mudstone units (Fig. 2). These intervals likely represent spatially restricted locally wet environments with higher representation of extra local and local pollen and spores (Fig. 7). The sandstone units in Somerset contain more spores suggesting a more local source for the palynomorphs, but the *Aulisporites* acme is still absent.

The taphonomic bias between local and regional pollen is further exacerbated by the higher pollen production rates of wind-blown pollen from the hinterland (e.g., conifers) compared to insect-pollinated palynomorph types such as Cycadales pollen, *Cycadopites* sp., *A. astigmosus* (e.g., Fægri & van der Pijl 1966).

The relatively wetter periods during the CPE should have supported the expansion of the hygrophyte vegetation living proximal to a lake. However, the proposed enhanced seasonal runoff associated with the CPE could have transported more regional pollen types to the lacustrine depositional setting of the DMF, leading to the underrepresentation of the more proximal local and extra local vegetation elements e.g., ferns or Bennettitales. A similar scenario was suggested by Bonis et al. (2010) from the Triassic/Jurassic boundary palynological assemblages of St. Audrie`s Bay (Somerset, UK) where the intensification of seasonal monsoonswas connected to the increase in hinterland Cheirolepidiaceae pollen and lower spore abundance.

Climate change reflected by the hinterland vegetation (regional pollen) might provide new criteria for tracking climate change during the CPE. However, interpreting the ecological signal of the regional hinterland pollen types is difficult due to the uncertainty in parent plants and in the uncertain assignment of dispersed pollen grains into the hygrophyte or xerophyte

groups. *Alisporites* species were most likely produced by seed ferns and although the parent plant is uncertain, with some placing them in transitional and/or hygrophyte groups (e.g., Visscher & Van der Zwan, 1981; Whiteside *et al.* 2015; Lindström *et al.* 2016; Mueller *et al.* 2016a, b). The increase in the total *Alisporites* and total spore abundance in the lower part of the DMF in the Strangman's Cove section coincides with a peak in freshwater algae (*P. mosellanum*) in the Lincombe Member (Fig. 8). This increase in algae suggests expansion of the lacustrine facies (i.e. the Lincombe Member), hence can be linked to a climatic interval with a relatively wetter season (Fig. 8), which is also supported by the increase in abundance of *Alisporites*.

Acritarchs in Somerset

Marine microplankton are known from some other Late Triassic mudstone units in the Cheshire Basin and the Midlands (Earp & Taylor 1986; Wilson & Evans 1990; Warrington & Ivimey-Cook 1992; Barclay et al. 1997) indicating possible marine influence, but with limited additional evidence for a marine incursions in the MMG depositional basins. The existence of halites in the MMG has always been contentious, with purely marine, sabkha and wind-blown origins considered (Hounslow & Ruffell 2006). Fauna from the Arden Sandstone Formation in the Worcester Graben includes possible marine bivalves *Nucula*?, *Thracia*? and *Pholadomya*? and shark teeth (Old *et al.* 1991), indicating possible marine connection. However, the frequent occurrence of colonial freshwater algae (*P. moesellanum*) in the Lincombe Member (South Devon) and in Somerset suggests freshwater conditions during the deposition of this lithological unit. The acritarchs are simple acanthomorph acritarchs (*Michrystridium*) with no significant stratigraphical value and could easily be reworked Palaeozoic forms. The acritarchs could be reworked and transported to the lakes during periodic flash floods. The source of the reworked palynomorphs ist likely Carboniferous or Devonian sediments 50-80 km to the west and north-west (Porter & Gallois, 2008). In

addition as Hounslow & Ruffell (2006) conclude, the marine microplankton may also have arrived in far-travelled aeolian dust, in part sourced from marine aerosols, as occurs in modern desert settings (Glennie & Evans 1976).

Conclusions

The Carnian Pluvial Episode during late Julian to early Tuvalian in the western Tethys is considered to be the one of the most pronounced climate change during the Triassic associated with higher precipitation rates and carbon cycle perturbation. The shift to relatively more humid conditions is manifested in the expansion of hygrophyte vegetation in many locations worldwide (Roghi et al. 2010). The palynological assemblages from four localities in the Wessex Basin, SW UK have been shown to track vegetation changes and palaeoclimate trends during the Carnian from a fluvio-lacustrine environment and in addition provide a palynostratigraphical framework for correlation.

The Dunscombe Mudstone Formation in South Devon and the Lipe Hill succession from Somerset contain a Julian (early Carnian) palynoflora, while the assemblage from the overlying Branscombe Mudstone Formation is likely Tuvalian (late Carnian) based on the co-occurrence of *Brodispora striata* and *Partitisporites quadruplices*. The presence of *Ricciisporites tuberculatus* also indicates a Tuvalian age for the Sutton Mallett section in Somerset. Based on the palynological assemblages and the chemostratigraphy, the stratigraphical range of the Dunscombe Mudstone Formation can be extended down into the Julian in contrast to previous Tuvalian age assignments of the Arden Sandstone Fm (Clarke 1965; Warrington 1970; Warrington et al. 1980; Barclay et al. 1997). A humidity signal associated with the CPE is not seen in the Wessex Basin successions where quantitative palynology suggests the dominance of xerophyte floral elements through the Dunscombe Mudstone Formation with only a few horizons of increased hygrophyte flora. The British

successions appear to lack an acme of *Aulisporites astigmosus* which has been linked to the shift to wetter climate as seen in the western Tethys or in the Germanic Basin. Firstly, the prevailing dry climatic conditions in the inner part of Pangea and the strong seasonality in precipitation might explain the lack of suitable permanent habitat for the hygrophyte vegetation. Secondly, the lack of a clear humid signal is likely caused by overrepresentation of the regional pollen rain in the lacustrine units leading to the predominance of xerophyte hinterland floral elements. The bias towards regional pollen rain is further enhanced by the higher pollen production rate of hinterland elements- mainly the conifers. In addition, the potential increase in continental runoff related to more humid conditions might have further increased the proportion of the regional hinterland floral elements in the palynological assemblages. Changes in the regional flora might provide a tool for recording climate change. A slight shift to wetter climate is inferred from increased *Alisporites* abundance in the hinterland flora that coincides with increase of fresh water algae suggesting the expansion of local lacustrine environments during a relatively wetter period.

Acknowledgements

WMK and VB acknowledge funding from the Faculty of Mathematics and Natural Sciences at the University of Oslo (Norway). Part of the research was funded by the RCN FRINATEK grant no. 213985 (WMK) and FRINATEK overseas travel grant 244926/BG (CSM/WMK). Mufak Said Naoroz (UiO) is thanked for his help in the processing of the palynological samples from the Wiscombe Park-1 Borehole and Somerset. The samples from the Strangman's Cove section were collected by Wolfram M. Kürschner, Steven Mueller, Ilias Kousis and Mark Hounslow in 2014. Ramues Gallois is gratefully acknowledged for guidance during this fieldwork, and use of his field-logs of the Strangman's Cove section. Samples from the outcrops in Somerset were collected by Wolfram M. Kürschner and Alastair Ruffell

744 in 2015. Sofie Lindström and an anonymous reviewer are thanked for the thorough reviews
745 and constructive comments which helped to improve the manuscript.

746

747

748 **References**

749 Abbink, O.A., Van Konijnenburg-Van Cittert, J.H.A. &Visscher, H. 2004. A sporomorph
750 ecogroup moder for the Northwest European Jurassic–Lower Cretaceous. Concepts and
751 framework. Netherlands Journal of Geosciences, 83, 17–38.

752

753 Arche, A. & López-Gómez, J. 2014. The Carnian Pluvial Event in Western Europe: New data
754 from Iberia and correlation with the Western Neotethys and Eastern North America–NW
755 Africa regions. Earth-Science Reviews, 128, 196–231,
756 https://doi.org/10.1016/j.earscirev.2013.10.012

757

758 Bachmann, G.H., Geluk, M.C., Warrington, G., Becker-Roman, A., Beutler, G., Hagdorn, H.,
759 Hounslow, M.W., Nitsch, E., Röhling, H.-G., Simon, T. & Szulc, A. 2010. Triassic. In:
760 Doornenbal, J.C. & Stevenson, A.G. (eds) Petroleum Geological Atlas of the Southern
761 Permian Basin Area, EAGE Publications, 149-173, Hounten, 1–342.

762

763 Balini M, Lucas S.G., Jenks J.F. & Spielmann, J.A. 2010. Triassic ammonoid biostratigraphy:
764 an overview. In: Lucas, S.G. (ed) The Triassic Timescale. Geological Society London Special
765 Publication, 334, 221–262.

766

767 Balme, B.E. 1995. Fossil in situ spores and pollen grains: an annotated catalogue: Review of
768 Palaeobotany and Palynology, 87, 81–323, https://doi.10.1016/0034-6667(95)93235-X
769
770 Barclay, W.J., Ambrose, K.,Chadwick, R.A.& Pharoah, T.C. 1997. Geology of the country
771 around Worcester. Memoir of the Geological Survey of Great Britain, British Geological
772 Survey, London, 1–157.
773
774 Batten, D.J. 2002. Palynofacies and petroleum potential. In: Jansonius, J. &McGregor D.C.
775 (eds) Palynology: Principles and Applications, American Association of Stratigraphic
776 Palynologists Foundation, 3, 1065–1084.
777
778 Berglund, B.E. 1973. Pollen dispersal and deposition in an area of southeastern Sweden –
779 some preliminary results. In: Birks, H.J.B. & West, R.G. (eds) Quaternary plant ecology,
780 Blackwells, Oxford, 117–129.
781
782 Bialik, O.M., Korngreen, D. & Benjamini, C. 2013. Carnian (Triassic) aridization on the
783 Levant margin: evidence from the M1 member, Mohilla Formation, Makhtesh Ramon, south
784 Israel. Facies, 59, 559–581, https://doi.10.1007/s10347-012-0321-5
785
786 Bonis, N.R. & Kürschner, W.M. 2012. Vegetation history, diversity patterns, and climate
787 change across the Triassic/Jurassic boundary. Paleobiology, 38, 240–264,
788 https://doi.10.1666/09071.1
789

790 Bonis, N.R., Ruhl, M. & Kürschner, W.M. 2010. Milankovitch-scale palynological turnover
791 across the Triassic–Jurassic transition at St. Audrie's Bay, SW UK. Journal of the Geological
792 Society, London, 167, 877–888, https://doi.org/10.1144/0016-76492009-141
793
794 Breda, A., Roghi, G., Furin, S., Meneguolo, R., Ragazzi, E., Fedele, P. & Gianolla, P. 2009.
795 The Carnian Pluvial Event in the Tofane area (Cortina d'Ampezzo, Dolomites, Italy).
796 Geo.Alp, 6, 80–115.
797
798 Cirilli, S. 2010. Upper Triassic–lowermost Jurassic palynology and palynostratigraphy: a
799 review. In: Lucas, S.G. (ed.) The Triassic Timescale, Geological Society, London, Special
800 Publications, 334, 285–314, https://doi.10.1144/SP334.12
801
802 Cirilli, S. & Eshet, Y. 1991. First discovery of Samaropollenites and the Onslow Microflora
803 in the Upper Triassic of Israel, and its phytogeographic implications. Palaeogeography,
804 Palaeoclimatology, Palaeoecology, 85, 207–212, https://doi.org/10.1016/0031-
805 0182(91)90160-S
806
807 Clarke, R.F.A. 1965. Keuper miospores from Worcestershire, England. Palaeontology, 8,
808 294–321.
809
810 Collister, J.W., Rieley, G., Stern, B., Eglinton, G. & Fry, B. 1994. Compound-specific $\delta^{13}C$
811 analyses of leaf lipids from plants with differing carbon dioxide metabolisms. Organic
812 Geochemistry 21, 619–627, https://doi.org/10.1016/0146-6380(94)90008-6
813

814 Cornet, B. 1977. The palynostratigraphy and age of the Newark Supergroup. PhD thesis, The
815 Pennsylvania State University.
816
817 Dal Corso, J., Gianolla, P., Newton, R.J., Franceschi, M., Roghi, G., Caggiati, M., Raucsik,
818 B., Budai, T., Haas, J. & Preto, N. 2015. Carbon isotope records reveal synchronicity between
819 carbon cycle perturbation and the "Carnian Pluvial Event" in the Tethys realm (Late Triassic).
820 Global and Planetary Change, 127, 79–90, https://doi.org/10.1016/j.gloplacha.2015.01.013
821
822 Dal Corso, J., Mietto, P., Newton, R.J., Pancost, R.D., Preto, N., Roghi, G. & Wignall, P.B.
823 2012. Discovery of a major negative δ13C spike in the Carnian (Late Triassic) linked to the
824 eruption of Wrangellia flood basalts. Geology, 40, 79–82, https://doi.org/10.1130/G32473.1
825
826 Demko, T.M., Dubiel, R.F., & Parrish, J.T. 1998. Plant taphonomy in incised valleys:
827 implications for interpreting paleoclimate from fossil plants. Geology, 26, 1119–1122,
828 https://doi.10.1130/0091-7613(1998)026<1119:PTIIVI>2.3.CO;2
829 De Zanche, V., Gianolla, P. & Roghi, G. 2000. Carnian stratigraphy in the Raibl/Cave del
830 Predil area (Julian Alps, Italy). Eclogae Geologicae Helvetiae, 93, 331–347,
831 https://doi.org/10.5169/seals-168826
832
833 Diefendorf, A.F. & Freimuth, E.J. 2017. Extracting the most from terrestrial plant-derived n-
834 alkyl lipids and their carbon isotopes from the sedimentary record: A review. Organic
835 Geochemistry, 103, 1–21, https://doi.org/10.1016/j.orggeochem.2016.10.016
836
837 Dunay, R.E. & Fisher, M.J. 1978. The Karnian palynofloral succession in the Northern
838 Calcareous Alps, Lunz-am-See, Austria. Pollen et Spores, 20, 177–187.

839 Earp, J. R. & Taylor, B. J. 1986. Geology of the country around Chester and Winsford.
840 Memoir of British Geological Survey, sheet 109, HMSO, London.
841
842 Fijałkowska-Mader, A. 2015. A record of climatic changes in the Triassic palynological
843 spectra from Poland. Geological Quarterly, 59, 615–653,
844 https://doi.http://dx.doi.org/10.7306/gq.1239
845
846 Fijałkowska-Mader, A., Heunisch, C. & Szulc, J. 2015. Keuper palynostratigraphy and
847 palynofacies of the Upper Silesia (Southern Poland). Annales Societatis Geologorum
848 Poloniae, 85, 637–661, http://dx.doi.org/10.14241/asgp.2015.025
849
850 Fisher, M.J. 1972. The Triassic palynofloral succession in England. Geoscience and Man, 4,
851 101–109, http://dx.doi.org/10.1080/00721395.1972.9989724
852
853 Fisher, M.J. 1985. Palynology of sedimentary cycles in the Mercia Mudstone and Penarth
854 Groups (Triassic) of southwest and central England. Pollen et Spores, 28, 95–112.
855
856 Franz, M., Nowak, K., Berner, U., Heunisch, c., Bandel, K., Röhling, H-G. & Wolfgamm, M.
857 2014. Eustatic control on epicontinental basins: The example of the Stuttgart Formation in the
858 Central European Basin (Middle Keuper, Late Triassic). Global and Planetary Change, 122,
859 305–329, http://dx.doi.org/10.1016/j.gloplacha.2014.07.010
860
861 Furin, S., Preto, N., Rigo, M., Roghi, G., Gianolla, P., Crowley, J.L. & Bowring, S.A. 2006.
862 High-precision U-Pb zircon age from the Triassic of Italy: Implications for the Triassic time

scale and the Carnian origin of calcareous nannoplankton and dinosaurs. Geology, 34, 1009–1012, https://doi.org/10.1130/G22967A.1

Fægri, K. & van der Pijl, L. 1966. The principles of pollination ecology. Pergamon Press, London.

Gallois, R.W. 2001. The lithostratigraphy of the Mercia Mudstone Group (mid to late Triassic) of the south Devon coast. Geoscience in South-West England, 10, 195–204.

Gallois, R.W. 2003. The distribution of halite (rock-salt) in the Mercia Mudstone Group (mid to late Triassic) in south-west England. Geoscience in south-west England, 10, 383-389.

Gallois, R.W. 2007. The stratigraphy of the Mercia Mudstone Groups succession (Mid-to Late Triassic) proved in the Wiscombe Park boreholes, Devon. Geoscience in south-west England, 11, 280–286.

Gallois, R. W. & Porter, R.J. 2006. The stratigraphy and sedimentology of the Dunscombe Mudstone Formation (late Triassic) of south-west England. Geoscience in south-west England 11, 174–182.

Golonka, J. 2007. Late Triassic and Early Jurassic palaeogeography of the world. Palaeogeography, Palaeoclimatology, Palaeoecology, 244, 297–307, https://doi.org/10.1016/j.palaeo.2006.06.041

887 Greene, A.R., Scoates, J.S., Weis, D., Katvala, E.C., Israel, S. & Nixon, G.T. 2010. The
888 architecture of oceanic plateaus revealed by the volcanic stratigraphy of the accreted
889 Wrangellia oceanic plateau. Geosphere, 6, 47–73, https://doi.10.1130/GES00212.1
890
891 Grimm, E.C. 1987. CONISS: a FORTRAN 77 program for stratigraphically constrained
892 cluster analysis by the method of incremental sum of squares. Computers & Geosciences, 13,
893 13–35.
894
895 Grimm, E.C. 1991–2001. Tilia, TiliaGraph and TGView Software. Illinois State Museum,
896 Springfield, Illinois, USA.
897
898 Glennie, K. W. & Evans, G. 1976. A reconnaissance of the recent sediments of the Ranns of
899 Kutch, India. Sedimentology, 23, 625-647.
900
901 Götz, A.E., Ruckwied, K. & Barbacka, M. 2011. Palaeoenvironment of the Late Triassic
902 (Rhaetian) and Early Jurassic (Hettangian) Mecsek Coal Formation (south Hungary):
903 implications from macro- and microfloral assemblages. Palaeobiodiversity and
904 Palaeoenvironments, 91, 75–88, https://doi:10.1007/s12549-010-0048-7
905 Götz, A.E., Ruckwied, K., Pálfy, J. & Haas, J. 2009. Palynological evidence of synchronous
906 changes within the terrestrial and marine realm at the Triassic/Jurassic boundary (Csővár
907 section, Hungary). Review of Palaeobotany and Palynology, 156, 401–409,
908 https://doi.org/10.1016/j.revpalbo.2009.04.002
909

910 Heunisch, C. 1999. Die Bedeutung der Palynologie für Biostratigraphie und Fazies in der
911 Germanischen Trias. In: Hauschke, N. & Wilde, V. (eds) Trias - Eine ganze andere Welt
912 Mitteleuropa im frühen Erdmittelalter, Dr. Friedrich Pfeil, Munich, 207–262
913
914 Hicks, S. & Hyvärinen, H. 1999. Pollen influx values measured in different sedimentary
915 environments and their palaeoecological implications. Grana, 38, 228–242,
916 https://doi.10.1080/001731300750044618
917
918 Hochuli, P.A. & Frank, S.M. 2000. Palynology (dinoflagellate cysts, spore-pollen) and
919 stratigraphy of the Lower Carnian Raibl Group in the Eastern Swiss Alps. Eclogae
920 Geologicae Helvetiae, 93, 429–443, https://doi.org/10.5169/seals-168832
921
922 Hochuli, P.A. & Vigran, J.O. 2010. Climate variations in the Boreal Triassic — Inferred from
923 palynological records from the Barents Sea. Palaeogeography, Palaeoclimatology,
924 Palaeoecology, 290, 20–42, https://doi.org/10.1016/j.palaeo.2009.08.013
925
926 Hornung, T., Brandner, R., Krystyn, L., Joachimsky, M.M. & Keim, L. 2007a.
927 Multistratigraphic constraints on the NW Tethyan “Carnian Crisis”. In: Lucas, S.G. &
928 Spielmann, J.A. (eds), The Global Triassic, New Mexico Museum of Natural History and
929 Science Bulletin, 41, 59–67,
930
931 Hornung, T., Krystyn, L. & Brandner, R. 2007b. A Tethys-wide mid-Carnian (Upper Triassic)
932 carbonate productivity decline: evidence for the Alpine Reingraben Event from Spiti (Indian
933 Himalaya). Journal of Asian Earth Sciences, 30, 285–230,
934 https://dx.doi.org/10.1016/j.jseaes.2006.10.001

935

936 Hounslow, M.W. McIntosh, G., Gallois, R.W. & Jenkins, G. 2002. Anisian, Ladinian and
937 Carnian non-marine magnetostratigraphic reference section: the coastal exposures between
938 Budleigh Salterton and Branscombe, South Devon, U.K (abstract). Geoscience in south-west
939 England, 10, 453.

940

941 Hounslow, M.W., McKie, T., & Ruffell, A.H. 2012. Permian to late Triassic post orogenic
942 collapse and rifting, arid deserts, evaporating seas and mass extinctions. In: Woodcock, N.H.
943 & Strachan, R.A. The Geological History of Britain and Ireland, Second revised edition, John
944 Wiley & Sons, Ltd, Chichester, 301–321, https://doi.10.1002/9781118274064.ch16

945

946 Hounslow, M.W. & Ruffell, A. 2006. Triassic-Seasonal Rivers, Dusty Deserts and Salty
947 Lakes. In: Brenchly, P.J. & Rawson, P. F. (eds) Geology of England and Wales, Geological
948 Society of London Publication, 295–324.

949

950 Howard, A.S., Warrington, G., Ambrose, K & Rees, J.G. 2008. A formational framework for
951 the Mercia Mudstone Group (Triassic) of England and Wales. British Geological Survey,
952 Keyworth, Nottingham, Research Report RR/08/04.

953

954 Jacobson, G.L. & Bradshaw, R.H.W. 1981. The selection of sites for palaeovegetational
955 studies. Quaternary Research, 16, 80–96.

956

957 Jeans, C.V. 1978. The origin of the Triassic clay assemblages of Europe with special
958 reference to the Keuper Marl and Rhaetic of parts of England. Philosophical Transactions of
959 the Royal Society of London Series A, 289, 549–639.

960

961 Keim, L., Spötl, C. & Brandner, R. 2006. The aftermath of the Carnian carbonate platform
962 demise: a basinal perspective (Dolomites, Southern Alps). Sedimentology, 53, 361–386,
963 https://doi.10.1111/j.1365-3091.2006.00768.x

964

965 Klaus, W. 1960. Sporen der karnischen Stufe der ostalpinen Trias. Jahrbuch der Geologischen
966 Bundesanstalt Sonderbände, 5, 107–184.

967

968 Kohn, M.J. 2010. Carbon isotope compositions of terrestrial C3 plants as indicators of
969 (paleo)ecology and (paleo)climate. PNAS, 107, 19691–19695,
970 https://doi.org/10.1073/pnas.1004933107

971

972 Korte, C., Kozur, H. & Veizer, J. 2005. $\delta^{13}C$ and $\delta^{18}O$ values of Triassic brachiopods and
973 carbonate rocks as proxies for coeval seawater and palaeotemperature. Palaeogeography,
974 Palaeoclimatology, Palaeoecology, 226, 287–306,
975 https://doi.org/10.1016/j.palaeo.2005.05.018

976

977 Kousis, I. 2015. *Palynology and sedimentology of the Dunscombe Formation, Mercia*
978 *Mudstone Group, South Devon, Southwest England*. MSc thesis, University of Oslo

979

980 Kozur, H. W. & G. H. Bachmann 2010. The Middle Carnian Wet Intermezzo of the Stuttgart
981 Formation (Schilfsandstein), Germanic Basin. Palaeogeography, Palaeoclimatology,
982 Palaeoecology, 290, 107–119, https://doi.org/10.1016/j.palaeo.2009.11.004

983

Kozur, H.W. & Weems, R.E. 2010. The biostratigraphic importance of conchostracans in the continental Triassic of the northern hemisphere. In: Lucas, S. (ed). Triassic Timescale. Geological Society, London, Special Publications, 334, 315–417, https://doi.org/10.1144/SP334.13

Kräusel, R. & Schaarschmidt, F. 1966. Die Keuperflora von Neuewelt bei Basel. IV. Pterophyllen und Taeniopteriden. Schweizerische Paläontologische Abhandlungen, 84, 1–64.

Kuerschner, W.M., Bonis, N.R., Krystyn, L. 2007. Carbon-isotope stratigraphy and palynostratigraphy of the Triassic–Jurassic transition in the Tiefengraben section — Northern Calcareous Alps (Austria). Palaeogeography, Palaeoclimatology, Palaeoecology, 244, 257–280, https://doi.org/10.1016/j.palaeo.2006.06.031

Kustatscher, E., Heunisch, C & Van Konijnenburg-Van Cittert, J.H.A. 2012. Taphonomical implications of the Ladinian megaflora and palynoflora of Thale (Germany). Palaios, 27, 753–764, https://doi.10.2110/palo.2011.p11-090r

Kutzbach, J.E. & Gallimore, R.G. 1989. Pangaean climates: Megamonsoons of the megacontinent. Journal of Geophysical Research, 94, 3341–3357, https://doi.10.1029/JD094iD03p03341

Kürschner, W.M. & Herngreen, G.F.W. 2010. Triassic palynology of central and northwestern Europe: a review of palynofloral diversity patterns and biostratigraphic subdivisions. Geological Society of London Special Publication, 334, 263–283, https://doi:10.1144/SP334.11

1009 Lindström, S., Erlström, M., Piasecki, S., Nielsen, L.H. & Mathiesen, A. 2017. Palynology
1010 and terrestrial ecosystem change of the Middle Triassic to lowermost Jurassic succession of
1011 the eastern Danish Basin. Review of Palaeobotany and Palynology, 244, 65–95,
1012 http://dx.doi.org/10.1016/j.revpalbo.2017.04.007
1013
1014 Lindström, S., Irmis, R.B., Whiteside, J.H., Smith, N.S., Nesbitt, S.J. & Turner, A.H. 2016.
1015 Palynology of the upper Chinle Formation in northern New Mexico, U.S.A.: implications for
1016 biostratigraphy and terrestrial ecosystem change during the Late Triassic (Norian–Rhaetian):
1017 Review of Palaeobotany and Palynology, 225, 106–131,
1018 https://doi.10.1016/j.revpalbo.2015.11.006
1019
1020 Litwin, R.J., Traverse, A. & Ash, S.R. 1991. Preliminary palynological zonation of the Chinle
1021 Formation, southwestern U.S.A., and its correlation to the Newark Supergroup. Review of
1022 Palaeobotany and Palynology, 68, 269–287, https://doi.10.1016/0034-6667(91)90028-2
1023
1024 López-Gómez, J., Escudero-Mozo, M.J., Martín-Chivelet, J., Arche, A., Lago, M. & Galé, C.
1025 2017. Western Tethys continental-marine responses to the Carnian Humid Episode:
1026 Palaeoclimatic and palaeogeographic implications. Global and Planetary Change, 148, 79–95,
1027 https://doi.org/10.1016/j.gloplacha.2016.11.016
1028
1029 Lucas, S.G. 2018. Late Triassic ammonoids: distribution, biostratigraphy and biotic events.
1030 In: Tanner, L.H. (ed.) The Late Triassic World, Topics in Geobiology 46, Springer, 237–261.
1031
1032 Lukeneder, S., Lukeneder, A., Harzhauser, M., İslamoğlu, Y., Krystyn, L. & Lein, R. 2012. A
1033 delayed carbonate factory breakdown during the Tethyan-wide Carnian Pluvial Episode along

1034 the Cimmerian terranes (Taurus, Turkey). Facies, 58, 279–296, https://doi.10.1007/s10347-
1035 011-0279-8
1036
1037 McKie, T. & Williams, B. 2009. Triassic palaeogeography and fluvial dispersal across the
1038 northwest European Basins. Geological Journal, 44, 711–741, https://doi.org/10.1002/gj.1201
1039
1040 Mehdi, D., Cirilli, S., Buratti, N., Kamoun, F. & Trigui, A. 2009. Palynological
1041 characterisation of the Lower Carnian of the KEA5 borehole (Koudiat El Halfa Dome;
1042 Central Atlas, Tunisia). Geobios, 42, 63–71, https://doi.10.1016/j.geobios.2008.06.002
1043
1044 Mietto, P., Manfrin, S., Preto, N. & Gianolla, P. 2008. Selected ammonoid fauna from Prati di
1045 Stuores/Stuores Wiesen and related sections across the Ladinian-Carnian boundary (Sputhern
1046 Alps, Italy). Rivista Italiana di Paleontolgia e Stratigrafia, 114, 377–429.
1047
1048 Mietto, P., Mafrin, S., Preto, N., Rigo, M., Roghi, G., Furin, S., Gianolla, P., Posenati, R.,
1049 Muttoni, G., Nicora, A., Buratti, N., Cirilli, S., Spötl, C., Ramezani, J. & Bowring, S.A. 2012.
1050 The Global Boundary Stratotype Section and Point (GSSP) of the Carnian Stage (Late
1051 Triassic) at Prati Di Stuores/Stuores Wiesen Section (Southern Alps, NE Italy). Episodes, 35,
1052 414–430.
1053
1054 Miller, C.S., Peterse, F., da Silva, A-C., Baranyi, V., Reichart, G.J. & Kürschner, W.M. 2017.
1055 Astronomical age constraints and extinction mechanisms of the Late Triassic Carnian crisis.
1056 Scientific Reports, 7:2557, https://doi.10.1038/s41598-017-02817-7
1057

1058 Moix, P., Beccaletto, L., Kozur, H.W., Hochard, C., Rosselet, F. & Stampfli, G.M. 2008. A
1059 new classification of the Turkish terranes and sutures and its implication for the paleotectonic
1060 history of the region. Tectonophysics, 451, 7–39, https://doi.org/10.1016/j.tecto.2007.11.044
1061
1062 Moix, P., Vachard, D., Allibon, J., Martini, R., Wernli, R., Kozur, H. & Stampfli, G. 2013.
1063 Palaeotethyan, Neotethyan and Huglu-Pindos series in the Lycian Nappes (SW Turkey):
1064 geodynamical implications. In: Tanner, L.H., Spielmann, J.A. & Lucas, S.G. (eds) The
1065 Triassic System. New Mexico Museum of Natural History and Science, 401–444.
1066
1067 Mueller, S., Hounslow, M.W. & Kürschner, W.M. 2016a. Integrated stratigraphy and
1068 palaeoclimate history of the Carnian Pluvial Event in the Boreal realm; new data from the
1069 Upper Triassic Kapp Toscana Group in central Spitsbergen (Norway). Journal of the
1070 Geological Society, 173, 186–202, https://doi.10.1144/jgs2015-028
1071
1072 Mueller, S., Krystyn, L. & Kürschner, W.M. 2016b. Climate variability during the Carnian
1073 Pluvial Phase — A quantitative palynological study of the Carnian sedimentary succession at
1074 Lunz am See, Northern Calcareous Alps, Austria. Palaeogeography, Palaeoclimatology,
1075 Palaeoecology, 441, 198–211, http://dx.doi.org/10.1016/j.palaeo.2015.06.008
1076
1077 Muttoni, G., Mazza, M., Mosher, D., Katz, M.E., Kent, D.V. & Balini, M. 2014. A Middle–
1078 Late Triassic (Ladinian–Rhaetian) carbon and oxygen isotope record from the Tethyan Ocean.
1079 Palaeogeography, Palaeoclimatology, Palaeoecology, 399, 246–259,
1080 https://doi.org/10.1016/j.palaeo.2014.01.018
1081

1082 Nakada, R., Ogawa, K., Suzuki, N., Takahashi, S. & Takahashi, Y. 2014. Late Triassic
1083 compositional changes of aeolian dusts in the pelagic Panthalassa: response to the continental
1084 climatic change. Palaeogeography, Palaeoclimatology, Palaeoecology, 393, 61–75,
1085 https://doi.org/10.1016/j.palaeo.2013.10.014
1086
1087 Oboh-Ikuenobe, F.E. & De Villiers, S.E. 2003. Dispersed organic matter in samples from the
1088 western continental shelf of Southern Africa: palynofacies assemblages and depositional
1089 environments of Late Cretaceous and younger sediments. Palaeogeography,
1090 Palaeoclimatology, Palaeoecology, 201, 67–88, https://doi.org/10.1016/S0031-
1091 0182(03)00510-8
1092
1093 Ogg, J.G. 2015. The mysterious Mid-Carnian "Wet Intermezzo" global event. Journal of
1094 Earth Science, 26, 181–191, https://doi.10.1007/s12583-015-0527-x
1095
1096 Old, R. A. Hamblin, R. J. O., Ambrose, K. & Warrington, G. 1991. Geology of the country
1097 around Redditch. Memoir of the British Geological Survey, sheet 183 (England and Wales),
1098 HMSO, London.
1099
1100 Olivera, D.E., Zavattieri, A.M. & Quatrocchio, M.E. 2015. The palynology of the Cañadón
1101 Asfalto Formation (Jurassic), Cerro Cóndor depocentre, Cañadón Asfalto Basin, Patagonia,
1102 Argentina: palaeoecology and palaeoclimate based on ecogroup analysis. Palynology, 39,
1103 362–386, http://dx.doi.org/10.1080/01916122.2014.988382
1104
1105 Orłowska-Zwolińska, T. 1983. Palynostratigraphy of the upper part of Triassic epicontinental
1106 sediments in Poland. Prace Instytutu Geologicznego, 54, 1–89.

Orłowska-Zwolińska, T. 1985. Palynological zones of the Polish epicontinental Triassic. Bulletin Academy of Sciences, Earth Sciences, 33, 107–119.

Pancost, R.D., Freeman, K.H., & Wakeham, S.G. 1999. Controls on the carbon-isotope compositions of compounds in Peru surface waters. Organic Geochemistry, 30, 319–340, https://doi.org/10.1016/S0146-6380(99)00004-2

Parrish, J.T. 1993. Climate of the supercontinent Pangea. The Journal of Geology, 101, 215–233.

Paterson, N.W., Mangerud, G. & Mørk, A. 2016. Late Triassic (early Carnian) palynology of shallow stratigraphical core 7830/5-U-1, offshore Kong Karls Land, Norwegian Arctic. Palynology, 41, 230–254, http://dx.doi.org/10.1080/01916122.2016.1163295

Planderová, E. 1972. A contribution to palynological research of Lunz Beds in West-Carpathian region. Geologické práce, Správy, 58, 57–77.

Planderová, E. 1980. Palynomorphs from Lunz Beds and from black clayey shales in basement of Vienna Basin (borehole LNV-7). Geologica Carpathica, 31, 267–294.

Porter, R.J. & Gallois, R.W. 2008. Identifying fluvio–lacustrine intervals in thick playa-lake successions: An integrated sedimentology and ichnology of arenaceous members in the mid–late Triassic Mercia Mudstone Group of south-west England, UK. Palaeogeography,

1131 Palaeoclimatology, Palaeoecology, 270, 381–398,
1132 https://doi.org/10.1016/j.palaeo.2008.07.020
1133
1134 Pott, C., Krings, M. & Kerp, H. 2008. The Carnian (Late Triassic) flora from Lunz in Lower
1135 Austria: paleoecological considerations. Palaeoworld, 17, 172–182,
1136 https://doi.org/10.1016/j.palwor.2008.03.001
1137
1138 Preto, N., Kustatscher, E. & Wignall, P.B. 2010. Triassic climates — State of the art and
1139 perspectives. Palaeogeography, Palaeoclimatology, Palaeoecology, 290, 1–10,
1140 https://doi.org/10.1016/j.palaeo.2010.03.015
1141
1142
1143 Reitz, E. 1985. Palynologie der Trias in Nordhessen und Südniedersachsen. Geologische
1144 Abhandlungen Hessen, 86, 1–36.
1145
1146 Rigo, M., Preto, N., Roghi, G., Tateo, F. & Mietto, P. 2007. A rise in the Carbonate
1147 Compensation Depth of western Tethys in the Carnian: deep-water evidence for the Carnian
1148 Pluvial Event. Palaeogeography, Palaeoclimatology, Palaeoecology, 246, 188–205,
1149 https://doi.org/10.1016/j.palaeo.2006.09.013
1150
1151 Roghi, G. 2004. Palynological investigations in the Carnian of the Cave del Prdil area
1152 (Julian Alps, NE Italy). Review of Palaeobotany and Palynology, 132, 1–35,
1153 https://doi.org/10.1016/j.revpalbo.2004.03.001
1154

1155 Roghi, G., Gianolla, P., Minarelli, L., Pilati, C. & Preto, N. 2010. Palynological correlation of
1156 Carnian humid pulses throughout western Tethys. Palaeogeography, Palaeoclimatology,
1157 Palaeoecology, 290, 89–106, https://doi.org/10.1016/j.palaeo.2009.11.006
1158
1159 Rostási, Á., Raucsik, B. & Varga, A. 2011. Palaeoenvironmental controls on the
1160 claymineralogy of Carnian sections from the Transdanubian Range (Hungary).
1161 Palaeogeography, Palaeoclimatology, Palaeoecology, 300, 101–112,
1162 https://doi.org/10.1016/j.palaeo.2010.12.013
1163
1164 Ruckwied, K., Götz, A.E., Pálfy, J. & Török, Á. 2008. Palynology of a terrestrial coal-bearing
1165 series across the Triassic/Jurassic boundary (Mecsek Mts, Hungary). Central European
1166 Geology, 51, 1–15, https://doi.10.1556/CEuGeol.51.2008.1.1
1167
1168 Ruffell, A. & Shelton, R.G. 1999. The control of sedimentary facies by climate during phases
1169 of crustal extension: examples from the Triassic of onshore and offshore England and
1170 Northern Ireland. Journal of the Geological Society, London, 156, 779–789,
1171 https://doi.org/10.1144/gsjgs.156.4.0779
1172
1173 Ruffell, A., Simms, M.J. & Wignall, P.B. 2016. The Carnian Humid Episode of the late
1174 Triassic: a review. Geological Magazine, 153, 271–284,
1175 https://doi.10.1017/S0016756815000424
1176
1177 Ruffell, A. & Warrington, G. 1988. An arenaceous member in the Mercia Mudstone Group
1178 (Triassic) west of Taunton, Somerset. Proceedings of the Ussher Society, 7, 102–103.
1179

1180 Ruhl, M., Kürschner, W.M., Krystyn, L. & 2009. Triassic–Jurassic organic carbon isotope
1181 stratigraphy of key sections in the western Tethys realm (Austria). Earth and Planetary
1182 Science Letters, 281, 169–187, http://dx.doi.org/10.1016/j.epsl.2009.02.020.
1183
1184 Scheuring, B.W. 1970. Palynologische und palynostratigraphische Untersuchungen des
1185 Keupers im Bölchentunnel (Solothurner Jura). Schweizerische Paläontologische
1186 Abhandlungen, 88, 1–119.
1187
1188 Scheuring, B.W. 1978. Mirofloren aus den Meridenkalken des Mte. San Giorgio (Kanton
1189 Tessin). Schweizerische Paläontologische Abhandlungen, 100, 1–205.
1190
1191 Schlager, W. & Schöllnberger, W. 1974. Das Prinzip stratigraphischer Wenden in der
1192 Schichtenfolge der Nordlichen Kalkalpen. Mitteilungen der Geologischen Gesellschaft Wien,
1193 66/67, 165–93.
1194
1195 Schulz, E. 1967. Sporenpaläontologische Untersuchungen rätoliassischer Schichten im
1196 Zentralteil des Germanischen Beckens. Paläontologische Abhandlungen Series B,
1197 Paläobotanik, 2, 541–633.
1198
1199 Sellwood, B.W. & Valdes, P.J. 2006. Mesozoic climates: General circulation models and the
1200 rock record. Sedimentary Geology, 190, 269–287,
1201 https://doi.org/10.1016/j.sedgeo.2006.05.013
1202
1203 Shukla, U.H., Bachmann, G.H. & Singh, I.B. 2010. Facies architecture of the Stuttgart
1204 Formation (Schilfsandstein, Upper Triassic), central Germany, and its comparison with

1205 modern Ganga system, India. Palaeogeography Palaeoclimatology Palaeoecology, 297, 110–
1206 128, https://doi.10.1016/j.palaeo.2010.07.019
1207
1208 Simms, M.J. & Ruffell, A.H. 1989. Synchroneity of climatic change and extinctions in the
1209 Late Triassic. Geology, 17, 265–268, https://doi.10.1130/0091-
1210 7613(1989)017<0265:SOCCAE>2.3.CO;2
1211
1212 Simms, M.J. & Ruffell, A.H. 1990. Climatic and biotic change in the Late Triassic. Journal of
1213 the Geological Society, London, 147, 321–327, https://doi.org/10.1144/gsjgs.147.2.0321
1214
1215 Sun, Y.D., Wignall, P.B., Joachimski, M.M., Bond, D.P.G., Grasby, S.E., Lai, X.L., Wang,
1216 L.N., Zhang, Z.T. & Sun, S. 2016. Climate warming, euxinia and carbon isotope perturbations
1217 during the Carnian (Triassic) Crisis in South China. Earth and Planetary Science Letters, 444,
1218 88–100, https://doi.org/10.1016/j.epsl.2016.03.037
1219
1220 Szulc, J. 2000. Middle Triassic evolution of the northern Peri-Tethys area as influenced by
1221 early opening of the Tethys Ocean. Annales Societatis Geologorum Poloniae, 70, 1–48.
1222
1223 Trotter, J.A., Williams, I.S., Nicora, A., Mazza, M. & Rigo, M. 2015. Long-term cycles of
1224 Triassic climate change: A new δ18O record from conodont apatite. Earth Planetary Science
1225 Letters, 415, 165–174, https://doi.org/10.1016/j.epsl.2015.01.038
1226
1227 Talbot, M.R., Holm, K., & Williams, M.A.J. 1994. Sedimentation in low-gradient desert
1228 margin systems: a comparison of the Late Triassic of northwest Somerset (England) and the

1229 late Quaternary of east-central Australia. Geological Society of America Special Paper, 289,
1230 97-117.
1231
1232 Vakhrameev, V.A. 1991. Jurassic and Cretaceous floras and climates of the Earth. Cambridge
1233 University Press, Cambridge, 1–250.
1234
1235 Van der Eem, J.G.L.A. 1983. Aspects of middle and late triassic palynology. 6. Palynological
1236 investigations in the Ladinian and lower Karnian of the Western Dolomites, Italy. Review of
1237 Palaeobotany and Palynology, 39, 189–300, https://doi.org/10.1016/0034-6667(83)90016-7
1238
1239 Van Konijnenburg-Van Cittert, J.H.A. & Van der Burgh, J. 1989. The flora from the
1240 Kimmeridgian (upper jurassic) of Culgower, Sutherland, Scotland. Review of Palaeobotany
1241 and Palynology, 61, 1–51, https://doi.org/10.1016/0034-6667(89)90060-2
1242
1243 van Veen, P.M. 1985. Stratigraphy of the Triassic in the Troms Area. Technical report,
1244 Oljedirektoratet Norge, 0D-85–36
1245
1246 Vigran, J.O., Mangerud, G., Mørk, A., Worsley, D. & Hochuli, P.A. 2014. Palynology and
1247 geology of the Triassic succession of Svalbard and the Barents Sea. NGU Special Publication,
1248 14, Geological Survey of Norway, https://doi.10.5167/uzh-99116
1249
1250 Visscher, H. & Krystyn, L. 1978. Aspects of late Triassic palynology. 4. A palynological
1251 assemblage from ammonoid-controlled late karnian (Tuvalian) sediments of Sicily. Review of
1252 Palaeobotany and Palynology, 26, 93–112, https://doi.org/10.1016/0034-6667(78)90007-6
1253

1254 Visscher, H., Van Houte, M., Brugman, W.A. & Poort, R.J. 1994. Rejection of a Carnian
1255 (Late Triassic) "pluvial event" in Europe. Review of Palaeobotany and Palynology, 83, 217–
1256 226, https://doi.org/10.1016/0034-6667(94)90070-1
1257
1258 Visscher, H. & Van der Zwan, C.J. 1981. Palynology of the circum-Mediterranean Triassic
1259 phytogeographical and palaeoclimatological implications. Geologische Rundschau, 70, 625–
1260 636.
1261
1262 Vollmer, T. Werner, R., Weber, M., Tougiannidis, N., Röhling, H-G. & Hambach, U. 2008.
1263 Orbital control on Upper Triassic Playa cycles of the Steinmergel-Keuper (Norian): A new
1264 concept for ancient playa cycles. Palaeogeography, Palaeoclimatology, Palaeoecology, 267,
1265 1–16, https://doi.org/10.1016/j.palaeo.2007.12.017
1266
1267 Warrington, G. 1967. The correlation of the Keuper by miospores. Nature, 214, 323–324,
1268 https://doi.10.1038/2141323a0
1269
1270 Warrington, G. 1970. The stratigraphy and palaeontology of the 'Keuper' Series of the central
1271 Midlands of England. Quarterly Journal of the Geological Society, 126, 183–223,
1272 https://doi.org/10.1144/gsjgs.126.1.0183
1273
1274 Warrington, G. 1971. Palynology of the New Red Sandstone sequence of the South Devon
1275 coast. Proceedings of the Ussher Society, 2, 307–315.
1276

1277 Warrington, G. 1974. Studies in the palynological biostratigraphy of the British Trias. I.
1278 Reference sections in west Lancashire and north Somerset. Review of Palaeobotany and
1279 Palynology, 17, 133–147, https://doi.org/10.1016/0034-6667(74)90095-5
1280
1281 Warrington, G. 1984. Late Triassic palynomorph records from Somerset. Proceedings of the
1282 Ussher Society, 6, 29–34.
1283 Warrington, G. 1997. The Lyme Regis Borehole, Dorset- palynology of the Mercia Mudstone,
1284 Penarth and Lias groups (Upper Triassic-Lower Jurassic). Proceedings of the Ussher Society,
1285 9, 153–157.
1286
1287 Warrington, G. 2004. Red rocks of the west - the tip of the iceberg. Open University
1288 Geological Society Journal, Symposium Edition 2004, 25, 28–32
1289
1290 Warrington, G., Audley-Charles, M. G., Elliott, R. E., Evans, W. B., Ivemey-Cook, H. C.,
1291 Kent, P. E., Robinson, P.L., Shotton, F. W., and Taylor, F. M. 1980. A correlation of Triassic
1292 rocks in the British Isles. Geological Society of London, Special Report, 13, 1–78.
1293
1294 Warrington, G. & Ivimey-Cook, H. C. 1992. Triassic, In: Cope, J. C. W., Ingham, J.K. &
1295 Rawson, P.F. (eds), Atlas of palaeogeography and lithofacies. Memoir of the Geological
1296 Society, London, 13, 97-106.
1297
1298 Warrington, G. & Williams, B.J. 1984. The North Curry Sandstone Member (late Triassic)
1299 near Taunton, Somerset. Proceedings of the Ussher Society, 6, 82–84.
1300

1301 Whiteside, J.H., Lindström, S., Irmis, R.B., Glasspool, I.J., Schaller, M.F., Dunlavey, M.,
1302 Nesbitt, S.J., Smith, N.D. & Turner, A.H. 2015. Extreme ecosystem instability suppressed
1303 tropical dinosaur dominance for 30 million years. Proceedings of the National Academy of
1304 Sciences, 112, 7909–7913, https://doi.10.1073/pnas.1505252112
1305
1306 Wilson, A. A. & Evans, W. B. 1990. Geology of the country around Blackpool. Memoir of
1307 the British Geological Survey, sheet 66, HMSO, London.
1308
1309 Wood, G.D., Gabriel, A.M. & Lawson, J.C. 1996. Palynological techniques – processing and
1310 microscopy. In: Jansonius, J., McGregor, D. C. (editors), Palynology: Principles and
1311 Applications. American Association of Stratigraphic Palynologists Foundation 1, 29–50.
1312
1313 Xu, G., Hannah, J.L., Stein, H.J., Mørk, A., Vigran, J.O., Bingen, B., Schutt, D.L. &
1314 Lundschein, B.A. 2014. Cause of Upper Triassic climate crisis revealed by Re–Os
1315 geochemistry of Boreal black shales. Palaeogeography, Palaeoclimatology, Palaeoecology,
1316 395, 222–232, https://doi.org/10.1016/j.palaeo.2013.12.027
1317
1318 Zhang, Y., Li, M., Ogg, J.G., Montgomery, P., Huang, C., Chen, Z-Q., Shi, Z., Enos, P. &
1319 Lehrmann, D.J. 2015. Cycle-calibrated magnetostratigraphy of middle Carnian from South
1320 China: Implications for Late Triassic time scale and termination of the Yangtze Platform.
1321 Palaeogeography, Palaeoclimatology, Palaeoecology, 436, 135–166,
1322
1323 Ziegler, A.M., Parrish, J.M., Jiping, Y., Gyllenhall, D., Rowley, D.B., Parrish, J.T.,
1324 Shangyou, N., Bekker, A. & Hulver, M.L. 1994. Early Mesozoic phytogeography and

climate. Philosophical Transactions of The Royal Society B Biological Sciences, 341, 297–305, https://doi.10.1098/rstb.1993.0115

Figure captions

Fig. 1. (**a**) Map of the UK and Ireland showing the position of the study area, (**b**) palaeogeography during the Late Triassic after Golonka (2007), the asterisk marks the position of the study area, (**c**) Mercia Mudstone lithostratigraphy of south-west England from Howard et al. (2008), names shown in italics are abandoned in the revised nomenclature, (**d, e**) outline geology maps and location of the four studied outcrops and the Wiscombe Park-1 Borehole, modified after Gallois & Porter (2006) and Porter & Gallois, (2008).

Fig. 2. Lithostratigraphy, sample positions and the relative pollen-spore abundances during the Carnian in the Wiscombe Park-1 core and in the Strangman's Cove outcrop section, Devon. Lithological log modified from Gallois (2007) and Gallois & Porter (2006). The stratigraphical subdivision is inferred from palynology and chemostratigraphy. The boundary between substages is indicated by a dashed line due to the uncertainty of the boundary position. Only the most abundant taxa are shown. The grey area of the curves is an exaggeration (3X) of the abundances plotted in black. The unidentified palynomorphs and encountered *Lycopodium* grains are shown as counts. A detailed lithological log with the exact position of the palynological samples is available in the Supplementary Data (Fig. S1).

Fig. 3. Lithostratigraphy, sample positions and the relative pollen-spore abundances during the Carnian in the Lipe Hill and Sutton Mallett sections, Somerset. Lithological log is modified after Ruffell & Warrington (1988). See Fig. 2 for details.

Fig. 4. Selected palynomorphs identified from the Mercia Mudstone Group. Taxon name is followed by lithostratigraphic unit and locality. Sample and slide numbers are in parentheses. Scale bar 10 µm: 1-13, 16-37. Scale bar 20 µm: 13-16. 1 *Brodispora striata*, Branscombe

Mudstone Formation, Strangman`s Cove (WE203/A). 2 *Porcellispora longdonensis*, Branscombe Mudstone Formation, Strangman`s Cove (WE203/A). 3 *Thomsonisporis toralis,* Sidmouth Mudstone Formation, WP-1 (109.11 m/1). 4 *Calamospora tener*, Sidmouth Mudstone Formation, WP-1 (111.98 m/1). 5 *Kyrtomisporis* sp., Sidmouth Mudstone Formation, WP-1 (111.98 m/1), 6 *Aratrisporites* sp., Sidmouth Mudstone Formation, WP-1 (111.98 m/1). 7 *Aratrisporites fimbriatus*, Sidmouth Mudstone Formation, WP-1 (111.98 m/1). 8 *Cycadopites* sp., Sidmouth Mudstone Formation, WP-1 (111.98 m/1). 9 *Lunatisporites acutus*, Dunscombe Mudstone Formation, Lipe Hill (LH 2/2). 10 *Aulisporites astigmosus*, Sidmouth Mudstone Formation, WP-1 (111.98 m/1). 11 cf. *Aulisporites astigmosus*, Sidmouth Mudstone Formation, WP-1 (109.11 m/1). 12 *Brachysaccus neomundanus*, Dunscombe Mudstone Formation, Strangman`s Cove (WE017/A). 13 *Ovalipollis lunzenis*, Branscombe Mudstone Formation, Strangman`s Cove (WE203/A). 14 *Alisporites grauvogeli*, Dunscombe Mudstone Formation, WP-1 (57.86 m/1). 15 *Ovalipollis ovalis*, Dunscombe Mudstone Formation, Strangman`s Cove (WE305/B). 16 *Triadispora aurea*, Sidmouth Mudstone Formation, WP-1 (111.98 m/1). 17 *Triadispora plicata*, Dunscombe Mudstone Formation, Lipe Hill (LH 2/2). 18 *Triadispora verrucata*, Sidmouth Mudstone Formation, WP-1 (111.98 m/1). 19 *Triadispora obscura*, Sidmouth Mudstone Formation, WP-1 (111.98 m/1). 20 *Duplicisporites granulatus*, Dunscombe Mudstone Formation, Strangman`s Cove (WE003/A). 21 *Patinasporites densus*, Branscombe Mudstone Formation, Strangman`s Cove (WE203/A). 22 *Triadispora crassa*, Sidmouth Mudstone Formation, WP-1 (111.98 m/2). 23 *Triadispora modesta*, Sidmouth Mudstone Formation, WP-1 (111.98 m/1). 24 *Partitisporites novimundanus*, Dunscombe Mudstone Formation, Strangman`s Cove (WE003/A). 25 *Praecirculina granifer*, Dunscombe Mudstone Formation, Strangman`s Cove (WE001/A). 26 *Camerosporites secatus*, Dunscombe Mudstone Formation, Sutton Mallett (SM 2/1). 27 *Duplicisporites mancus*, Branscombe Mudstone

Formation, Strangman`s Cove (WE203/A). 28 *Partitisporites scurrilis,* Dunscombe Mudstone Formation, Strangman`s Cove (WE103/A). 29 *Partitisporites tenebrosus?,* Branscombe Mudstone Formation, Strangman`s Cove (WE203/A). 30 *Partitisporites maljawkinae,* Dunscombe Mudstone Formation, Strangman`s Cove (WE302/A). 31 *Partitisporites quadruplices,* Branscombe Mudstone Formation, Strangman`s Cove (WE203/B). 32 *Ricciisporites tuberculatus*, Dunscombe Mudstone Formation, Sutton Mallett (SM 2/1). 33 *Plaesiodictyon mosellanum*, Dunscombe Mudstone Formation, Strangman`s Cove (WE017/A). 34 acritarch indet., Dunscombe Mudstone Formation, Lipe Hill (LH 2/2). 35 acritarch indet same as 34 with different focus, Dunscombe Mudstone Formation, Lipe Hill (LH 2/2). 36 *Micrhystridium* sp., Dunscombe Mudstone Formation, Lipe Hill (LH 5/1). 37 *Botryococcus braunii*, Dunscombe Mudstone Formation, Strangman`s Cove (WE018/A).

Fig. 5. Chrono-, bio- and palynostratigraphical schemes for the Germanic Keuper, Alpine, Boreal and North America during the Carnian-Norian. Tethys ammonoid zones are from Mietto et al. (2008) and Balini et al (2010). I Kürschner & Herngreen (2010); II Heunisch (1999); III Orłowska-Zwolińska (1983, 1985); Fijałkowska-Mader *et al.* (2015); IV Roghi 2004; V Roghi *et al.* (2010), VI Van der Eem (1983); VII Van Veen 1985; VIII Vigran *et al.* 2014; IX Cornet 1977; X Litwin et al. (1991). Volcanic events from Dal Corso et al. (2012) and Moix *et al.* (2008, 2013). The characteristic spore-pollen events refer to the first and last occurrences of selected palynomorphs in the Southern Permian Basin mainly Germany and Poland as summarized in Kürschner & Herngreen (2010).

Fig. 6. Correlation of the Wiscombe Park-1 core and the Strangman's Cove section with $\delta^{13}C_{TOC}$ bulk isotope values, calcareous marker horizons (Gallois & Porter 2006) and the range of the key biostratigraphically important pollen taxa. Horizons with increased

hygrophyte vegetation elements are indicated. Black diamond symbols mark the samples included in the palynological analysis. The boundary between substages is indicated by a dashed line due to the uncertainty of the boundary position. The grey area is the correlation suggested by Gallois & Porter (2006) based on the lithology. Detailed lithological log of the Strangman's Cove section with the palynological sample locations is in the Supplementary Data (Fig. S1). SMF = Sidmouth Mudstone Formation, Jul. = Julian. Tuv. = Tuvalian. BMF = Branscombe Mudstone Formation.

Fig. 7. Conceptual model of the relationship between sampling size (lake diameter) and the relative proportion of pollen grains originating from different habitats around inferred lake deposits of the DMF as applied to Late Triassic palynomorph types. Modified after Jacobson & Bradshaw (1981).

Fig. 8. Stratigraphy, lithostratigraphy and climatic interpretation of selected palynomorph groups in the Strangman's Cove section. The boundary between substages is indicated by a dashed line due to the uncertainty of the boundary position. For the position of the palynological samples see Fig. 3. Detailed log with the position of the palynological samples is available in the Supplementary Data (Fig. S1). The total abundance of spores, *Alisporites* spp., algae and interpreted negative isotope excursions are indicated. BMF= Branscombe Mudstone Fm.

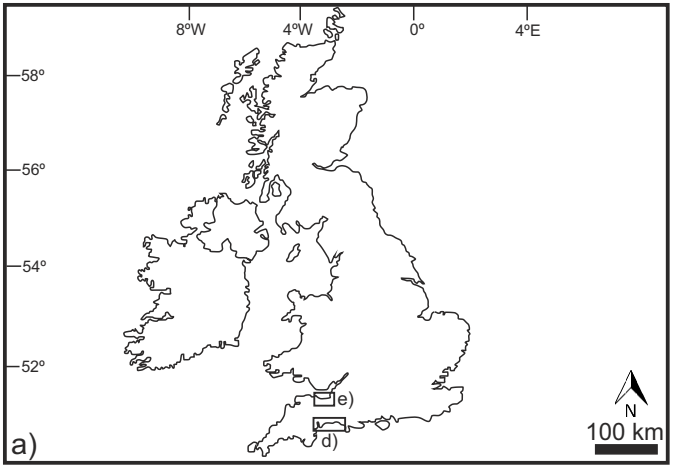
8°W
4°W
0°
4°E
58°
56°
54°
52°
e)
d)
N
100 km
a)

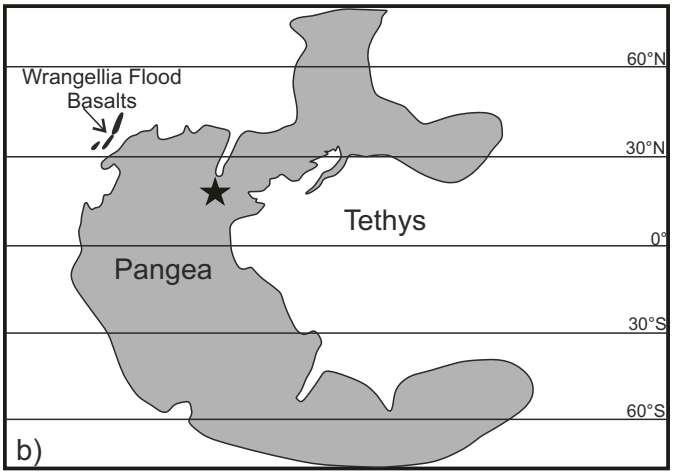
Wrangellia Flood Basalts
Tethys
Pangea
60°N
30°N
0°
30°S
60°S
b)

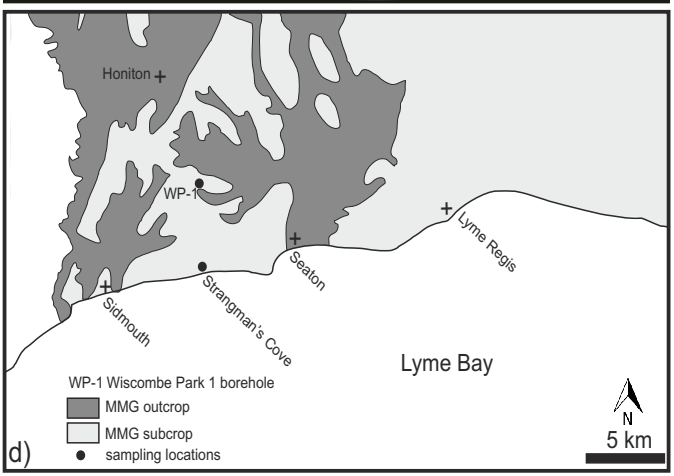
Honiton
WP-1
Seaton
Lyme Regis
Sidmouth
Strangman's Cove
Lyme Bay
WP-1 Wiscombe Park 1 borehole
MMG outcrop
MMG subcrop
sampling locations
N
5 km
d)

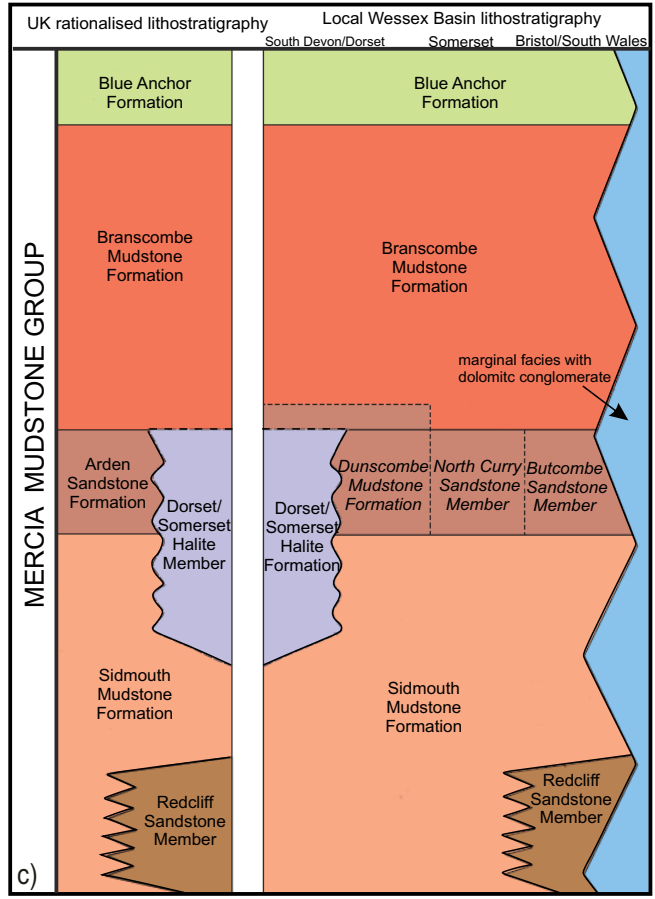
UK rationalised lithostratigraphy
Local Wessex Basin lithostratigraphy
South Devon/Dorset
Somerset
Bristol/South Wales
MERCIA MUDSTONE GROUP
Blue Anchor Formation
Blue Anchor Formation
Branscombe Mudstone Formation
Branscombe Mudstone Formation
marginal facies with dolomitc conglomerate
Arden Sandstone Formation
Dorset/ Somerset Halite Member
Dorset/ Somerset Halite Formation
Dunscombe Mudstone Formation
North Curry Sandstone Member
Butcombe Sandstone Member
Sidmouth Mudstone Formation
Sidmouth Mudstone Formation
Redcliff Sandstone Member
Redcliff Sandstone Member
c)

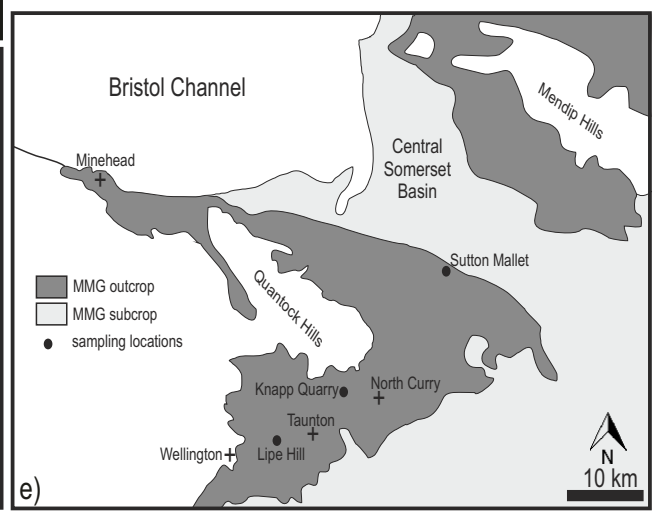
Bristol Channel
Mendip Hills
Central Somerset Basin
Minehead
Sutton Mallet
Quantock Hills
MMG outcrop
MMG subcrop
sampling locations
Knapp Quarry
North Curry
Taunton
Wellington
Lipe Hill
N
10 km
e)

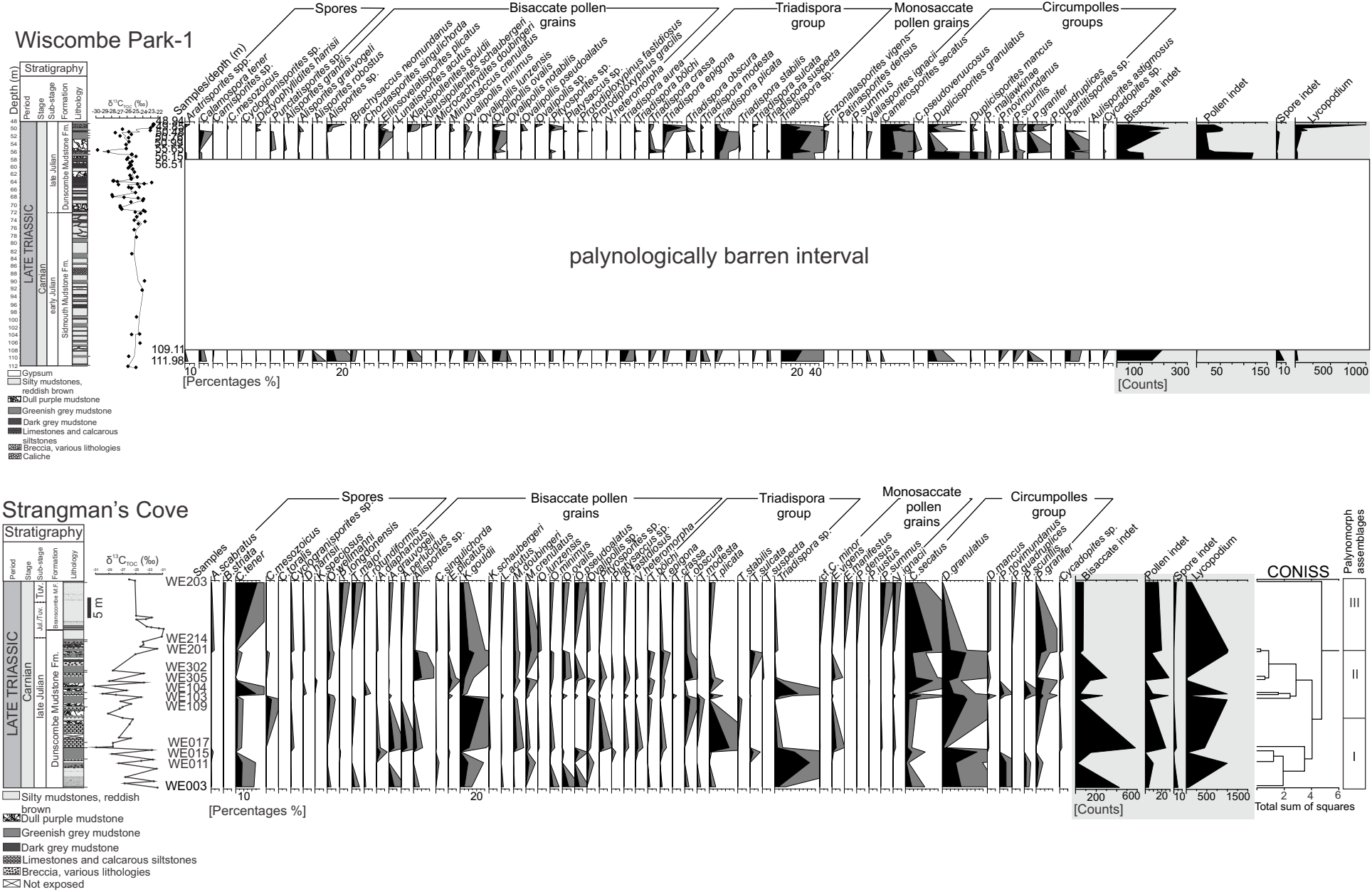
Wiscombe Park-1
Stratigraphy
Depth (m)
Period
Stage
Sub-stage
Formation
Lithology
LATE TRIASSIC
Carnian
late Julian
early Julian
Dunscombe Mudstone Fm.
Sidmouth Mudstone Fm.
δ13CTOC (‰)
Samples/depth (m)
Spores
Bisaccate pollen grains
Triadispora group
Monosaccate pollen grains
Circumpolles groups
A.ratisporites spp.
C.amisporites sp.
C.mesozoicus
C.tener
Cyclogranisporites sp.
Dictyophyllidites harrisii
Punctatisporites sp.
Alisporites grandis
Alisporites gravsvogelii
Alisporites robustus
Alisporites sp.
Brachysaccus neomundanus
Chordasporites singulichorda
Ellipsovelatisporites plicatus
Lunatisporites acutus
Klausipollenites gouldii
Microcachrydites doubingeri
Minutosaccus crenulatus
Ovalipollis minimus
Ovalipollis lunzensis
Ovalipollis ovalis
Ovalipollis pseudoalatus
Ovalipollis notabilis
Pityosporites sp.
Platysaccus sp.
Protodiploxypinus fastidiosus
Protodiploxypinus gracilis
V.heteromorpha
Triadispora aurea
Triadispora bolchi
Triadispora crassa
Triadispora epigona
Triadispora obscura
Triadispora modesta
Triadispora plicata
Triadispora stabilis
Triadispora sulcata
Triadispora suspecta
Triadispora sp.
Enzonalasporites vigens
Patinasporites densus
P.summus
Vallasporites ignacii
Camerosporites secatus
C.pseudoverrucosus
Duplicisporites granulatus
Duplicisporites mancus
P.majawkinae
P.novimundanus
P.scurrilis
P.granifer
P.quadruplices
Partitisporites sp.
Aulisporites astigmosus
Cycadopites sp.
Bisaccate indet
Pollen indet
Spore indet
Lycopodium
palynologically barren interval
56.51
109.11
111.98
[Percentages %]
[Counts]
Gypsum
Silty mudstones, reddish brown
Dull purple mudstone
Greenish grey mudstone
Dark grey mudstone
Limestones and calcarous siltstones
Breccia, various lithologies
Caliche
Strangman's Cove
Stratigraphy
Jul./Tuv.
Tuv.
Brantscombe M.F.
5 m
Samples
A.scabratus
B.striata
C.tener
C.mesozoicus
C.coralis
C.granisporites sp.
D.harrisii
K.specilosus
O.brelmanni
T.major
T.rotundiformis
A.diaphanous
A.gravsvogelii
A.robustus
A.sp.
C.singulichorda
E.plicatus
K.gouldii
K.schaubergeri
L.acutus
M.doubingeri
O.crenulatus
O.lunzensis
O.minimus
O.ovalis
O.pseudoalatus
O.sp.
P.fastidiosus
P.sp.
V.heteromorpha
T.bolchi
T.epigona
T.crassa
T.obscura
T.modesta
T.plicata
T.stabilis
T.sulcata
T.suspecta
Triadispora sp.
cf.C.minor
E.vigens
E.manifestus
P.densus
P.summus
V.ignacii
C.secatus
D.granulatus
D.mancus
P.novimundanus
P.quadruplices
P.scurrilis
P.granifer
Cycadopites sp.
Bisaccate indet
Pollen indet
Spore indet
Lycopodium
WE203
WE214
WE201
WE302
WE305
WE104
WE103
WE109
WE017
WE015
WE011
WE003
[Percentages %]
[Counts]
CONISS
Total sum of squares
Palynomorph assemblages
I
II
III
Silty mudstones, reddish brown
Dull purple mudstone
Greenish grey mudstone
Dark grey mudstone
Limestones and calcarous siltstones
Breccia, various lithologies
Not exposed

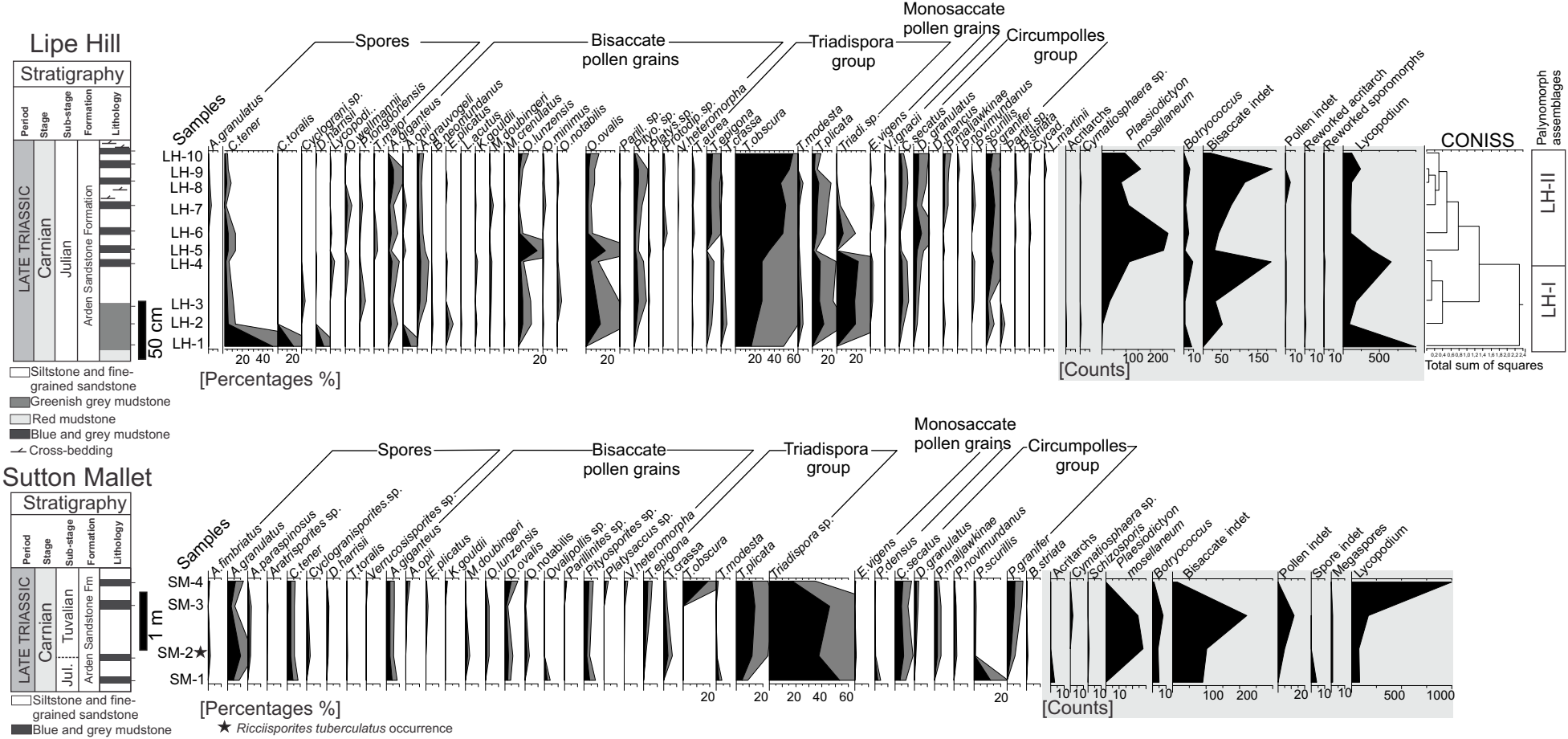
Lipe Hill
Stratigraphy
Period
Stage
Sub-stage
Formation
Lithology
LATE TRIASSIC
Carnian
Julian
Arden Sandstone Formation
50 cm
Siltstone and fine-grained sandstone
Greenish grey mudstone
Red mudstone
Blue and grey mudstone
Cross-bedding
Spores
Bisaccate pollen grains
Triadispora group
Monosaccate pollen grains
Circumpolles group
Samples
A.granulatus
C.tener
C.toralis
Cyclograni.sp.
D.harrisii
Lycopodi..
O.wellmannii
T.longobhensis
T.major
A.gigantеus
A.opii
E.grauvogelі
E.plicatus
K.acutus
K.gouldii
M.doubingeri
O.lunzensis
O.minimus
O.notabilis
O.ovalis
Perill. sp.
Pityo. sp.
Platys. sp.
Protodip. sp.
V.heteromorpha
V.aurea
T.epigona
T.crassa
T.obscura
T.modesta
T.plicata
Triadi.-sp.
E.vigens
V.lonacii
C.secatus
D.granulatus
P.maljawkinae
P.novimundanus
P.scurrillis
P.granifer
Patil. sp.
B.striata
Cycad.
L.martinii
Acritarchs
Cymatiosphaera sp.
Plaesiodictyon mosellaneum
Botryococcus
Bisaccate indet
Pollen indet
Reworked acritarch
Reworked sporomorphs
Lycopodium
LH-10
LH-9
LH-8
LH-7
LH-6
LH-5
LH-4
LH-3
LH-2
LH-1
[Percentages %]
[Counts]
CONISCA
Total sum of squares
Palynomorph assemblages
LH-II
LH-I
Sutton Mallet
Stratigraphy
Period
Stage
Sub-stage
Formation
Lithology
LATE TRIASSIC
Carnian
Tuvalian
Jul.
Arden Sandstone Fm
1 m
Siltstone and fine-grained sandstone
Blue and grey mudstone
Spores
Bisaccate pollen grains
Triadispora group
Monosaccate pollen grains
Circumpolles group
Samples
A.fimbriatus
A.granulatus
A.paraspinosus
Aratrisporites sp.
C.tener
Cyclogranisporites sp.
D.harrisii
T.toralis
Verrucosisporites sp.
A.gigantеus
A.opii
E.plicatus
K.gouldii
M.doubingeri
O.lunzensis
O.ovalis
O.notabilis
Ovalipollis sp.
Parillinites sp.
Pityosporites sp.
Platysaccus sp.
V.heteromorpha
T.epigona
T.crassa
T.obscura
T.modesta
T.plicata
Triadispora sp.
E.vigens
P.densus
C.secatus
D.granulatus
P.maljawkinae
P.novimundanus
P.scurillis
P.granifer
B.striata
Acritarchs
Cymatiosphaera sp.
Schizosporis
Plaesiodictyon mosellaneum
Botryococcus
Bisaccate indet
Pollen indet
Spore indet
Megaspores
Lycopodium
SM-4
SM-3
SM-2★
SM-1
[Percentages %]
[Counts]
★ Ricciisporites tuberculatus occurrence

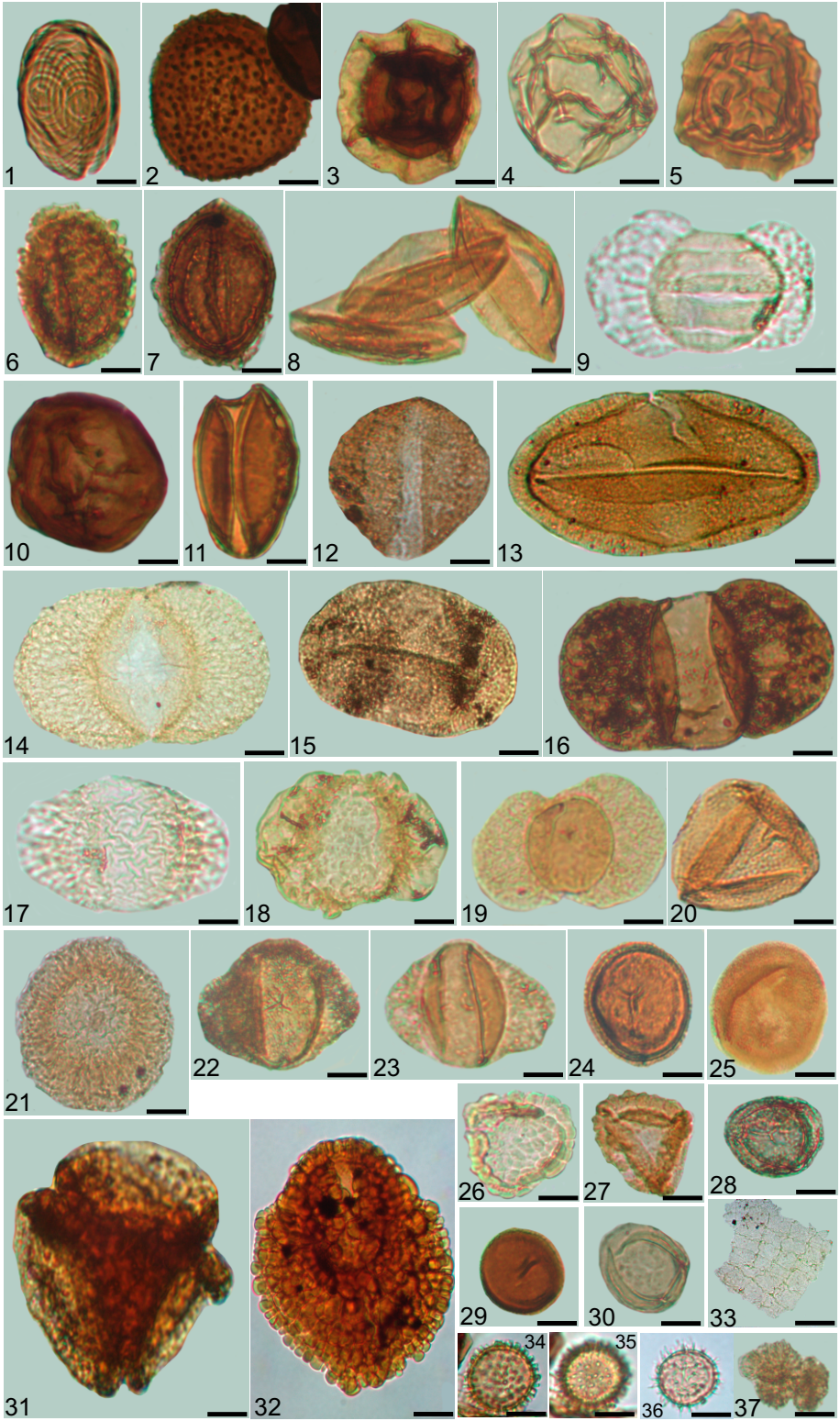
1
2
3
4
5
6
7
8
9
10
11
12
13
14
15
16
17
18
19
20
21
22
23
24
25
26
27
28
29
30
31
32
33
34
35
36
37

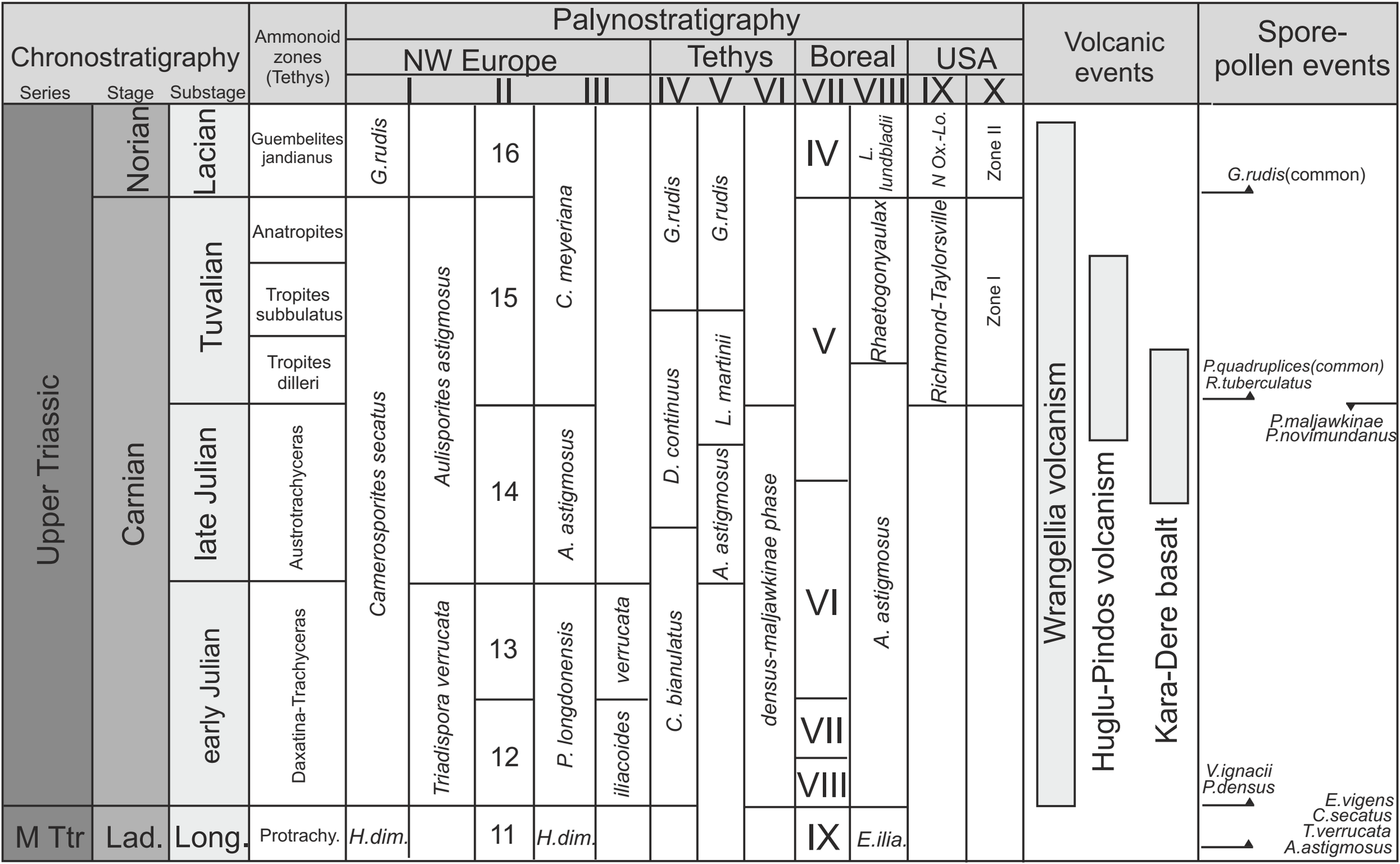
Chronostratigraphy
Series
Stage
Substage
Ammonoid zones (Tethys)
Palynostratigraphy
NW Europe
I
II
III
Tethys
IV
V
VI
Boreal
VII
VIII
USA
IX
X
Volcanic events
Spore-pollen events
Upper Triassic
Norian
Carnian
Lacian
Tuvalian
late Julian
early Julian
Guembelites jandianus
Anatropites
Tropites subbulatus
Tropites dilleri
Austrotrachyceras
Daxatina-Trachyceras
G.rudis
Camerosporites secatus
Aulisporites astigmosus
Triadispora verrucata
16
15
14
13
12
C. meyeriana
A. astigmosus
P. longdonensis
verrucata
iliacoides
G.rudis
D. continuus
C. bianulatus
G.rudis
L. martinii
A. astigmosus
densus-maljawkinae phase
IV
V
VI
VII
VIII
L. lundbladii
Rhaetogonyaulax
A. astigmosus
N Ox.-Lo.
Richmond-Taylorsville
Zone II
Zone I
Wrangellia volcanism
Huglu-Pindos volcanism
Kara-Dere basalt
G.rudis(common)
P.quadruplices(common)
R.tuberculatus
P.maljawkinae
P.novimundanus
V.ignacii
P.densus
E.vigens
C.secatus
T.verrucata
A.astigmosus
M Ttr
Lad.
Long.
Protrachy.
H.dim.
H.dim.
IX
E.ilia.

A. astigmosus
T. verrucata, T. aurea
Partitisporites spp.
P.quadruplices
P.densus, E. vigens
Carnian
early Julian
late Julian
Sidmouth Mudstone
Dunscombe Mudstone Formation
Samples (depth, m)
Calcareous marker beds
Wiscombe Park-1
δ13CTOC(‰)
TOC%
Hygrophyte/ xerophyte ratio
CIE-5
CIE-4
CIE-3
CIE-2
IIE
-31 -29 -27 -25 -23 -21
0 1 2 3
0 0.1 0.2
Strangman's Cove
δ13CTOC(‰)
TOC%
Hygrophyte/ xerophyte ratio
CIE-5
CIE-4
CIE-3
CIE-2
IIE
-34 -30 -26 -22 -18
0 2 4
0 0.24 0.48 0.72
Calcareous marker beds
Samples
Lincombe Member
Dunscombe Mudstone Formation
late Julian
Jul./Tuv.
Carnian
BMF
SMF
Tuv.
Cycadopites sp.
P.densus
P. quadruplices
Partitisporites spp.
B. striata
P.longdonensis

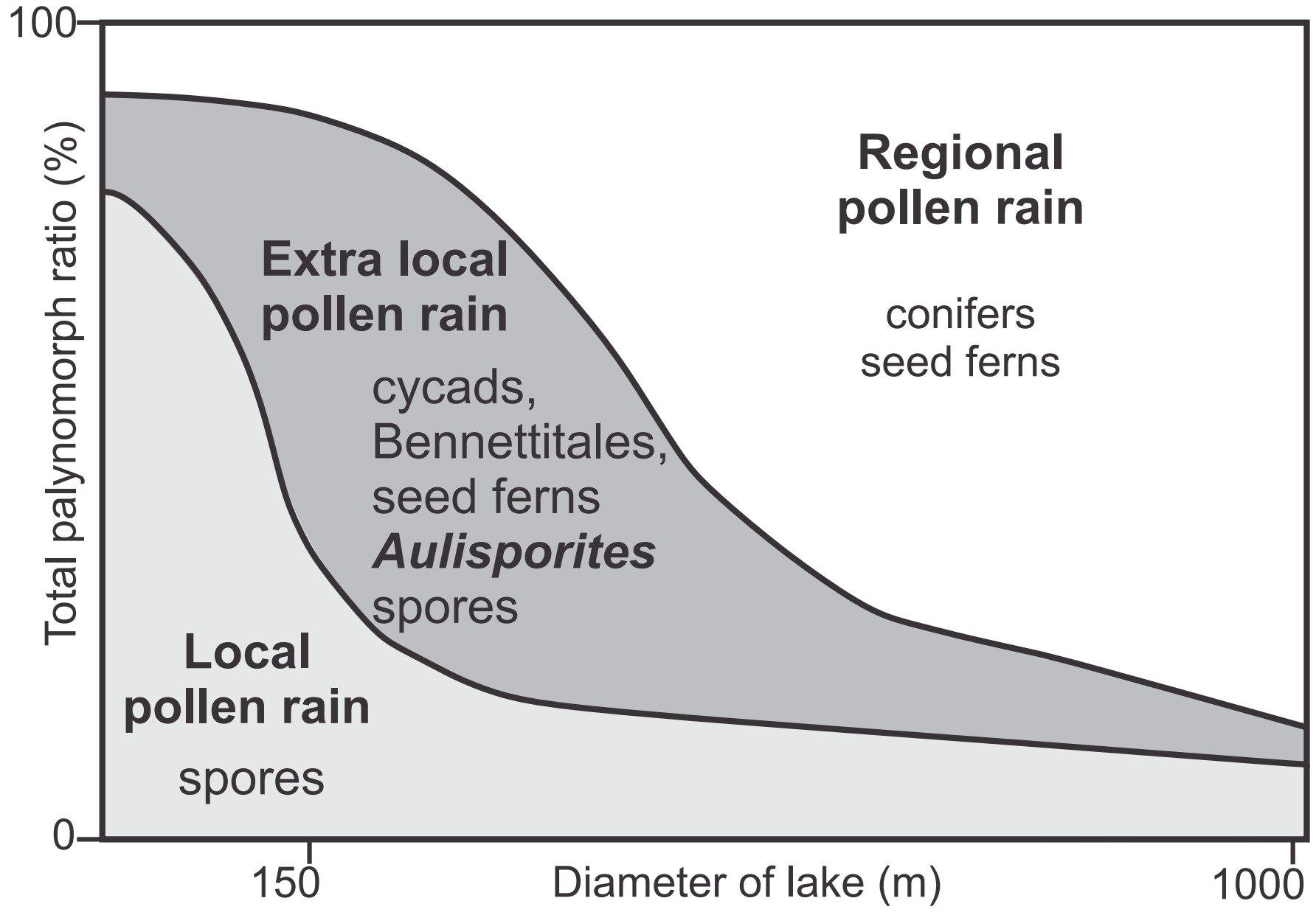
100
0
Total palynomorph ratio (%)
Regional
pollen rain
conifers
seed ferns
Extra local
pollen rain
cycads,
Bennettitales,
seed ferns
Aulisporites
spores
Local
pollen rain
spores
150
Diameter of lake (m)
1000

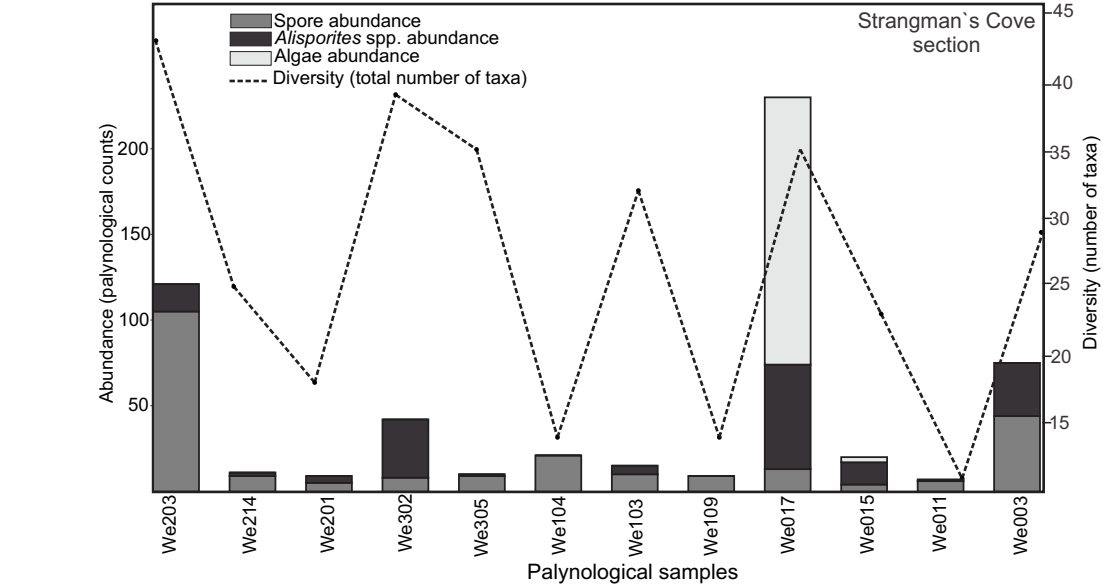

Lithostratigraphy	BMF	Dunscombe Mudstone Fm					Lincombe M.	Dunscombe M.F.	
Substages	Tuvalian	Julian/Tuvalian			late Julian				
$\delta^{13}C_{TOC}$				CIE-5		CIE-4		CIE-3	
Climate	wetter?	drier?	wetter?	drier?	wetter?	drier	wetter	drier	wetter

Supplementary Data

A continental record of the Carnian Pluvial Episode (CPE) from the Mercia Mudstone Group: palynology and climatic implications

Viktória Baranyi, Charlotte S. Miller, Alastair Ruffell, Mark W. Hounslow & Wolfram M. Kürschner

Contents

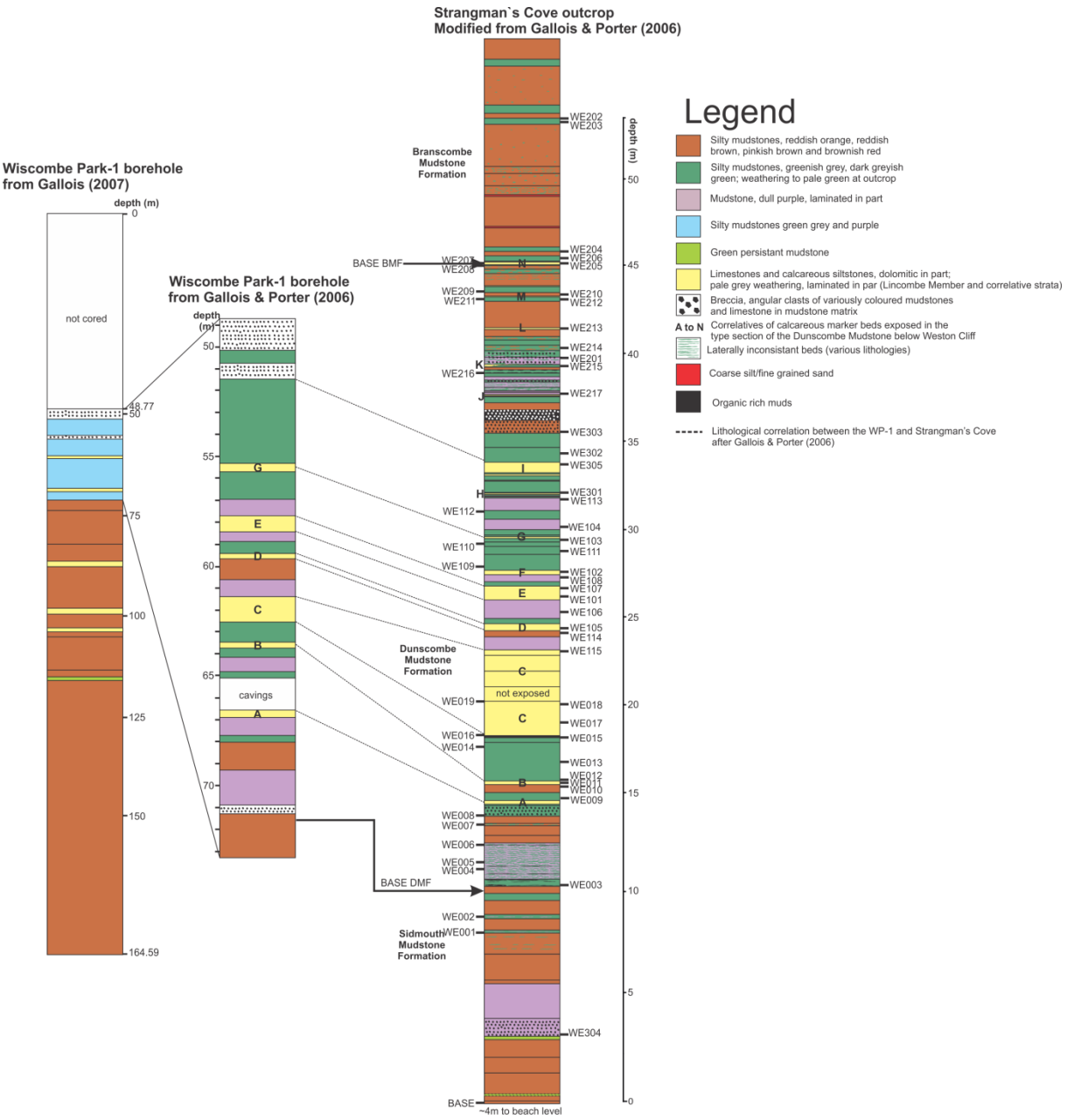

Fig. S1. Detailed lithological log the Strangman`s Cove section with the exact position of the palynological samples and its correlation (Gallois & Porter 2006) to the WP-1 borehole core. DMF = Dunscombe Mudstone Formation, BMF = Branscombe Mudstone Formation.

Detailed description of the Mercia Mudstone Group lithostratigraphic units in the Wessex Basin

Sidmouth Mudstone Formation

The formation was originally defined by Gallois (2001) and later adapted to the national re-assessment by Howard et al. (2008). The type section is in the South Devon coast between Sidmouth [SY 129 873] and Weston Mouth [SY 163 879]. Its base is defined at the top of the Pennington Point Mbr of the underlying Otter Sandstone Fm (Gallois, 2004) in the same section, and in south Devon it has been divided into five members (Gallois, 2001, 2004). At the type section the formation consists predominantly of massive red-brown mudstone and siltstone with common grey-green reduction patches and spots. The mudstones are mostly structureless, with a blocky weathering habit. Units consisting of thin beds of grey-green dolomitic siltstone and very fine-grained sandstone, interbedded with mudstone, occur at intervals throughout the formation. In the type section, Gallois (2007) indicates the "*Sidmouth Mudstone comprises c. 180 m of relatively uniform red-brown mudstones and orange-brown muddy siltstones in stacked sequences of small-scale rhythms, 0.5 to 1.5 m thick, in which fissile-weathering, brownish red, silty mudstones pass up into reddish orange, muddy siltstones*". Gypsum and/or anhydrite also occur predominantly in the upper part of the formation as nodules and veins. Caliche nodules occur in the lowest member of the formation. Age is probably latest Anisian or earliest Ladinian at its base (Hounslow & McIntosh, 2003) through Ladinian to probably Carnian in its upper parts (this paper). It is devoid of macrofossils.

Arden Sandstone Formation

Howard et al. (2008) define this formation, with a type section in the Canal cutting [SP 2118 6744] at Shrewley in Warwickshire (Old et al., 1991). Howard et al. (2008) describe **t**he lithology of the formation as "*consisting of grey, green and purple mudstone interbedded with paler grey-green to buffcoloured siltstone and fine to medium-grained, varicoloured (green, brown, buff, mauve) sandstone; thin pebble beds occur locally. Laminated and thinly interbedded sediments are commonly extensively bioturbated and show structures indicative of thixotropic deformation. Invertebrate and vertebrate macrofossils are present, locally in abundance, and miospores and burrows are common. The siltstones and finer sandstones show small-scale ripple drift cross-bedding; thicker sandstone beds show trough and planar crossbedding. The proportion of fine to coarse clastics varies laterally within the formation. The thicker sandstone units, composed of several individual beds, have a lenticular geometry and occupy the inferred former courses of distributary channels in a deltaic or estuarine environment. The formation is differentiated from the reddish brown, blocky weathering mudstones of adjacent formations by its predominantly greenish grey colour, the presence of a significant (though commonly subordinate) proportion of sandstone, the predominance of finely laminated lithologies throughout, and its comparatively fossiliferous nature.*" The base of the formation is placed at the change from underlying red mudstone to non-red units, and on the South Devon coast may be at the breccia (Howard et al. 2008) at around sample WE008 in Fig. S1 (50 cm below bed A), and ca. 71m in the Wiscombe Park Borehole. Its thickness is 7-8 m in the midlands and upto 24 m thick in S. Devon. On palynological evidence, primarily from the Midlands, its age is late Carnian. It contains a variety of rather poorly documented macrofossils (Old et al., 1991; Barclay *et al*., 1997).

Dunscombe Mudstone Formation

The formation was defined by Gallois (2001) and later slightly revised by Gallois & Porter (2006), with a type section at the series of cliff faces below Weston Cliff (SY 168 880 to 171 880; Gallois & Porter, 2006). There the formation consists of 38 m to 43 m of interbedded and interlaminated green, purple, red and grey mudstones, mudstone breccias, silty dolomitic limestones, siltstones and fine-grained sandstones. The dolomitic beds form prominent, pale weathering markers in the cliffs. The breccias and dark grey mudstones, can give rise to water seepage lines in the cliff outcrops. At the type section the formation can be divided in three divisions, following Jeans (1978), a 'lower calcareous group' (containing beds informal A and B; Fig. s1), and 'middle sandstone group' containing beds C to E, and an 'upper calcareous group' containing beds F to N (Gallois & Porter, 2006; Fig. s1).

In the Wiscombe Park boreholes the base of the formation is at the base of a partially dolomitised breccia (at 71 m; Gallois, 2007) which marks a lithological change from the predominantly red-brown mudstone of the Sidmouth Mudstone Formation to interbedded green and purple mudstones with thin dolomitic and dark grey mudstones. In the Strangman's cove section, Gallois & Porter (2006) used the base of the formation as the first grey mudstone just below sample position WE003 (Fig. s1), and the upper boundary at the top of bed N (location of WE205).

Lenticular beds of siltstone and fine-grained calcareous sandstone are present throughout, but dominate in the middle division of the Dunscombe Mudstone Formation. These calcareous or sandy beds (designates as A-N, Fig. S1) form prominent pale weathering marker beds in the cliff. At outcrops on the Devon coast, the thickest of these units (bed C) has been named the Lincombe Member (Porter & Gallois 2008) (Fig. S1). In Somerset, lenticular sandstones similar to the Lincombe Member are recorded in the lower part of the formation between Lipe Hill and Norton Fitzwarren between Knapp and Stathe and between Moorlinch and Sutton Mallet (e.g., Ruffell & Warrington 1988; Gallois, 2003), but their age relationship or correlation to the Lincombe Member is unclear. The mudstone breccias consist of angular predominantly clasts in a mudstone matrix and were formed by dissolution of gypsum/anhydrite and halite, with cliff falls revealing residual white gypsum patches within the breccias. Correlations with boreholes suggest that the breccias probably pass laterally into thick beds of salt (Gallois, 2003). The formation contains a variety of macrofossils and trace fossils (Porter and Gallois, 2008). Based on this study the formation is Julian-earliest Tuvalian in age.

Branscombe Mudstone Formation

The formation was originally defined by Gallois (2001), and later adapted to the national re-assessment by Howard et al. (2008). The type section is on the Devon coast between Weston Cliff and Branscombe Mouth [SY 171 879 to 207 881] with higher units at Haven Cliff, east of Seaton [SY 256 898 to 260 897]). Gallois (2001) divided this into four members in the type section. The formation predominantly consists of red-brown mudstone and siltstone with a blocky weathering habit. Fairly frequent green mudstone or green to red fine-grained sandstone beds (5 mm to 10 cm thick) occur particularly in the upper or mid parts of the formation (as well as rare black mudstone in mid parts), and a ca. 10 m thick Red Rock Gypsum Member occurs in the coastal outcrops. In the type section Gallois (2001) and Gallois & Porter (2006) defined its base at the top of bed N (which we use here), whereas Howard et al. (2008) revised it down to around the base of bed J.

In south Devon, Somerset and Gloucestershire, the highest 10 to 20 m include common beds of greenish grey mudstone (Haven Cliff Mudstone Mbr, in south Devon, part of 'Tea Green

Marls' further N), giving rise to markedly colour-banded sections were exposed . Based on this study and magnetostratigraphic data (Hounslow et al. 2004) the age of the formation is Late Carnian (this study) to around the Norian- Rhaetian boundary (Kent et al. 2017). The formation is devoid of macrofossils, but contains palynomorphs in its uppermost parts.

Blue Anchor Formation

The type section of the formation is in north Somerset at Blue Anchor cliff [ST 0385 4368], where it is 36.54 m thick (Warrington and Whittaker, 1984; Howard et al. 2008). The formation typically consists of rhythmically bedded pale grey to green, dolomitic silty mudstones, siltstones and argillaceous limestones. At the type section it also contains extensive thick beds of gypsum, but these are rarely preserved elsewhere unless locally in boreholes. Often its base is taken as a prominent bed of dolomitic limestone, as in Devon (Gallois, 2001), although in North Somerset it is taken at the top of the highest occurrence of a major red mudstone (Warrington and Whittaker, 1984; Hounslow et al. 2004)- the boundary is likely diachronous and may be erosive (Howard et al. 2008). Based on magnetostratigraphy its age is from around the Norian-Rhaetian boundary into the early Rhaetian (Kent et al. 2017; Hounslow & Muttoni, 2010). It contains a fairly restricted macrofauana and diverse palynology (Hounslow et al. 2004).

Sample locations

In Devon two localities were sampled. A total of 56 samples were taken from a coastal outcrop at **Strangman`s Cove** (SY 1718 8795, 49º50´48´´N, 7º32´33´´W) (Fig. 1) and 34 samples were analysed from the **Wiscombe Park-1 borehole** (WP-1) (SY 1819 9382, 49º51´07´´N, 7º32´30´´W) (Fig. 1) borehole. The Wiscombe Park-1 borehole was drilled by the British Gypsum Ltd in 1972 to a depth of 164.59 m, and the interval between 48.77 m and 164.59 m was continuously cored (Gallois 2007). The core is housed at the British Geological Survey National Geoscience Data Centre at Keyworth, Nottingham, UK.

In Somerset three localities were sampled: **Knapp Quarry** (Knapp, North Curry, ST 3050 2536, 51º01´25´´N, 2º59´30´´W) (seven samples), **Sutton Mallet** (north of Bridgwater, 51º07´25´´N, 2º53´49´´W) (four samples) and **Lipe Hill** (between Taunton and Wellington, from ST 1872 2150 to ST 186 215 50º59´13´´N, 3º09´36´´W) (ten samples) (Fig. 1). The Lipe Hill exposes one of the successions that formed the basis for the CPE (Ruffell et al, 2015). It exposes a succession starting with a conglomeratic basal beds followed by fine-grained, cross-laminated sandstone and grey-dark grey mudstones (Ruffell & Warrington 1988). Knapp Quarry (Warrington & Williams 1984) comprises of fine-grained, pale grey to cream coloured, cross-bedded and ripple-drift cross-laminated sandstones interbedded with blue and grey mudstones (Ruffell & warrington, 1988). At Sutton Mallet 2 m of fine and medium grained sandstone are interbedded with 5-15 cm blue-grey mudstones. All three sandstones are channel deposits, each with a basal channel-lag deposit, cutting down into the Sidmouth Mudstone, unlike the Lincombe Member which is several metres above the base of the Dunscombe Mudstone Formation.

Laboratory techniques

Palynological processing

Ten to twenty grams of sediment were crushed and in order to calculate palynomorph concentration, one tablet containing Lycopodium spores was added to each sample at the start of processing. All samples were treated with 10% HCl to dissolve the carbonate fraction. To dissolve the silicates, the samples were treated with hot concentrated HF (65ºC) in a water bath for two days. The organic residue was sieved with a 250 µm and a 15 µm mesh. To separate heavy minerals (e.g., pyrite) from the organic particles, heavy liquid ($ZnCl_2$) was added to the organic residue between 250 µm and 15 µm. Slides were mounted using epoxy resin (Entellan) as the mounting medium. Microscopy was carried out with a Zeiss Standard Trinocular (328883) microscope connected to an AxioCam ERc5s camera and Zen 2011 software.

Organic carbon isotope analysis and TOC

For $\delta^{13}C_{TOC}$ analyses, 36 samples from the Strangman's Cove outcrop were homogenized and treated sequentially with 0.1M and 1M HCl for 24 hours, before being rinsed to neutrality with MilliQ water (18.2 MΩ cm) and dried at 40°C for 4 days. Each step, involving a change of reagent or water, was preceded by centrifugation (10 min at 1500 rpm) to prevent the loss of fine material in suspension. The resulting powders were weighed into tin cups. Samples were first measured for % TOC using a Fisons NA1500 NCS and then for isotopes using the Fisons NA1500 NCS coupled with a Thermo Delta plus IR-MS. Ratios were normalised using the laboratory standard GQ (a powdered Graphite-Quartzite). The precision obtained for repeat analysis was better than ± 0.19‰ (1σ). The analyses were carried out at the GeoLab, Department of Earth Sciences, at the University of Utrecht.

Table S1. *Botanical affinity, proposed habitat and ecological affinity of the identified palynomorphs. NA= not assigned*

Taxa	Botanical affinity*	Habitat (SEG)†	Type	Ecology‡
Anapiculatisporites	moss?	river/lowland	local/extra-local	hygrophyte
Aratrisporites spp.	lycopsid	river	local	hygrophyte
Calamospora tener	Equisetales	river	local	hygrophyte
Carnisporites	Filicales	river	local	hygrophyte
Conbaculatisporites	Dipteridaceae	river	local	hygrophyte
Concavisporites	Matoniaceae	river/lowland	local/extra-local	hygrophyte
Converrucosisporites	Dicksoniaceae	lowland	local/extra-local	
Cyclogranisporites/Cyclotriletes	Osmundaceae	river/lowland	local/extra-local	hygrophyte
Dictyophyllidites	Filicales	lowland	extra-local	hygrophyte
Kraeuselisporites	lycopsid	river	local	hygrophyte
Kyrtomisporis	fern	river/lowland	local/extra-local	hygrophyte
Lycopodiacidites	lycopsids	river	local	hygrophyte
Osmundacidites	Osmundaceae	river/lowland	local/extra-local	hygrophyte
Porcellispora longdonensis	liverwort	river	local/extra-local	hygrophyte
Rogalskaiasporites	Moss?	river	local	hygrophyte
Thomsonisporites toralis	NA	NA	NA	hygrophyte
Todisporites	Osmundaceae	river/lowland	local/extra-local	hygrophyte
Verrucosisporites	Filicales	river	local	hygrophyte
Alisporites spp.	seed fern	upland/lowland	regional/extra-local	hygrophyte?
Brachysaccus	conifer	upland	regional	xerophyte
Chordasporites	conifer/seed fern	upland	regional	xerophyte
Ellipsovelatisporites	conifer	upland	regional	xerophyte
Lunatisporites	Podocarpaceae	upland	regional	xerophyte
Klausipollenites spp.	Voltziales	upland	regional	xerophyte
Microcachrydites	Podocarpaceae	upland	regional	xerophyte
Minutosaccus	Voltziaceae	upland	regional	xerophyte
Ovalipollis spp.	Voltziaceae	upland	regional	xerophyte
Parillinites	conifer?	upland	regional	xerophyte
Pityosporites	conifer/seed fern	upland/lowland		xerophyte
Platysaccus	Podocarpaceae	upland	regional	xerophyte
Protodiploxypinus	conifer/seed fern	upland/lowland		xerophyte
Sulcatisporites	conifer?	upland	regional	xerophyte
Triadispora spp.	Voltziaceae	upland	regional	xerophyte
Voltziaceaesporites	Voltziaceae	upland	regional	xerophyte
Enzonalasporites	Majonicaceae	upland	regional	xerophyte
Patinasporites	Majonicaceae	upland	regional	xerophyte
Pseudoenzonalasporites	Majonicaceae	upland	regional	xerophyte
Vallasporites	Majonicaceae	upland	regional	xerophyte
Aulisporites	Bennettitales	lowland	extra-local	hygrophyte
Brodispora striata	NA	lowland	local	hygrophyte
Camerosporites	Cheirolepidiaceae	upland	regional	xerophyte
Cycadopites	Cycadophyte	lowland	regional	hygrophyte
Duplicisporites	Cheirolepidiaceae	upland	regional	xerophyte
Lagenella martinii	NA	river/lowland	local	hygrophyte
Partitisporites	Cheirolepidiaceae	upland	regional	xerophyte
Praecirculina	Cheirolepidiaceae	upland	regional	xerophyte

*Botanical affinities from Balme (1995), Roghi (2004), Roghi *et al.* (2010), Raine *et al.* (2011), Bonis & Kürschner (2012), Fijałkowska-Mader (2015), Lindström *et al.* (2016), Paterson et al. (2016)

†Habitats from Abbink *et al.* (2004), Kustatscher et al. (2012), Paterson et al. (2016)

‡Ecology from Visscher & Van der Zwan (1981), Roghi (2004), Roghi *et al.* (2010), Fijałkowska-Mader (2015), Mueller *et al.* (2016a, b), Paterson et al. (2016)

Table 2. *Compilation of the sedimentological, palynological and geochemical characteristics of CPE successions across Europe.* N.D. No data/not determined

Location	Sedimentology	Palynology	Carbon cycle	Climatic interpretation	References
„British Keuper" Mercia Mudstone Group, Wessex Basin)	Switch from evaporitic playa and red-bed facies to greenish purple mudstones and sandstones of an alluvial-fluvial-lacustrine series in the late Julian	Xerophyte palynomorphs predominant during the entire Julian *Aulisporites astigmosus* acme missing in the Julian	Five negative carbon isotope excursions during the late Julian Initial isotope excursions at the early/late Julian boundary	Minor humid pulse with a prevailing relatively drier background climate	This study, Miller et al. (2017)
"Schilfsandstein," Germany	Switch from evaporitic playa lakes (Grabfeld Formation) to fluvial-deltaic sandstones (Stuttgart Formation)	Hygrophyte vegetation and *Aulisporites astigmosus* acme in the late Julian	N.D.	Minor humid pulse with a prevailing relatively drier background climate	Visscher et al. (1994)
Iberian Peninsula	Switch from evaporitic beds to coarse grained clastic deposits (Manuel Formation), multiple clastic intervals	Mainly xerophyte assemblages *Aulisporites astigmosus* acme missing	N.D.	Multiple short-lived humid episodes in the Carnian punctuated by drier intervals	Arche & López-Gómez (2014); López-Gómez et al. (2017)
Boreal Realm (Svalbard)	Transition from offshore marine mudstones to prodelta and deltaic siltstones-sandstones	Hygrophyte palynomorphs predominant in the Carnian, *Aulisporites astigmosus* acme in the Julian 1	Negative carbon isotope excursion at the Julian 1 and 2 boundary	Relatively drier and warmer climate in the Julian 1 and shift to increased humidity in the Julian 2	Mueller et al. (2016a)
Dolomites (Western Tethys)	Platform carbonates are covered by carbonate-clastic ramp deposits and four distinct siliciclastic intervals in the late Julian-early Tuvalian	Clastic intervals associated with the increase of hygrophyte palynomorphs *Aulisporites astigmosus* acme in the Julian 2	Negative carbon isotope excursion at the Julian 1 and 2 boundary	Multiple humid pulses during the late Julian Return to drier climate in the Tuvalian	Roghi (2004); Roghi et al. (2010)
Raibl Group (Northern Calcareous Alps)	Platform carbonates covered by a mixed carbonate-clastic series with three siliciclastic intervals in the late Julian-early Tuvalian	Clastic intervals associated with the increase of hygrophyte palynomorphs *Aulisporites astigmosus* acme in the Julian 2	N.D.	Multiple humid pulses during the late Julian Return to drier climate in the Tuvalian	Roghi et al. (2010)
Lunz area (Northern Calcareous Alps)	Switch from pelagic marls (Partnach Formation) and limestones (Reifling Formation) to organic rich shales (Reingraben Formation) and deltaic sandstones (Lunz Formation) with coals in the Julian 2	Increase of hygrophyte palynomorphs in the Julian 2 *Aulisporites astigmosus* acme in the early Julian 2	Negative carbon isotope excursion at the Julian 1 and 2 boundary	Multiple humid pulses during the late Julian Return to drier climate in the Tuvalian	Roghi et al. (2010); Dal Corso et al. (2015); Mueller et al. (2016b)
Transdanubian Range (NW Hungary)	Pelagic and platform carbonates are interrupted by a mixed carbonate clastic, mainly marl sequence in the Julian 2	Increase of hygrophyte palynomorphs in the late Julian	Negative carbon isotope excursion at the Julian 1 and 2 boundary	Shift to more humid climate in the Julian 2	Góczán et al. (1983); Góczán & Oravecz-Scheffer (1996a, b); Haas et al. (2012); Dal Corso et al. (2015)

Spores Sidmouth Formation

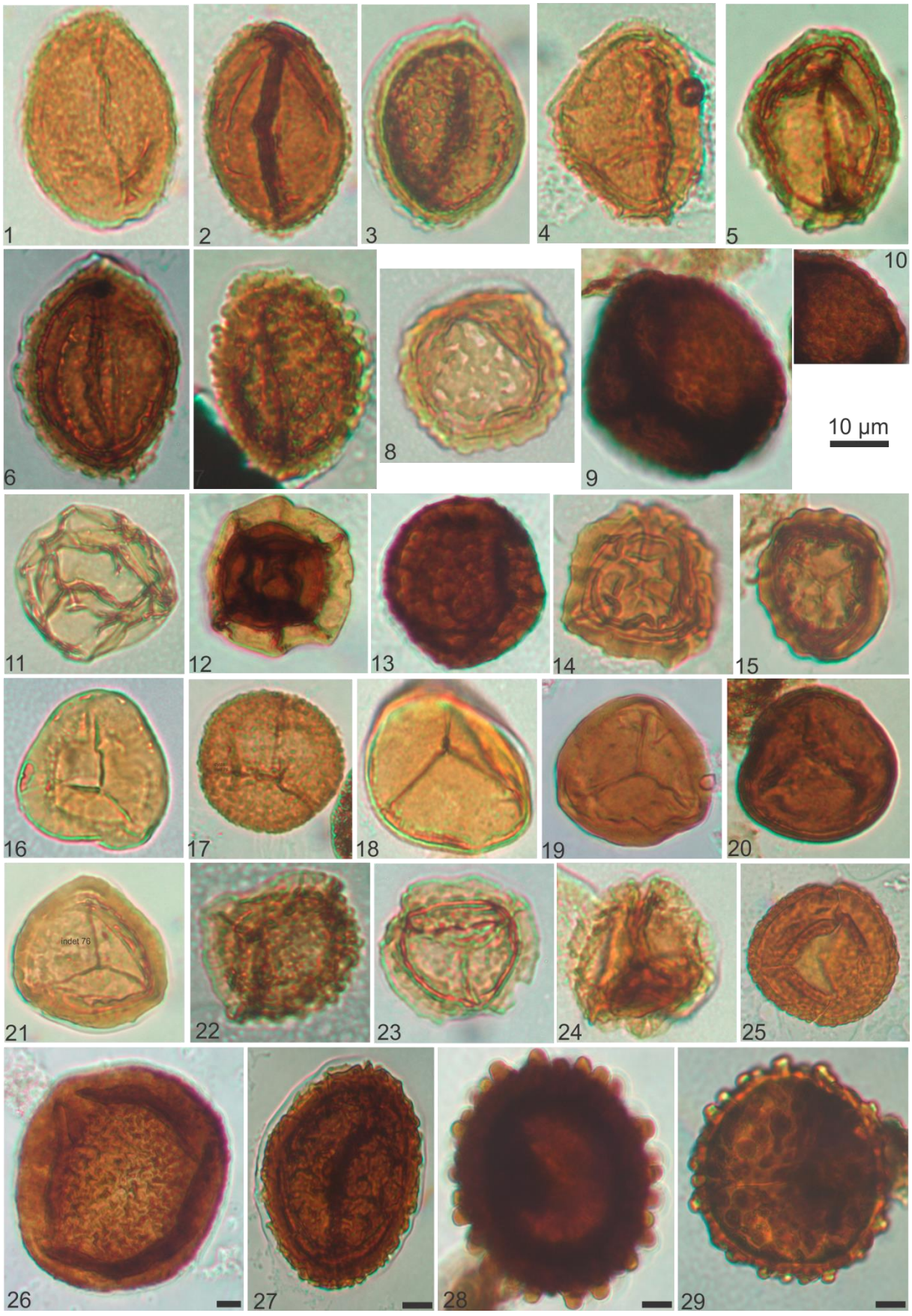

Spores in the Sidmouth Formation with the indication of sample name, or code and slide number

1 *Aratrisporites granulatus* (111.98 m/1)

2 *Aratrisporites granulatus* (111.98 m/1)

3 *Aratrisporites* sp. (111.98 m/2)

4 *Aratrisporites fimbriatus* (109.11 m/1)

5 *Aratrisporites fimbriatus* (111.98 m/1)

6 *Aratrisporites fimbriatus* (111.98 m/1)

7 *Aratrisporites* sp. (111.98 m/1)

8 *Uvaesporites gadensis* (111.98 m/1)

9 *Verrucosisporites morulae* (111.98 m/1)

10 *Verrucosispoirtes morulae* high resolution same as 10, (111.98 m/1)

11 *Calamospora tener* (111.98 m/1)

12 *Thomsonisporis toralis* (109.11 m/1)

13 *Lycopodiacidites* sp. (109.11 m/1)

14 *Kyrtomispories* sp. (111.98 m/1)

15 spore indet A (111.98 m/1)

16 *Rogalskaiasporites* sp. (111.98 m/1)

17 *Cyclogranisporites* sp. (111.98 m/1)

18 *Punctatisporites* (111.98 m/1)

19 spore indet B (111.98 m/1)

20 *Punctatisporites* (111.98 m/1)

21 spore indet C (111.98 m/1)

22 cf *Kraeuselisporites* sp. (111.98 m/1)

23 cf *Kraeuselisporites* (111.98 m/1)

24 cf *Kraeuselisporites* sp. (111.98 m/1)

25 *Verrucosispoirtes morulae* (111.98 m/1)

26 *Cyclotriletes* sp. (111.98 m/1)

27 *Aratrisporites* sp. (111.98 m/1)

28 megaspore indet (111.98 m/1)

29 megaspore indet (109.11 m/1)

Pollen grains Sidmouth Formation

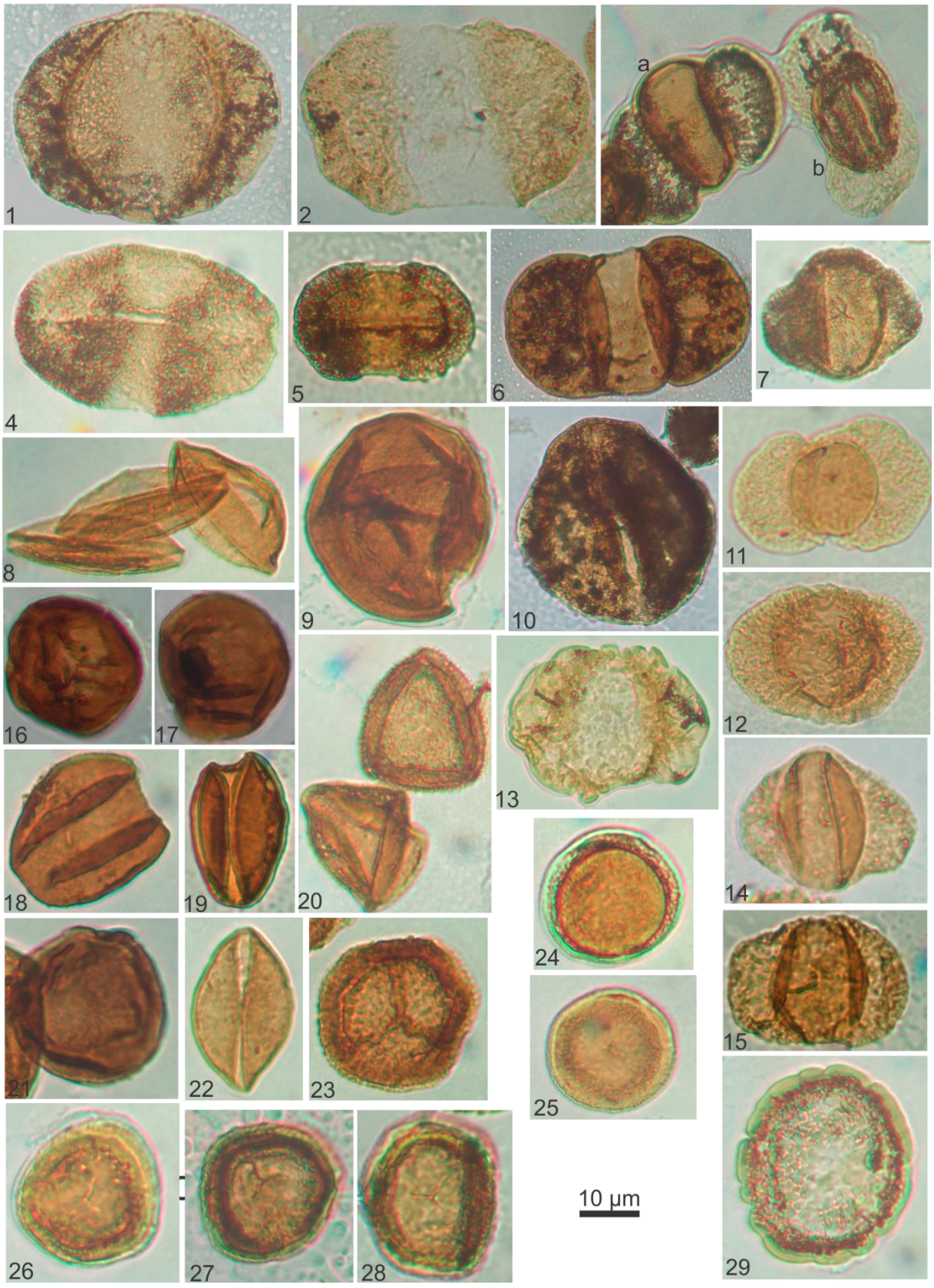

Pollen grains in the Sidmouth Mudstone Formation with the indication of sample name, or code and slide number

1 *Alisporites opii* (WP-1 111.98 m/1)

2 *Alisporites robostus* (WP-1 111.98 m/1)

3 a) *Triadispora aurea* b) *Lunatisporites acutus* (WP-1 111.98 m/1)

4 *Ovalipollis ovalis* (WP-1 111.98 m/1)

5 *Ovalipollis notabilis* (WP-1 109.11 m/1)

6 *Triadispora aurea* (WP-1 111.98 m/1)

7 *Triadispora crassa* (WP-1 111.98 m/2)

8 *Cycadopites* sp. (WP-1 111.98 m/1)

9 *Araucariacites australis* (WP-1 111.98 m/1)

10 *Brachysaccus neomundanus* (WP-1 109.11 m/1)

11 *Triadispora obscura* (WP-1 111.98 m/1)

12 *Triadispora plicata* (WP-1 111.98 m/1)

13 *Triadispora verrucata* (WP-1 111.98 m/1)

14 *Triadispora modesta* (WP-1 111.98 m/1)

15 *Triadispora staplini* (WP-1 109.11 m/1)

16 *Aulisporites astigmosus* (WP-1 111.98 m/1)

17 *Aulisporites astigmosus* (WP-1 111.98 m/1)

18 *Aulisporites astigmosus* (WP-1 111.98 m/1)

19 cf. *Aulisporites astigmosus* (WP-1 109.11 m/1)

20 *Duplicisporites granulatus* (WP-1 111.98 m/1)

21 *Aulisporites astigmosus* (WP-1 111.98 m/1)

22 *Cycadopites* sp. (WP-1 111.98 m/2)

23 *Vallasporites ignacii* (WP-1 111.98 m/2)

24 *Partitisporites novimundanus* (WP-1 109.11 m/2)

25 *Partitisporites novimundanus* (WP-1 111.98 m/1)

26 *Partitisporites scurrilis* (WP-1 111.98 m/1)

27 *Partitisporites scurrilis* (WP-1 109.11 m/1)

28 *Partitisporites scurrilis* (WP-1 109.11 m/1)

29 *Camerosporites secatus* (WP-1 111.98 m/1)

Palynomorphs in the Dunscombe Mudstone Formation

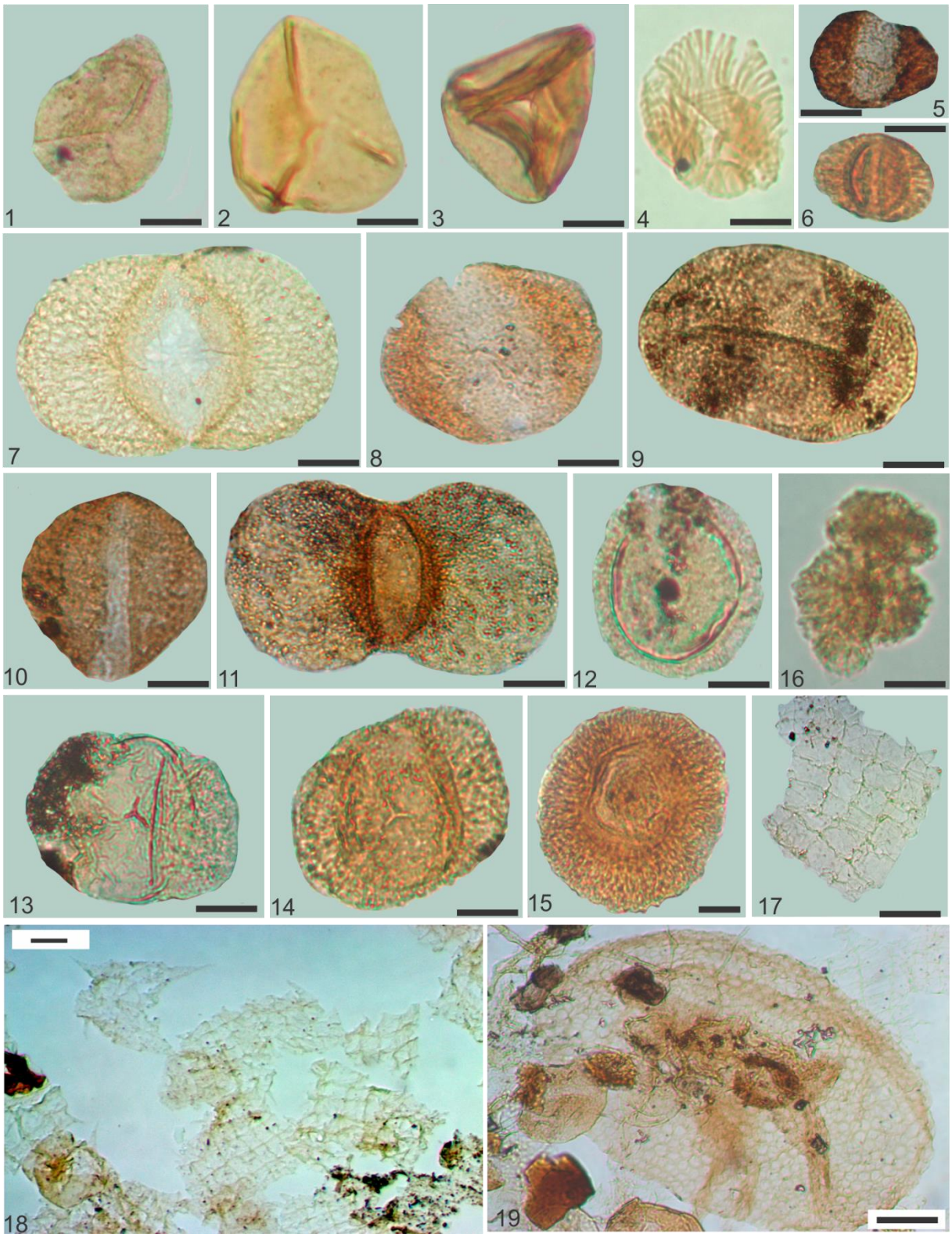

Palynomorphs in the Dunscombe Mudstone Formation with the indication of sample name, or code and slide number, scale bar 1-6, 16-17: 10 µm; 7-15, 18-19: 20 µm

1 *Deltoidospora* sp. (WE016/A)

2 *Deltoidospora* sp. (WE213/A)

3 *Concavisporites toralis* (WE016/A)

4 *Brodispora striata* (WE111/A)

5 *Triadispora epigona* (WE017/A)

6 *Triadispora modesta* (WE201/A1)

7 *Alisporites grauvogeli* (WP-1 57.86 m/1)

8 *Alisporites* sp. (WE017/A)

9 *Ovalipollis ovalis* (WE305/B)

10 *Brachysaccus neomundanus* (WE017/A)

11 *Platysaccus* sp. (WE015/A)

12 *Enzonalasporites vigens* (WP-1 56.15 m/1)

13 *Triadispora plicata* (WE103/A)

14 *Triadispora crassa* (WE305/C)

15 *Patinasporites iustus* (WE305/C)

16 *Botryococcus braunii* (WE018/A)

17 *Plaesiodictyon mosellanum* (WE017A)

18 *Plaesiodictyon mosellanum* (WE017A)

19 insect remain, probably an egg? (WE017/A)

Circumpolles pollen in the Dunscombe Formation

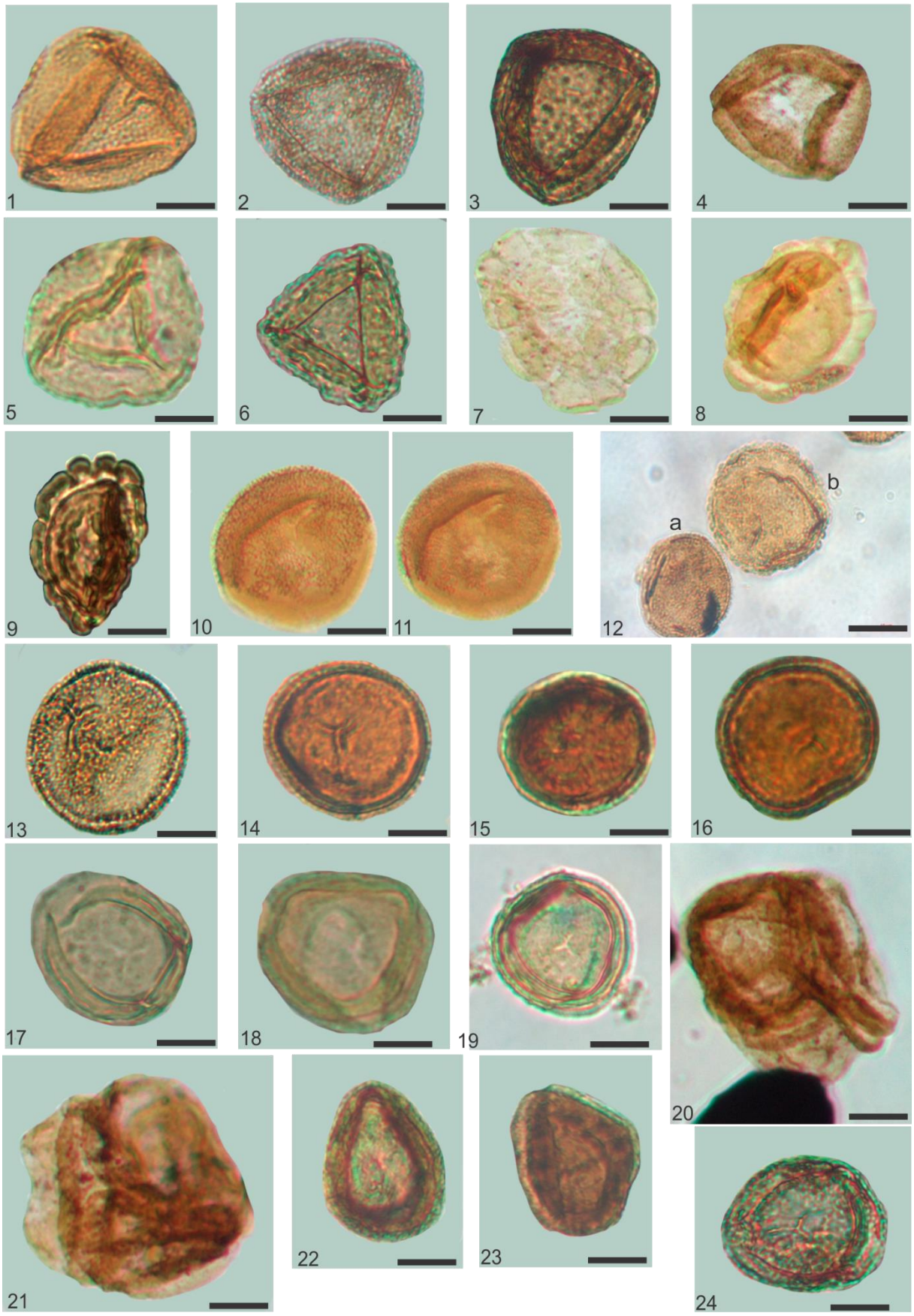

Circumpolles pollen in the Dunscombe Mudstone Formation with the indication of sample name, or code and slide number, scale bar 10 µm

1 *Duplicisporites granulatus* (WE003/A)

2 *Duplicisporites granulatus* (WE103/A)

3 *Duplicisporites granulatus* (WE305/B)

4 *Duplicisporites granulatus* (WE213/A)

5 *Duplicisporites mancus* (WE302/B)

6 *Duplicisporites mancus* (WE103/A)

7 *Camerosporites secatus* (WE213/A)

8 *Camerosporites secatus* (WE21/3A)

9 *Camerosporites secatus* (WE305/B)

10 *Praecirculina granifer* (WE001/A)

11 same as 10 *Praecirculina granifer* (WE001/A), different focus

12 a *Praecirculina granifer*, b *Camerosporites pseudoverrucosus* (WE015/A)

13 *Praecirculina granifer* (WE015/A)

14 *Partitisporites novimundanus* (WE003/A)

15 *Partitisporites novimundanus* (WP-1 49.8 5m/1)

16 *Partitisporites novimundanus* (WE201/A)

17 *Partitisporites maljawkinae* (WE302/A)

18 *Partitisporites maljawkinae* (WP-1 50.99 m/1)

19 *Partitisporites maljawkinae* (WP-1 55.65 m/1)

20 *Partitisporites quadruplices* (WE213/A)

21 *Partitisporites quadruplices* (WE213/A)

22 *Partitisporites scurrilis* (WE016/A)

23 *Partitisporites scurrilis* (WP-1 48.94 m/1)

24 *Partitisporites scurrilis* (WE103/A)

Palynomorphs in the Branscombe Mudstone Formation I

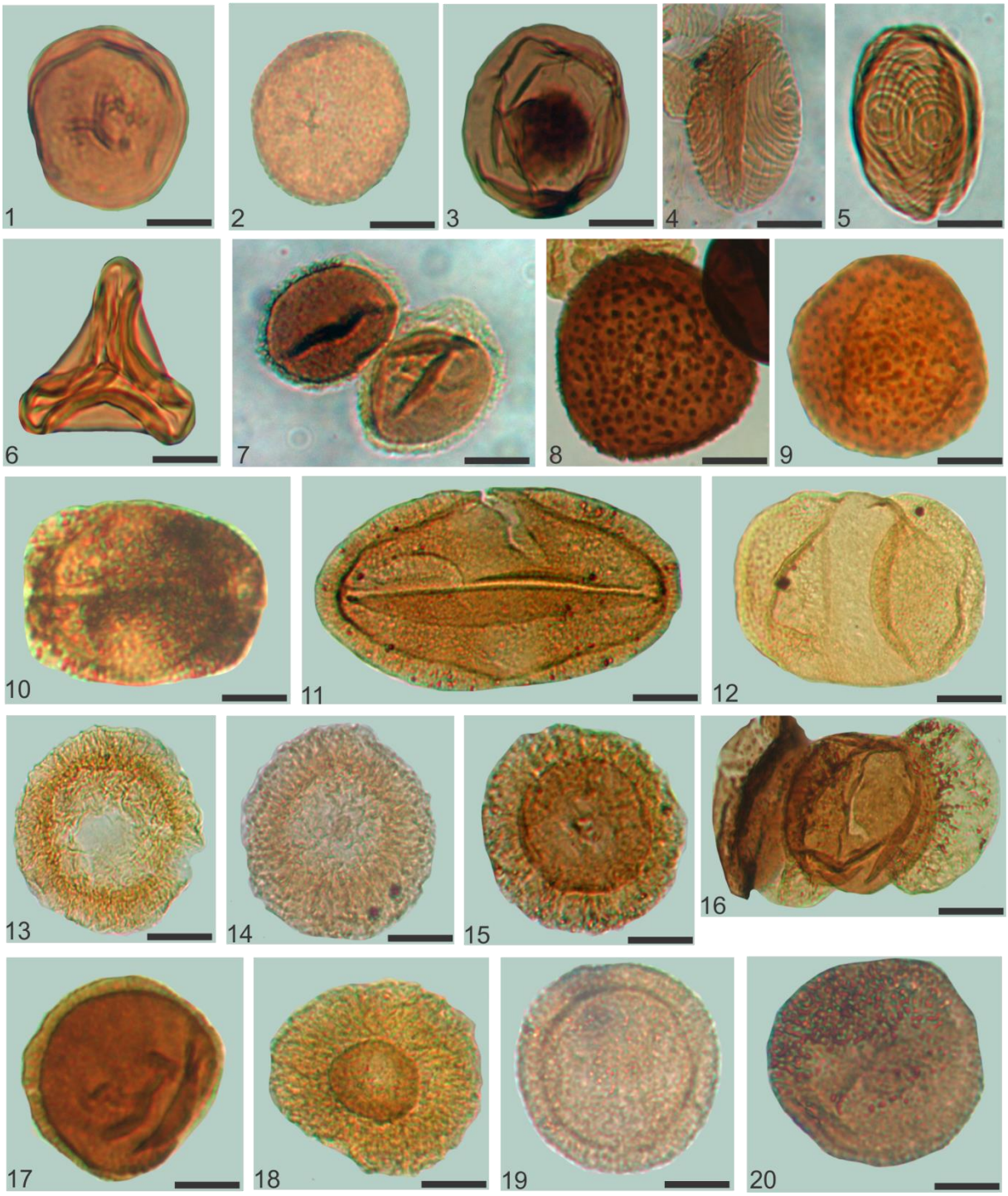

Palynomorphs in the Branscombe Mudstone Formation I with the with the indication of sample name, or code and slide number, scale bar 10 µm

1 *Todisporites rotundiformis* (WE203/C)

2 *Cyclogranisporites* sp. (WE203/B)

3 *Calamospora tener* (WE203/A)

4 *Brodispora striata* WE203/A)

5 *Brodispora striata* (WE203/A)

6 *Concavisporites toralis* (WE203/A)

7 a, b *Aratrisporites granulatus* (WE203/A)

8 *Porcellispora longdonensis* (WE203/A)

9 *Porcellispora longdonensis* (WE203/A)

10 *Ovalipollis minimus* (WE203/A)

11 *Ovalipollis lunzenis* (WE203/A)

12 *Alisporites grandis* (WE203/A)

13 *Patinasporites densus* (WE203/A)

14 *Patinasporites densus* (WE203/A)

15 *Patinasporites iustus* (WE203/A)

16 *Pityosporites* sp. (WE203/A)

17 *Enzonalasporites vigens* (WE203/A)

18 *Patinasporites explanatus* (WE203/A)

19 *Enzonalasporites manifestus* (WE203/B)

20 *Pseudoenzonalasporites summus* (WE203/A)

Palynomorphs in the Branscombe Mudstone Formation II

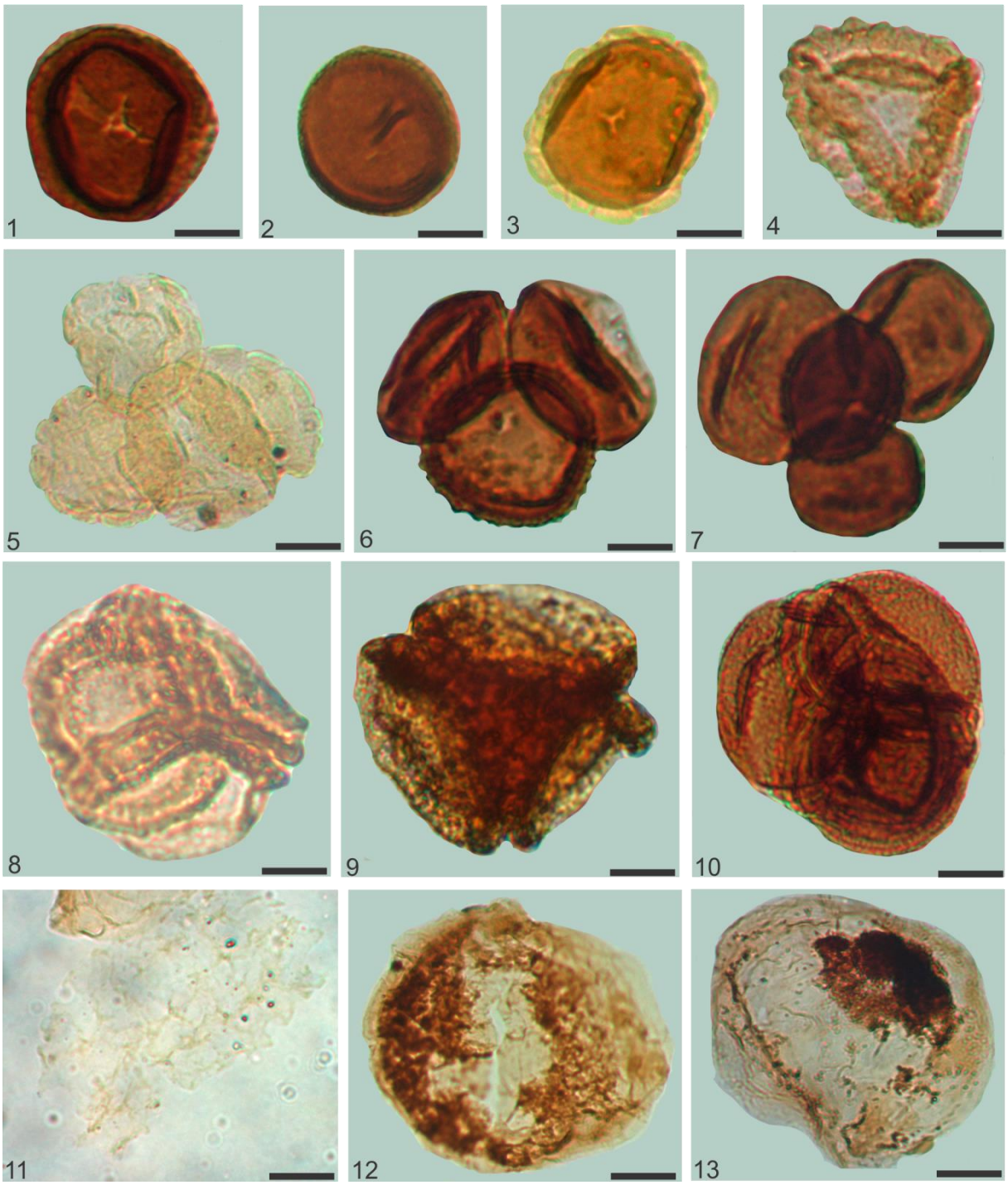

Palynomorphs in the Branscombe Mudstone Formation II with the indication of sample name, or code and slide number, scale bar 10 µm

1 *Partitisporites tenebrosus*? (WE203/A)

2 *Partitisporites tenebrosus*? (WE203/A)

3 *Camerosporites secatus* (WE203/A)

4 *Duplicisporites mancus* (WE203/A)

5 *Camerosporites secatus* (WE203/A)

6 *Partitisporites tenebrosus*? (WE203/B)

7 *Partitisporites tenbrosus?* (WE203/B)

8 *Partitisporites quadruplices* (WE203/B)

9 *Partitisporites quadruplices* (WE203/B)

10 *Partitisporites* sp. (WE203/C)

11 *Plaesiodictyon mosellanum* (WE203/B)

12 *Schizosporis* sp. (WE203/A)

13 *Schizosporis* sp. (WE203/A)

Somerset palynomorphs

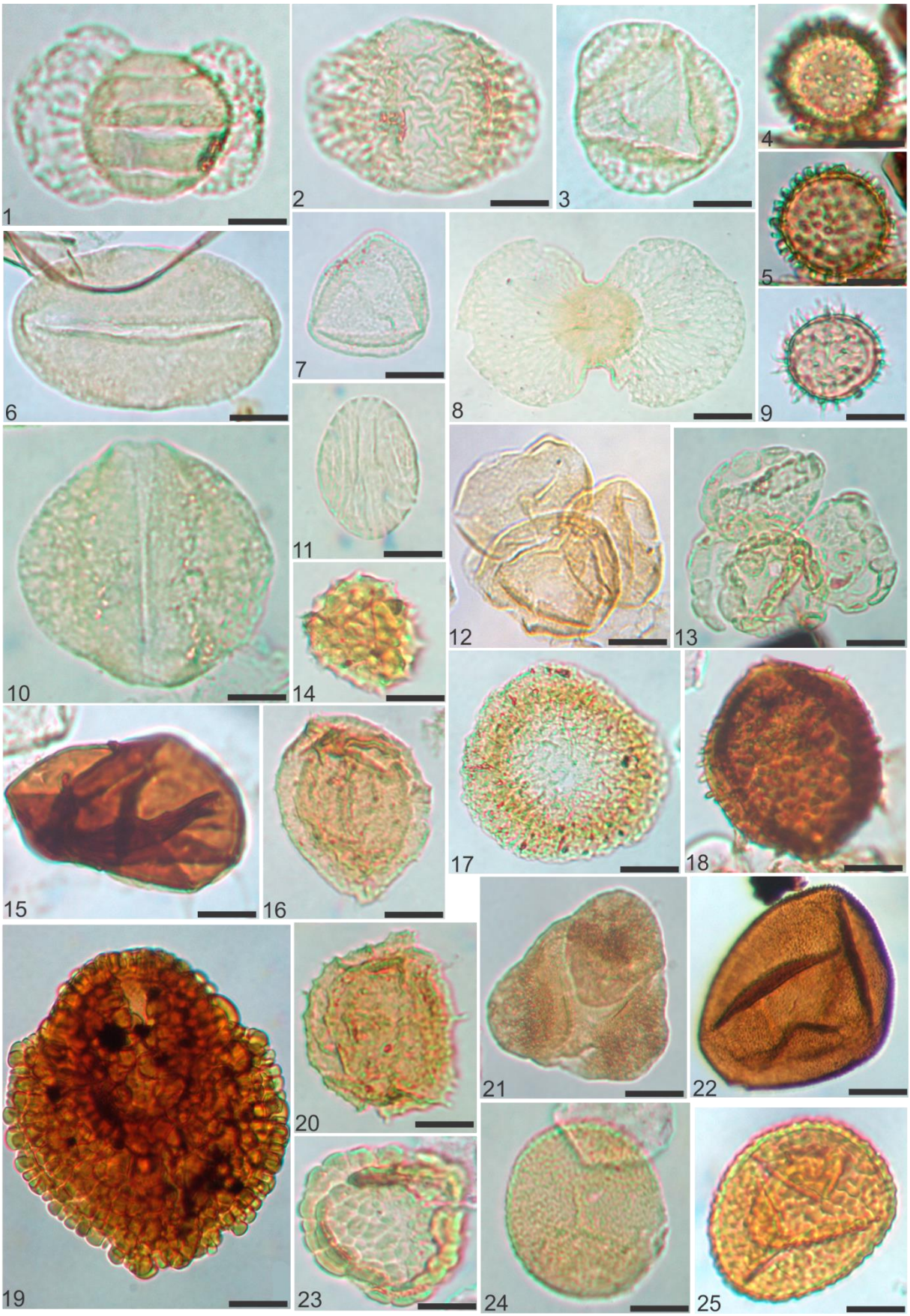

Somerset palynomorphs with the indication of sample name, or code and slide number, scale bar 10 µm. SM = Sutton Mallet, LH = Lipe Hill

1 *Lunatisporites acutus* (LH 2/2)

2 *Triadispora plicata* (LH 2/2)

3 Bisaccate indet with three airbags (LH 2/2)

4 acritach indet (LH 2/2)

5 acritarch indet same as 4 with different focus (LH 2/2)

6 *Ovalipollis ovalis* (LH 2/2)

7 *Duplicisporites granulatus* (LH 4/1)

8 *Platysaccus* sp. (LH 5/1)

9 *Micrhystridium* sp. (LH 2/2)

10 *Alisporites grauvogeli* (LH 7/1)

11 *Brodispora striata* (LH 9/1)

12 *Duplicisporites granulatus* tetrad (LH 8/1)

13 *Camerosporites secatus* tetrad (LH 7/1)

14 *Gibeosporites lativerrucosus* (SM 2/1)

15 cf. *Aulisporites astigmosus* (SM 3/1)

16 *Aratrisporites scabratus* (SM 3/1)

17 *Patinasporites densus* (SM 2/1)

18 *Porcellispora longdonensis* (SM 3/1)

19 *Ricciisporites tuberculatus* (SM 2/1)

20 *Aratrisporites paraspinosus* (SM 2/1)

21 bisaccate indet with three airbags (SM 4/1)

22 *Cyclotriletes* sp. (SM 4/1)

23 *Camerosporites secatus* (SM 2/1)

24 *Cyclogranisporites* sp. (SM 4/1)

25 *Converrucosisporites tumolosus* (SM 4/1)

List of all identified palynomorphs in alphabetic order

Spores

Anapiculatisporites sp.

Aratrisporites fimbriatus (Klaus, 1960) Playford & Dettmann, 1965

Aratrisporites granulatus (Klaus 1960) Playford & Dettmann 1965

Aratrisporites paraspinosus Klaus 1960

Aratrisporites scabratus Klaus 1960

Aratrisporites sp.

Calamospora tener (Leschik, 1955) De Jersey, 1962

Carnisporites sp.

Conbaculatisporites mesozoicus Klaus, 1960

Concavisporites toralis (Leschik, 1955) Nilsson, 1958

Converrucosisporites tumulosus (Leschik, 1956) Roghi 2004

Cyclogranisporites sp.

Cyclotriletes sp.

Dictyophyllidites harrisii Couper, 1958

Kraeuselisporites sp.

Kyrtomisporis laevigatus Mädler 1964

Kyrtomisporis speciosus Mädler 1964

Lycopodiacidites sp.

Osmundacidites wellmanni Couper, 1953

Porcellispora longdonensis (Clarke, 1965) Scheuring, 1970

Rogalskaiasporites sp.

Thomsonisporites toralis Leschik, 1955

Todisporites major Couper, 1958

Todisporites rotundiformis (Maljavkina, 1943) Pocock, 1970

Verrucosisporites moroluae Klaus, 1960

Bisaccate pollen grains

Alisporites diaphanous (Pautsch, 1958) Lund, 1977

Alisporites grandis (Cookson, 1953) Dettmann, 1963

Alisporites perlucidus Pautsch, 1973

Alisporites opii (Daugherty, 1941) Jansonius, 1962

Alisporites robostus Nilsson, 1958

Alisporites sp.

Brachysaccus neomundanus (Leschik, 1956) Mädler, 1964

Chordasporites singulichorda Klaus, 1960

Ellipsovelatisporites plicatus Klaus, 1960

Lunatisporites acutus (Leschik, 1955) Scheuring, 1970

Klausipollenites gouldii Dunay & Fisher, 1979

Klausipollenites schaubergeri (Potonie & Klaus, 1954) Jansonius, 1962

Minutosaccus crenulatus Dolby & Balme, 1976

Ovalipollis lunzensis Klaus, 1960

Ovalipollis minimus Scheuring, 1970

Ovalipollis notabilis Scheuring, 1970

Ovalipollis ovalis (Krutzsch, 1955) Scheuring, 1970

Ovalipollis sp.

Parillinites sp.

Pityosporites sp.

Platysaccus sp.

Protodiploxypinus fastidiosus (Jansonius, 1962) Warrington, 1974

Protodiploxypinus gracilis Scheuring, 1970

Sulcatisporites sp.

Triadispora aurea Scheuring, 1978

Triadispora bölchi Scheuring, 1970

Triadispora epigona Scheuring, 1970

Triadispora crassa Klaus, 1964

Triadispora obscura Scheuring, 1970

Triadispora modesta Scheuring, 1970

Triadispora plicata Klaus, 1964

Triadispora stabilis (Scheuring, 1970) Scheuring, 1978

Triadispora sulcate Scheuring, 1978

Triadispora suspecta Scheuring, 1970

Triadispora verrucata (Schulz, 1966) Scheuring, 1970

Triadispora sp.

Voltziaceaesporites heteromorpha Klaus, 1964

Monosaccate pollen grains

Enzonalasporites vigens (Leschik, 1956) Scheuring, 1970

Enzonalasporites manifestus Leschik, 1956

Patinasporites densus (Leschik, 1956) Scheuring, 1970

Patinasporites explanatus (Leschik, 1956)

Patinasporites iustus Klaus, 1960

Pseudoenzonalasporites summus Scheuring, 1970

Vallasporites ignacii Leschik, 1956

Non-saccate pollen grains

Aulisporites astigmosus (Leschik, 1955) Klaus, 1960

Camerosporites pseudoverrucosus

Camerosporites secatus (Leschik, 1955) Scheuring, 1970

Cycadopites sp.

Duplicisporites granulatus Leschik, 1956

Duplicisporites mancus Klaus, 1960

Lagenella martinii Klaus, 1960

Partitisporites maljawkinae (Klaus, 1960) Van der Eem, 1983

Partitisporites novimundanus (Leschik, 1956) Van der Eem, 1983

Partitisporites scurillis (Scheuring, 1970) Van der Eem, 1983

Partitisporites quadruplices (Scheuring, 1970) Van der Eem, 1983

Partitisporites tenebrosus (Scheuring, 1970) Van der Eem, 1983

Partitisporites sp.

Praecirculina granifer (Leschik, 1956) Klaus, 1960

Incertea sedis

Brodispora striata Clarke, 1965

Aquatic palynomorphs

Botryococcus braunii Kützing, 1849

Cymatiosphaera sp.

Micrihystridium sp.

Plaesiodictyon mosellanum Wille, 1970

Schizosporis sp.

Table S3 Wiscombe Park-1 palynofacies

Depth	Dry weight	Lycopodium (added)	Lycopodium (counted)	Bisaccates	Monosaccates	Non-saccate pollen	Spores	Charcoal	Cuticles	Plant tissues	Woody fragments	AOM	Algae	Botryococcus	Plaesiodictyon	Fungi	Total
48.94m	5.33g	12077	19	8	2	3	0	300	0	2	17	9	0	10	0	0	351
49.85m	5.66g	12077	5	32	5	6	1	257	0	0	14	26	0	0	0	0	341
50.48m	5.85g	12077	21	59	1	22	2	250	0	4	10	35	0	0	0	0	383
50.76m	5.33g	12077	2	33	0	16	0	6	0	9	0	250	0	0	0	0	314
50.99m	5.31g	12077	23	202	4	22	2	30	0	7	0	45	0	0	2	0	314
51.75m	6.01g	12077	22	9	0	1	0	19	0	53	2	227	0	3	0	0	314
55.30m	6.35g	12077	1000	8	0	1	7	95	0	64	3	8	0	0	0	0	186
55.65m	5.42g	12077	1	22	0	21	0	7	0	1	0	275	0	0	0	0	326
56.15m	5.78g	12077	6	56	0	58	0	18	0	5	4	180	0	1	0	0	322
56.51m	5.33g	12077	18	55	0	96	6	24	1	7	8	135	0	0	0	0	332
57.86m	5.87g	12077	1000	6	0	5	1	31	2	180	15	45	0	0	0	0	285
60.00m	5.68g	12077	1000	0	0	4	1	22	0	82	14	17	0	0	0	0	140
62.61 m	5.60g	12077	1000	0	0	0	5	14	0	106	0	12	0	0	0	0	137
63.68m	5.51g	12077	1000	1	0	0	0	86	3	81	14	40	0	0	0	0	225
64.00m	15.7g	12077	133	0	0	0	0	286	0	10	10	10	0	0	0	0	316
64.66m	5.59g	12077	7	0	0	0	0	4	0	12	1	300	0	0	0	0	317
65.29m	5.65g	12077	1000	10	0	1	5	145	0	38	14	140	0	6	0	0	359
66.59m	5.83g	12077	1000	3	0	3	1	46	0	148	5	57	0	0	0	0	263
67.89m	6.36g	12077	1000	3	0	0	2	54	0	69	6	59	0	0	0	0	193
69.04m	10.38g	12077	1000	17	0	3	4	28	0	177	11	39	0	0	0	0	279
70.03m	15.5g	12077	638	2	0	0	0	36	0	126	17	130	1	0	0	0	312
70.37m	6.49g	12077	1000	1	0	0	1	13	0	155	26	13	0	0	0	0	209
70.80m	9.61g	12077	1000	0	0	0	1	18	0	110	20	43	0	0	0	0	192
71.11m	5.56g	12077	1000	1	0	2	4	28	0	63	10	20	0	0	0	3	128
71.31m	6.40g	12077	465	0	0	0	0	78	0	56	6	170	0	0	0	0	310
72.84m	6.62g	12077	750	6	0	0	1	62	0	30	7	250	0	0	0	0	356
74.71m	10.06g	12077	452	11	4	0	0	200	0	80	3	25	0	0	0	0	323
82.45m	6.23g	12077	1000	2	0	1		75	2	60	21	120	0	0	0	0	281
91.94m	6.47g	12077	175	0	0	0	0	11	0	9	7	300	0	0	0	0	327
105.68m	10.28g	12077	711	7	0	11	7	23	0	220	5	43	0	0	0	0	316
109.11m	9.53g	12077	3	233	0	30	4	10	1	20	14	7	0	0	0	0	319
111.70m	10.18g	12077	147	2	0	2	2	148	0	116	25	30	0	1	0	0	326
111.98m	10.20g	12077	9	187	0	35	11	58	1	25	7	0	2	0	0	0	326
126.45m	10.01g	12077	374	8	0	2	3	127	0	132	8	52	0	0	0	0	332

Table S4 Wiscombe Park-1 palynological counts

Taxa/depth	48.94m	49.85m	50.48m	50.76m	50.99m	55.30m	55.65m	56.15m	56.51m	60.00m	62.61m	63.68m	64.00m	64.49m	65.29m	65.90m	66.59m	67.89m	69.04m	70.03m	70.37m	70.80m	71.11m	71.41m	71.46m	71.87m	82.45m	105.68m	109.11m	111.69m	111.98m	126.45m
Aratrisporits fimbriatus	0	0	0	0	0	0	0	0	0	0	0	0	0	0	0	0	0	0	0	0	0	0	0	0	0	0	0	0	0	0	*	0
Aratrisporites granulatus	0	0	0	0	0	0	0	0	0	0	0	0	0	0	0	0	0	0	0	0	0	0	0	0	0	0	0	0	0	0	*	0
Aratrisporites paraspinosus	0	0	0	0	0	0	0	0	0	0	0	0	0	0	0	0	0	0	0	0	0	0	0	0	0	0	0	0	*	0	0	0
Aratrisporites sp.	2	0	0	0	0	0	0	0	2	0	0	0	0	0	0	0	0	0	0	0	0	0	0	0	0	0	0	0	0	0	4	0
Calamospora tener	0	0	0	7	16	1	2	1	3	0	0	0	0	0	1	1	1	0	0	1	0	0	0	0	0	0	1	1	5	1	10	1
Carnisporites sp.	0	0	0	0	0	0	0	0	0	0	0	0	0	0	0	0	0	0	0	0	0	0	0	0	0	0	0	0	1	0	0	0
Conbaculatisporites mesozoicus	0	1	0	0	0	0	0	0	0	0	0	0	0	0	0	0	0	0	0	0	0	0	0	0	0	0	0	0	0	0	0	0
Concavisporites toralis	0	0	0	0	0	0	0	0	0	0	0	0	0	0	0	0	0	0	0	0	0	0	0	0	0	0	0	0	0	0	0	0
Cyclogranisporites sp.	0	0	0	0	0	0	0	0	0	0	0	0	0	0	0	0	0	0	0	0	0	0	0	0	0	0	0	0	0	0	1	0
Cyclotriletes sp.	0	0	0	0	0	0	0	0	0	0	0	0	0	0	0	0	0	0	0	0	0	0	0	0	0	0	0	0	0	0	*	0
Dictyophyllidites harrisii	2	1	5	1	0	1	0	0	0	1	1	0	1	1	0	1	1	1	1	1	1	1	1	1	1	1	0	1	0	1	1	1
Kreauselisporites sp.	0	0	0	0	0	0	0	0	0	0	0	0	0	0	0	0	0	0	0	0	0	0	0	0	0	0	0	0	0	0	*	0
Kyrtomisporites sp.	0	0	0	0	0	0	0	0	0	0	0	0	0	0	0	0	0	0	1	0	0	0	0	0	0	0	0	0	0	0	*	0
Lycopodiacidites sp.	0	0	0	0	0	0	0	0	0	0	0	0	0	0	0	0	0	0	0	0	0	0	0	0	0	0	0	0	*	0	0	0
Punctatisporites sp.	0	0	0	0	4	0	7	0	0	0	0	0	0	0	0	0	0	0	0	0	0	0	0	0	0	0	0	0	0	0	0	0
Rogalskaiasporites sp.	0	0	0	0	0	0	0	0	0	0	0	0	0	0	0	0	0	0	0	0	0	0	0	0	0	0	0	0	0	0	*	0
Thomsonisporites toralis	0	0	0	0	0	0	0	0	0	0	0	0	0	0	0	0	0	0	0	0	0	0	0	0	0	0	0	0	*	0	0	0
Todisporites major	0	0	0	0	0	0	0	0	0	0	0	0	0	0	0	0	0	0	0	0	0	0	0	0	0	0	0	0	0	0	0	0
Todisporites rotundiformis	0	0	0	0	0	0	0	0	0	0	0	0	0	0	0	0	0	0	0	0	0	0	0	0	0	0	0	0	0	0	2	0
Uvaesporites sp.	0	0	0	0	0	0	0	0	0	0	0	0	0	0	0	0	0	0	0	0	0	0	0	0	0	0	0	0	0	0	*	0
Verrucosisporites moruluae	0	0	0	0	0	0	0	0	0	0	0	0	0	0	0	0	0	0	0	0	0	0	0	0	0	0	0	0	0	0	*	0
Alisporites grandis	0	0	0	0	0	0	3	0	0	0	0	0	0	0	0	0	0	0	0	1	0	0	0	0	0	0	0	0	0	0	0	0
Alisporites grauvogeli	0	3	5	5	2	0	0	0	1	0	0	0	0	0	0	0	0	0	0	1	0	0	0	0	0	0	0	0	6	0	3	0
Alisporites opii	0	0	0	0	0	0	1	0	0	0	0	0	0	0	0	0	0	0	0	0	0	0	0	0	0	0	0	0	0	0	0	0
Alisporites perlucidus	0	0	0	0	0	0	0	0	0	0	0	0	0	0	0	0	0	0	0	0	0	0	0	0	0	0	0	0	0	0	0	0
Alisporites robostus	0	0	0	0	0	0	0	0	1	0	0	0	0	0	0	0	0	0	0	0	0	0	0	0	0	0	0	0	0	0	17	0
Alisporites sp.	7	6	5	4	0	0	0	1	0	0	0	0	0	0	0	0	0	0	0	0	0	0	0	0	0	0	0	0	20	1	38	0
Brachysaccus neomundanus	0	1	0	0	1	0	0	1	0	0	0	0	0	0	0	0	0	0	0	0	0	0	0	0	0	0	0	0	7	0	6	0
Chordasporites singulichorda	1	1	0	0	0	0	0	0	0	0	0	0	0	0	0	0	0	0	0	0	0	0	0	0	0	0	0	0	0	0	0	0
Ellipsoveltisporites plicatus	3	3	10	0	21	0	0	1	1	0	0	0	0	0	0	0	0	0	0	0	0	0	0	0	0	0	0	0	0	0	0	1
Lunatisporites acutus	0	2	0	0	0	0	0	0	0	0	0	0	0	0	0	0	0	0	1	0	0	0	0	0	0	0	0	0	2	0	2	0
Klausipollenites gouldii	5	14	10	6	0	0	0	0	1	0	0	0	0	0	0	0	0	0	1	0	0	0	0	1	0	0	0	0	8	1	23	0
Klausipollenites schaubergeri	4	0	0	0	0	0	0	0	0	0	0	0	0	0	0	0	0	0	0	0	0	0	0	0	0	0	0	0	0	0	0	0
Microcachrydites doubingeri	2	2	0	0	0	0	0	0	0	0	0	0	0	0	0	0	0	0	0	0	0	0	0	0	0	0	0	0	1	0	1	0
Minutosaccus crenulatus	1	2	5	3	0	0	0	0	0	0	0	0	0	0	0	0	0	0	0	0	0	0	0	0	0	0	0	0	3	0	0	0
Ovalipollis minimus	1	6	5	0	9	0	0	1	0	0	0	0	0	0	0	0	0	0	0	0	0	0	0	0	0	0	0	0	13	0	12	1
Ovalipollis lunzensis	0	0	0	0	3	0	0	0	0	0	0	0	0	0	0	0	0	0	0	0	0	0	0	0	0	0	0	0	0	0	10	0
Ovalipollis ovalis	6	6	10	15	26	0	9	14	3	0	0	0	0	0	0	1	0	0	0	0	0	0	0	0	0	0	0	0	27	0	26	1
Ovalipollis notabilis	0	0	0	0	0	0	0	1	1	0	0	0	0	0	0	0	0	0	0	0	0	0	0	0	0	0	0	0	0	0	6	0
Ovalipollis sp.	3	0	0	0	0	0	0	0	0	0	0	0	0	0	0	0	0	0	1	0	0	0	0	0	0	0	0	1	0	0	0	0
Pityosporites sp.	0	20	6	0	2	0	0	7	2	0	0	0	0	0	0	0	0	0	0	0	0	0	0	0	0	0	0	0	4	0	5	0
Platysaccus sp.	0	0	0	3	1	0	0	1	1	0	0	0	0	0	0	0	0	0	0	0	0	0	0	0	0	0	0	0	1	0	0	0
Protodiploxypinus fastidiosus	0	0	0	9	0	0	1	1	0	0	0	0	0	0	0	0	0	0	0	1	0	0	0	0	0	0	0	0	4	0	0	0
Protodiploxypinus gracilis	0	0	1	0	0	0	0	0	0	0	0	0	0	0	0	0	0	0	0	0	0	0	0	0	0	0	0	0	0	0	0	0
Sulcatisporites karuseli	0	0	0	0	0	0	0	0	0	0	0	0	0	0	0	0	0	0	0	0	0	0	0	0	0	0	0	0	1	0	0	0
Triadispora aurea	0	0	0	0	0	0	0	0	0	0	0	0	0	0	0	0	0	0	0	0	0	0	0	0	0	0	0	0	26	0	16	0
Triadispora bölchi	0	1	2	6	0	0	1	0	0	0	0	0	0	0	0	0	0	0	1	0	0	0	0	0	0	0	0	0	0	0	2	0
Triadispora crassa	2	5	3	1	2	0	7	24	0	0	0	0	1	0	0	0	0	0	1	0	0	0	0	0	0	0	0	1	8	1	4	0
Triadispora epigona	0	62	27	15	12	0	1	2	0	0	0	0	0	0	0	0	1	0	0	0	0	0	0	0	0	0	0	0	7	0	5	0
Triadispora obscura	0	1	5	8	0	0	8	10	0	0	0	0	0	0	0	0	0	1	0	1	0	0	0	0	0	0	0	0	11	0	11	1
Triadispora modesta	0	3	0	1	1	0	1	3	0	0	0	0	0	0	0	0	0	0	0	0	0	0	0	0	0	0	0	0	5	1	12	1
Triadispora plicata	2	7	14	10	41	0	24	16	14	0	0	0	0	0	0	0	0	0	1	0	0	0	1	0	0	0	0	0	8	0	4	0
Triadispora stabilis	0	0	0	0	0	0	2	1	0	0	0	0	0	0	0	0	0	0	1	1	0	0	0	0	0	0	0	0	0	0	1	0
Triadispora sulcata	2	0	0	2	0	0	0	0	0	0	0	0	0	0	0	0	0	0	0	0	0	0	0	0	0	0	0	0	3	0	1	0
Triadispora suspecta	0	0	0	0	0	0	0	3	0	0	0	0	0	0	0	0	0	0	0	0	0	0	0	0	0	0	0	0	3	0	5	0
Triadispora verrucata	0	0	0	0	0	0	0	0	0	0	0	0	0	0	0	0	0	0	0	0	0	0	0	0	0	0	0	0	0	0	*	0
Triadispora sp.	5	65	42	75	100	1	62	95	35	0	0	1	0	1	1	0	1	1	1	1	1	1	0	0	0	0	1	1	65	1	54	1
Vitreisporites	0	1	0	0	0	0	0	0	0	0	0	0	0	0	0	0	0	0	0	0	0	0	0	0	0	0	0	0	0	0	0	0
Voltziaceaesporites heteromorpha	0	0	0	1	1	0	1	0	0	0	0	0	0	0	0	0	0	0	0	0	0	0	0	0	0	0	0	0	2	0	1	0

Table S4 (cont.) Wiscombe Park-1 palynological counts (cont.)

Enzonalasporites vigens	2	0	0	4	4	0	2	0	0	0	0	0	0	0	0	0	0	0	0	0	0	0	0	0	0	0	0	0	0	0	0	0	0	0
Enzonalasporites manifestus	0	0	0	0	1	0	0	0	0	0	0	0	0	0	0	0	0	0	0	0	0	0	0	0	0	0	0	0	0	0	0	0	0	0
Patinasporites densus	0	0	0	0	0	0	0	0	1	0	0	0	0	0	0	0	0	0	0	0	0	0	0	0	0	0	0	0	0	0	0	0	0	0
Patinasporites iustus	0	0	0	0	0	0	0	0	0	0	0	0	0	0	0	0	0	0	0	0	0	0	0	0	0	0	0	0	0	0	0	0	0	0
Pseudoenzonalasporites summus	0	0	0	0	1	0	0	0	0	0	0	0	0	0	0	0	0	0	0	0	0	0	0	0	0	0	0	0	0	0	0	0	0	0
Vallasporites ignacii	0	1	0	0	6	0	1	0	0	0	0	0	0	0	0	0	0	0	0	1	0	0	0	0	0	0	0	0	0	1	0	6	0	
Camerosporites secatus	31	58	78	20	40	1	50	30	70	1	0	0	0	0	1	0	0	0	0	0	0	0	0	1	0	0	1	1	0	0	5	0		
Camerosporites pseudoverruucosus	0	0	0	0	1	0	9	3	0	0	0	0	0	0	1	0	0	0	0	0	0	0	0	0	0	0	0	0	0	0	0	0		
Duplicisporites granulatus	13	17	30	35	2	0	23	18	100	0	1	0	0	1	0	0	0	0	1	0	0	0	0	0	0	0	0	0	15	1	35	1		
Duplicisporites mancus	2	3	7	1	2	0	4	0	23	0	0	0	0	0	0	0	1	0	0	0	0	0	0	0	0	0	0	0	0	0	1	0		
Partitisporites maljawkinae	0	0	0	0	2	0	6	7	6	0	0	0	1	0	0	0	0	0	0	0	0	0	0	0	0	0	0	0	0	0	0	0		
Partitisporites novimundanus	1	5	1	3	5	0	10	11	0	1	0	0	0	0	0	0	0	0	0	0	0	0	0	0	0	0	0	1	10	1	1	0		
Partitisporites scurillis	5	11	10	12	2	0	7	13	10	0	0	0	0	0	0	0	0	0	0	0	0	0	0	0	0	0	0	0	11	0	3	0		
Partitisporites quadruplices	1	0	0	0	0	0	0	0	0	0	0	0	0	0	0	0	0	0	0	0	0	0	0	0	0	0	0	0	0	0	0	0		
Partitisporites sp.	0	0	0	20	7	0	51	10	28	0	0	0	0	0	0	0	0	0	0	1	0	0	0	0	0	0	0	0	17	0	18	0		
Praecirculina granifer	9	18	20	0	3	0	36	35	0	0	0	0	0	0	0	0	1	0	1	0	0	0	1	0	0	0	0	1	0	0	21	0		
Aulisporites astigmosus	0	0	0	0	0	0	0	0	0	0	0	0	0	0	0	0	0	0	0	0	0	0	0	0	0	0	0	0	1	0	2	0		
cf. Aulisporites astigmosus	0	0	0	0	0	0	0	0	0	0	0	0	0	0	0	0	0	0	0	0	0	0	0	1	0	0	0	0	0	0	0	0		
Cycadopites sp.	1	2	0	0	1	0	1	3	1	0	0	0	0	0	0	0	0	0	0	0	0	0	0	0	0	0	0	0	5	0	0	0		
																				0	0	0	0	0	0	0	0	0		0		0		
Pollen indet	37	55	55	48	20	0	26	38	120	0	0	0	0	0	0	0	0	0	0	0	0	0	0	0	0	0	0	0	1	0	0	0		
Bisaccate indet	52	220	146	125	185	0	39	53	112	0	0	0	0	0	0	0	0	0	0	0	0	0	0	0	0	0	0	0	195	0	150	0		
Spore indet	0	0	0	2	3	0	1	0	1	0	0	0	0	0	0	0	0	0	0	0	0	0	0	0	0	0	0	0	2	0	8	0		
Botryococcus	0	0	0	0	0	0	0	0	0	0	0	0	0	0	0	0	0	0	0	0	0	0	0	1	0	0	0	0	0	0	0	0		
Lycopodium	1000	86	170	42	88	†	16	28	33	†	†	†	†	†	†	†	†	†	†	†	†	†	†	†	†	†	†	†	16	†	40	†		
†only qualitative analysis, all slides																																		
scanned, presence= 1, absence=0																																		
***encountered after counting**																																		

Tanble S5 Strangman's Cove palynofacies

Samples	Dry weight (g)	Lycopodium (added)	Lycopodium (counted)	Bisaccates	Monosaccates	Non-saccate pollen	Spores	Charcoal	Brown-black wood	Cuticles	Plant tissues	Woody fragments	AOM	Resin	Algae indet	Botryococcus	Plaesiodictyon	Fungi	Total:
WE203	8	12077	47	93	44	27	37	67	6	0	23	0	15	0	28	0	0	5	340
WE204	8	12077	700	2	0	0	0	206	0	0	21	0	76	0	0	0	0	2	305
WE206	8	12077	567	2	0	0	2	188	0	0	13	0	110	0	0	0	0	8	315
WE207	8	12077	224	0	0	0	0	20	0	0	53	0	230	0	0	0	0	8	303
WE208	8	12077	391	6	3	3	6	56	0	0	3	0	231	0	0	10	0	10	318
WE209	8	12077	1000	0	0	0	0	35	0	0	4	0	50	0	0	0	0	7	89
WE212	8	12077	82	12	1	5	0	260	0	0	10	0	25	0	0	0	0	2	313
WE213	8	12077	51	3	0	5	1	285	0	0	4	1	10	0	0	0	0	0	309
WE214	8	12077	315	41	5	25	11	85	0	0	11	0	137	0	0	5	0	0	320
WE201	8	12077	635	52	3	8	0	156	0	0	43	0	32	0	0	1	0	5	295
WE216	8	12077	148	0	0	0	0	300	0	2		5	9	0	0	0	0	0	316
WE217	8	12077	1000	3	1	5	0	35	0	0	16	0	77	3	0	0	5	29	145
WE303	8	12077	68	7	1	3	1	275	0	1	18	0	6	0	0	0	1	3	313
WE302	8	12077	14	150	11	26	15	25	0	0	10	0	95	0	0	0	0	0	332
WE305	8	12077	3	100	4	20	6	100	133	0	4	1	0	0	0	0	0	0	368
WE 301	8	12077	5	0	0	0	2	13	16	0	3	7	300	0	4	1	1	4	347
WE112	8	12077	1000	10	3	2	6	42	0	0	13	0	65	0	0	0	0	6	141
WE104	8	12077	1000	86	1	10	30	120	0	0	22	0	81	0	0	0	0	0	350
WE103	8	12077	5	133	8	35	45	33	0	0	18	6	100	0	0	0	0	1	378
WE110	8	12077	6	27	3	24	14	23	0	0	0	5	235	0	0	0	0	0	331
WE111	8	12077	703	12	1	10	11	200	0	0	10	7	92	0	0	0	0	20	343
WE109	8	12077	431	40	0	7	1	210	0	0	6	6	46	0	0	0	0	0	316
WE108	8	12077	310	3	1	2	9	12	0	0	0	0	280	5	0	13	0	8	325
WE107	8	12077	1000	2	0	4	4	48	0	0	33	0	103	0	0	0	0	100	194
WE114	8	12077	1000	11	0	2	8	57	0	0	5	4	60	0	0	0	0	5	147
WE115	8	12077	220	0	0	0	2	26	0	0	41	0	28	0	0	0	212	2	309
WE019	8	12077	26	10	0	0	1	32	0	1	20	5	27	0	0	0	208	2	304
WE018	8	12077	91	1	0	0	0	62	0	0	22	6	100	0	0	2	128	18	321
WE017	8	12077	36	123	0	0	6	50	0	0	20	5	9	0	0	1	155	28	369
WE016	8	12077	37	1	0	0	0	93	10	0	4	4	211	0	0	0	0	0	323
WE015	8	12077	3	165	5	9	44	16	0	0	8	0	88	0	0	3	0	0	338
WE014	8	12077	1000	22	4	14	9	111	0	0	13	1	155	0	0	2	0	1	331
WE013	8	12077	1000	17	1	19	2	80	0	2	22	0	182	0	0	6	0	9	331
WE012	8	12077	297	24	0	16	0	225	0	0	1	11	51	0	0	0	0	2	328
WE011	8	12077	1003	67	0	6	20	130	0	0	0	14	66	0	0	0	1	30	304
WE010	8	12077	1000	6	0	0	4	26	0	3	130	4	97	0	0	22	29	6	321
WE009	8	12077	1000	12	1	11	8	172	0	0	6	0	96	0	0	2	0	3	308
WE008	8	12077	54	7	0	0	0	295	6	1	7	1	8	0	0	0	0	0	325
WE007	8	12077	1000	5	1	0	3	130	0	1	19	0	64	0	2	6	0	0	231
WE006	8	12077	912	1	0	0	2	160	0	0	15	0	134	0	0	0	0	0	312
WE005	8	12077	358	5	0	2	7	270	5	0	7	0	12	0	0	0	0	0	308
WE004	8	12077	28	23	3	0	0	260	30	0	10	5	20	1	0	0	0	0	352
WE003	8	12077	9	152	3	11	26	191	20	0	13	20	0	0	1	0	0	0	437
WE002	8	12077	163	1	0	0	1	305	2	0	2	0	5	0	0	0	0	0	316
WE001	8	12077	184	22	0	5	5	240	0	0	30	2	20	0	0	0	0	0	324
WE304	8	12077	311	0	0	0	1	106	37	2	51	0	120	0	3	0	0	1	320

Table S6 Strangman's Cove palynological counts

Taxa and samples	WE203	WE214	WE201	WE302	WE305	WE104	WE103	WE109	WE017	WE015	WE011	WE003
Aratrisporites sp.	0	2	0	*	*	0	0	0	0	3	0	1
Aratrisporites granulatus	*	0	0	0	0	0	0	0	0	0	0	0
Calamospora tener	77	1	2	0	4	18	1	2	8	0	6	25
Carnisporites sp.	0	0	0	0	*	0	0	0	0	0	0	0
Conbaculatisporites sp.	0	0	1	1	0	0	0	4	0	0	0	0
Concavisporites toralis	*	0	0	0	0	0	0	0	0	0	0	0
Cyclogranisporites sp.	1	2	0	3	1	0	0	0	4	0	0	1
Dictyophyllidites harrisii	*	1	*	0	0	1	0	0	0	0	0	0
Kyrtomisporites laevigatus	0	0	0	0	*	0	0	0	0	0	0	0
Kyrtomisporites speciosus	0	0	0	0	3	0	0	0	0	0	0	0
Osmundacidites wellmannii	0	3	2	4	0	0	9	2	0	0	0	5
Porcellispora longdonensis	12	0	0	0	0	0	0	0	0	1	0	0
Todisporites major	13	0	0	0	0	0	0	1	0	0	0	10
Todisporites rotundiformis	1	0	0	*	0	2	0	0	0	0	0	2
Alisporites diaphanous	0	1	0	0	0	0	0	0	5	13	0	0
Alisporites grandis	*	0	0	0	0	0	0	0	0	0	0	0
Alisporites grauvogeli	5	0	0	0	1	0	4	0	21	0	0	23
Alisporites opii	0	0	0	0	*	0	0	0	1	0	0	0
Alisporites perlucidus	4	0	0	1	0	0	0	0	23	0	0	0
?Alisporites robostus (big)	0	0	0	0	0	0	0	0	12	0	0	0
Alisporites sp.	7	1	4	33	0	0	1	0	0	0	0	8
Brachysaccus neomundanus	0	0	0	0	1	0	0	0	0	0	0	0
Chordasporites singulichorda	0	1	0	0	0	0	0	0	1	0	1	0
Ellipsoveltisporites plicatus	0	1	*	10	19	0	7	0	0	2	0	0
Lunatisporites acutus	3	0	0	*	0	0	3	0	1	1	0	3
Klausipollenites gouldii	10	15	12	18	18	2	4	18	33	1	7	16
Klausipollenites schaubergeri	4	0	0	0	0	0	0	0	2	0	0	0
Microcachrydites doubingeri	2	3	2	6	10	0	0	1	13	0	0	2
Minutosaccus crenulatus	2	10	4	0	18	1	5	0	6	2	3	0

Table S6 (cont.) Strangman's Cove palynological counts (cont.)

Ovalipollis lunzensis	0	2	0	1	0	0	0	0	2	0	0	0
Ovalipollis minimus	4	0	1	4	4	0	1	0	6	1	0	12
Ovalipollis ovalis	23	0	2	26	7	0	12	0	0	18	0	45
Ovalipollis sp.	2	2	0	0	12	0	0	2	5	1	2	0
Pityosporites sp.	7	0	0	10	7	0	2	0	16	0	0	1
Platysaccus sp.	1	0	0	3	1	0	2	0	1	5	0	0
Protodiploxypinus fastidiosus	3	0	0	8	8	0	7	0	6	0	0	0
Protodiploxypinus gracilis	0	0	0	0	0	0	0	0	0	2	0	0
Rimaesporites sp.	1	0	0	5	2	0	1	0	*	0	0	1
Triadispora bölchi	1	0	2	2	10	1	0	1	0	0	0	3
Triadispora crassa	1	0	0	0	0	0	6	0	0	0	0	0
Triadispora epigona	0	2	3	5	7	1	5	0	8	4	0	3
Triadispora modesta	0	0	0	1	0	0	4	2	0	0	0	5
Triadispora obscura	3	4	2	32	0	1	5	4	0	0	0	6
Triadispora plicata	7	0	0	8	21	0	20	0	76	3	0	9
Triadispora stabilis	0	0	0	0	0	0	0	1	0	0	0	0
Triadispora sulcata	0	0	4	1	0	0	1	0	0	12	0	0
Triadispora suspecta	0	0	0	2	0	0	0	0	0	0	0	0
Triadispora sp.	0	2	0	2	15	21	27	0	10	72	31	15
Vitreisporites sp.	0	9	0	0	8	0	0	0	0	0	0	0
Voltziaceaesporites heteromorpha	0	0	0	3	0	0	3	0	9	3	0	0
Enzonalasporites vigens	7	0	0	14	1	0	2	0	16	2	0	0
Enzonalasporites manifestus	18	0	0	*	0	0	0	0	1	0	0	0
Patinasporites densus	7	0	0	1	0	0	1	0	1	0	0	0
Patinasporites explanatus	*	0	0	0	0	0	0	0	0	0	0	0
Patinasporites iustus	0	0	0	0	*	0	0	0	0	0	0	0
Pseudoenzonalasporites summus	16	0	0	*	0	0	0	0	2	0	0	0
Vallasporites ignacii	9	1	0	2	1	0	3	0	3	1	0	0
Araucariacites sp.	1	0	0	1	1	0	0	0	0	0	0	1
Camerosporites secatus	24	48	6	42	125	2	70	3	8	24	1	26
Duplicisporites granulatus	1	15	21	62	29	10	96	19	5	128	12	76
Duplicisporites mancus	4	2	0	4	3	0	13	0	2	0	0	0

Table S6 (cont.) Strangman's Cove palynological counts (cont.)

Partitisporites novimundanus	0	0	0	0	0	4	8	0	0	0	6	27
Partitisporites scurrilis	0	0	0	0	0	6	14	0	0	0	2	7
Partitisporites tenebrosus	*	0	0	0	0	0	0	0	0	0	0	0
Partitisporites indet	*	0	0	0	0	0	0	0	0	0	0	0
Praecirculina granifer	0	18	4	1	33	4	31	3	0	0	2	1
Cycadopites sp.	0	2	0	5	1	0	0	0	3	0	0	0
Brodispora striata	3	0	0	0	0	0	0	0	0	0	0	0
Bisaccate indet	78	73	44	306	141	43	263	40	583	148	20	426
Pollen indet	16	20	8	29	0	9	28	5	25	0	10	4
Spore indet	3	0	0	0	0	0	0	0	3	0	1	5
Lycopodium (counted)	133	1020	1000	21	29	1000	27	1000	450	33	1000	56
*** encountered after counting**												

Table S7 Somerset palynofacies

Lipe Hill	Dry weight	Lycopodium (added)	Lycopodium (counted)	Bisaccates	Non-saccate poller	Monosaccates	Spores	Cuticle	Plant tissues	Woody fra	Charcoal	AOM	Resin	Plaesiodictyon	Botryococcus	Acritarch	Fungi	Total:
S-15-01	14.9 g	12077	95	0	1	0	5	0	200	30	41	28	0	0	1	1	3	307
S-15-02	16.3 g	12077	23	178	7	0	7	1	100	10	34	5	0	2	0	0	18	344
S-15-03	16 g	12077	47	151	12	0	8	0	27	16	75	10	0	8	0	0	1	307
S-15-04	17.8 g	12077	56	67	5	0	1	0	127	16	50	16	0	30	0	0	1	312
S-15-05	15.6 g	12077	95	87	5	0	5	0	36	32	100	17	0	32	1	0	0	315
S-15-06	16.9 g	12077	50	155	37	1	8	0	38	10	33	2	0	100	2	1	1	387
S-15-07	16. 2 g	12077	21	200	17	2	3	0	47	0	16	0	0	38	0	0	5	323
S-15-08	17.2 g	12077	45	217	20	5	3	0	26	7	21	0	1	26	1	0	0	327
S-15-09	16.1 g	12077	45	110	16	1	8	0	90	7	70	0	0	25	0	0	0	327
S-15-10	15.5 g	12077	48	180	17	0	0	0	35	3	45	0	0	27	0	0	0	307
Sutton Mallet																		
SM-15-01	16.2 g	12077	43	3	0	0	1	0	250	10	41	0	0	0	0	0	0	305
SM-15-02	16.2 g	12077	20	110	11	0	15	0	110	32	37	0	0	6	1	0	0	322
SM-15-03	14.7 g	12077	19	112	16	2	2	0	107	35	38	0	0	8	0	0	0	320
SM-15-04	16.2 g	12077	10	30	15	0	5	1	224	0	11	1	2	10	1	0	0	300

Table S8 Lipe Hill palynological counts

Taxa/Samples	LH-01	LH-02	LH-03	LH-04	LH-05	LH-06	LH-07	LH-08	LH-09	LH-10
Aratrisporites fimbriatus	0	0	0	0	0	0	1	0	0	0
Aratrisporites granulatus	0	*	0	0	1	0	4	2	1	0
Calamospora tener	6	13	11	6	12	14	2	8	6	4
Concavisporites toralis	2	0	0	0	0	0	0	0	0	0
Cyclogranisporites sp.	0	0	4	0	0	0	*	0	0	0
Dictyophyllidites harrisii	1	*	*	1	0	0	0	0	0	1
Lycopodiacidites sp.	0	0	0	5	0	1	0	0	1	0
Osmundacidites wellmannii	0	*	0	5	0	3	9	0	1	2
Porcellispora longdonensis	0	0	7	1	0	1	4	1	0	1
Todisporites major	0	*	0	0	4	4	0	1	0	1
Alisporites gignateus	0	11	5	15	3	12	7	17	23	0
Alisporites opii	1	0	0	0	3	0	5	0	0	0
Alisporites grauvogeli	0	2	11	15	9	7	6	5	7	8
Brachysaccus neomundanus	0	1	1	0	0	0	0	0	0	0
Ellipsovelatisporites plicatus	0	8	0	1	0	0	0	1	0	*
Lunatisporites acutus	0	1	0	0	0	0	0	0	0	0
Klausipollenites gouldii	0	2	0	3	0	0	1	0	0	0
Microcachrydites doubingeri	0	1	2	3	1	0	5	0	1	0
Minutosaccus crenulatus	0	1	0	0	0	0	1	0	0	0
Ovalipollis lunzensis	0	15	15	7	62	5	1	3	6	12
Ovalipollis minimus	0	1	0	1	1	*	4	2	3	1
Ovalipollis notabilis	0	*	5	1	1	0	0	2	1	0
Ovalipollis ovalis	0	52	40	16	65	8	7	13	13	16
Parillinites sp.	0	0	1	0	0	0	0	1	0	0
Pityosporites sp.	0	6	15	12	5	6	10	15	20	3
Platysaccus sp.	0	0	1	0	2	0	0	0	0	0
Protodiploxypinus gracilis	0	*	0	0	0	0	0	0	0	0
Protodiploxypinus sp.	0	0	0	0	*	5	1	1	3	1

Table S8 (cont.) Lipe Hill palynological counts (cont.)

Triadispora aurea	0	1	0	1	0	3	1	3	3	*
Triadispora epigona	0	6	8	10	*	18	17	15	23	22
Triadispora crassa	0	7	5	3	3	0	0	2	*	0
Triadispora obscura	2	75	95	107	113	176	200	160	242	210
Triadispora modesta	0	6	5	3	1	1	2	6	0	*
Triadispora plicata	0	40	25	32	4	16	20	22	7	10
Triadispora sp.	0	67	65	87	0	23	5	1	0	0
Voltziaceaesporites heteromorpha	0	*	0	0	0	0	1	0	*	1
Enzonalasporites vigens	0	*	3	3	0	0	5	0	1	0
Vallasporites ignacii	0	0	0	0	*	1	0	1		0
Camerosporites secatus	0	5	11	10	2	1	8	10	11	5
Duplicisporites granulatus	0	4	6	10	11	29	10	15	20	18
Duplicisporites mancus	0	0	0	0	0	1	0	0	0	0
Partitisporites maljawkinae	0	3	1	0	2	0	7	6	9	10
Partitisporites novimundanus	0	1	0	0	1	1	1	1	3	1
Partitisporites scurillis	0	0	3	4	0	0	5	3	1	0
Partiti/Prae indet	0	5	0	0	0	0	0	0	0	0
Praecirculina granifer	0	9	4	30	16	23	33	22	19	23
cf. Aulisporites astigmosus	0	*	*	0	0	0	0	0	0	0
Cycadopites sp.	0	0	0	0	0	1	0	0	1	2
Lagenella martinii	0	0	0	0	0	0	0	0	4	0
Brodispora striata	0	0	0	0	0	1	*	2	2	1

Table S8 (cont.) Lipe Hill palynological counts (cont.)

Cymatiosphaera	0	1	0	0	0	0	0	1	0	0
Plaesidictyon	0	3	32	113	255	274	110	80	161	95
Botryococcus	8	1	1	9	1	5	2	4	6	0
Bisaccate indet	0	53	33	187	31	42	77	115	190	20
Pollen indet	0	0	1	1	0	0	0	5	0	0
Spore indet	0	0	0	0	0	0	0	0	0	0
Reworked acritarch	1	2	0	0	*	*	0	0	0	0
Reworked sporomoph	0	0	0	1	*	0	0	0	0	0
Lycopodium (counted)	1000	84	180	662	395	107	109	115	239	115
***encountered after counting**										

Table S9 Sutton Mallett palynological counts

Taxa/Sample	SM-01	SM-02	SM-03	SM-04
Anapiculatisporites sp.	0	1	0	0
Aratrisporites fimbriatus	0	4	0	2
Aratrisporites granulatus	2	38	10	20
Aratrisporites paraspinosus	0	5	5	0
Aratrisporites sp.	0	0	1	0
Calamospora tener	2	11	10	10
Concavisporites toralis	0	0	0	0
Cyclogranisporites sp.	0	5	2	0
Dictyophyllidites harrisii	0	2	3	0
Gibeosporites lativerrucosus	0	*	0	0
Porcellispora longdonensis	0	0	*	*
Thomsonisporis toralis	0	1	*	0
Verrucosisporites sp.	0	0	*	2
Alisporites giganteus	2	11	11	10
Alisporites grauvogeli	0	0	1	*
Alisporites opii	0	0	2	5
Ellipsovelatisporites plicatus	0	0	3	1
Lunatisporites acutus	0	0	1	0
Klausipollenites gouldii	0	0	0	2
Microcachrydites doubingeri	0	6	1	*
Minutosaccus crenulatus	0	1	0	*
Ovalipollis lunzensis	0	6	5	0
Ovalipollis minimus	0	0	0	*
Ovalipollis ovalis	1	11	4	16
Ovalipollis notabilis	0	7	1	4
Ovalipollis sp.	1	0	0	0
Parillinites sp.	0	0	0	3
Pityosporites sp.	2	8	10	11
Platysaccus sp.	0	0	*	5

Table S9 (cont.) Sutton Mallett palynological counts (cont.)

Triadispora aurea	0	0	0	1
Triadispora epigona	0	3	10	11
Triadispora crassa	0	13	5	3
Triadispora obscura	0	0	0	62
Triadispora modesta	1	1	*	2
Triadispora plicata	2	46	51	40
Triadispora stabilis	0	0	*	0
Triadispora sp.	25	145	165	58
Voltziaceaesporites heteromorpha	0	0	1	5
Enzonalasporites vigens	0	2	0	1
Patinasporites densus	1	1	*	1
Vallasporites ignacii	0	0	*	0
Camerosporites secatus	2	27	18	21
Duplicisporites granulatus	0	2	5	5
Duplicisporites mancus	0	1	*	1
Partitisporites maljawkinae	0	10	9	6
Partitisporites novimundanus	0	4	3	1
Partitisporites scurillis	6	2	3	2
Praecirculina granifer	0	12	20	20
Brodispora striata	0	2	*	1
Riccisporites tuberculatus	0	*	0	0

Table S9 (cont.) Sutton Mallett palynological counts (cont.)

Cymatiosphaera sp.	0	2	0	
Schizosporis sp.	0	0	1	*
Plaesiodictyon mosellaneum	0	24	28	0
Botryococcus braunii	1	8	4	5
Bisaccate indet	14	222	102	90
Pollen indet	0	12	5	0
Spore indet		0	0	4
Megaspores indet	0	1	1	1
Reworked acritarchs	0	0	0	3
Lycopodium (counted)	1000	168	75	80
***encountered after counting**				

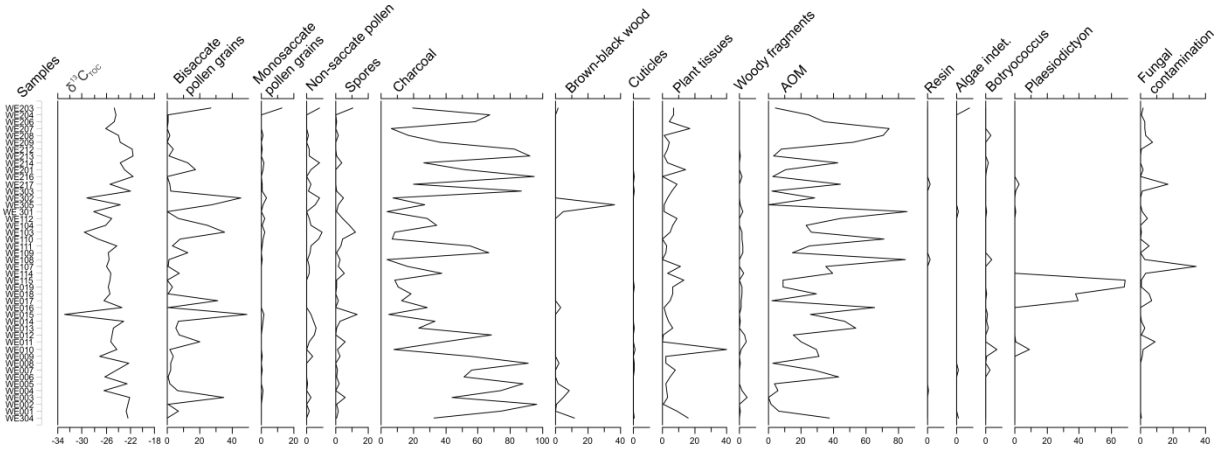

Fig. S2. Relative abundance (%) of the different palynofacies groups and the variation in the bulk organic carbon isotope values from the Strangman's Cove outcrop section. The diagram is plotted from data in Table S5 and Table S10.

Coefficient of determination (R^2) from the linear regression analysis of the palynofacies groups and bulk organic carbon isotope values:

TOC-bulk organic carbon R^2=0.34

Spores-bulk organic carbon R^2=0.27

Total pollen grains-bulk organic carbon R^2=0.20

Charcoal-bulk organic carbon R^2=0.36

AOM-bulk organic carbon R^2=0.11

Plant tissues-bulk organic carbon R^2=0.005

Woody fragments-bulk organic carbon R^2=2.87-5

Algae-bulk organic carbon R^2=0.01

Fungal contamination-bulk organic carbon R^2=0.01

Samples	δ13C	TOC
WE202	-27,38	0,06
WE203	-24,69	0,44
WE204	-24,34	0,14
WE206	-24,72	0,29
WE207	-26,05	0,08
WE208	-23,97	0,12
WE209	-23,72	0,10
WE210	-22,69	0,12
WE211	-22,17	0,11
WE212	-21,61	0,43
WE213	-21,60	0,38
WE214	-23,70	0,11
WE201	-22,93	0,14
WE215	-23,82	0,82
WE216	-21,48	0,31
WE217	-25,37	0,07
WE303	-21,99	0,36
WE302	-29,121	0,84
WE305	-23,629	0,81
WE301	-28,09	0,67
WE113	-25,578	0,05
WE112	-25,041	0,09
WE104	-26,052	0,14
WE103	-29,58	1,49
WE110	-27,404	1,52
WE111	-24,258	0,11
WE109	-25,624	0,18
WE108	-25,484	0,07
WE107	-25,976	0,07
WE101	-25,392	0,09
WE106	-25,765	0,10
WE105	-25,826	0,11
WE114	-25,233	0,06
WE115	-25,394	0,04
WE19	-25,634	0,13
WE18	-25,378	0,11
WE17	-26,346	0,17
WE16	-23,403	0,18
WE15	-32,844	4,56
WE14	-23,11	0,12
WE13	-24,74	0,08
WE11	-25,20	0,04
WE10	-24,18	0,09
WE9	-27,03	0,19
WE8	-22,24	0,50
WE6	-26,18	0,08
WE5	-22,51	0,17
WE4	-26,29	0,37
WE3	-22,14	0,22
WE1	-22,70	0,10
WE304	-22,37	0,17

Table S10 Strangman's Cove bulk carbon isotope ratios and TOC

Supplementary References

Abbink, O.A., Van Konijnenburg-Van Cittert, J.H.A. &Visscher, H. 2004. A sporomorph ecogroup moder for the Northwest European Jurassic–Lower Cretaceous. Concepts and framework. Netherlands Journal of Geosciences, 83, 17–38.

Arche, A. & López-Gómez, J. 2014. The Carnian Pluvial Event in Western Europe: New data from Iberia and correlation with the Western Neotethys and Eastern North America–NW Africa regions. Earth-Science Reviews, 128, 196–231, https://doi.org/10.1016/j.earscirev.2013.10.012

Balme, B.E. 1995. Fossil in situ spores and pollen grains: an annotated catalogue: Review of Palaeobotany and Palynology, 87, 81–323, https://doi.10.1016/0034-6667(95)93235-X

Bonis, N.R. & Kürschner, W.M. 2012. Vegetation history, diversity patterns, and climate change across the Triassic/Jurassic boundary. Paleobiology, 38, 240–264, https://doi.10.1666/09071.1

Dal Corso, J., Gianolla, P., Newton, R.J., Franceschi, M., Roghi, G., Caggiati, M., Raucsik, B., Budai, T., Haas, J. & Preto, N. 2015. Carbon isotope records reveal synchronicity between carbon cycle perturbation and the "Carnian Pluvial Event" in the Tethys realm (Late Triassic). Global and Planetary Change, 127, 79–90, https://doi.org/10.1016/j.gloplacha.2015.01.013

Fijałkowska-Mader, A. 2015. A record of climatic changes in the Triassic palynological spectra from Poland. Geological Quarterly, 59, 615–653, https://doi.http://dx.doi.org/10.7306/gq.1239

Gallois, R.W. 2001. The lithostratigraphy of the Mercia Mudstone Group (mid to late Triassic) of the south Devon coast. Proceedings of the Ussher Society, 10, 195-204.

Gallois, R.W. 2003. The distribution of halite (rock-salt) in the Mercia Mudstone Group (mid to late Triassic) in south-west England. Geoscience in south-west England, 10, 383-389.

Gallois, R.W. 2004. The type section of the junction of the Otter Sandstone Formation and the Mercia Mudstone Group (mid Triassic) at Pennington Point, Sidmouth. Geoscience in south-west England, 11, 51-58.

Gallois, R.W. 2007. The stratigraphy of the Mercia Mudstone Group succession (mid to late Triassic) proved in the Wiscombe Park boreholes, Devon. Geoscience in south-west England, 11, 280-286.

Gallois, R.W. & Porter, R.J. 2006. The stratigraphy and sedimentology of the Dunscombe Mudstone Formation (late Triassic). Geoscience in south-west England, 11, 174-182.

Góczán, F., Haas, J., Lőrincz, H. & Oravecz-Scheffer, A. 1983. Faciological and stratigraphic evaluation of a Carnian key section (borehole Hévíz 6, Keszthely Mts, Hungary). Magyar Állami Földtani Inézet Évi Jelentése 1981-ről, 263–293 (in Hungarian with English abstract)

Góczán, F. & Oravecz–Scheffer, A. 1996a. Tuvalian sequences of the Balaton Highland and the Zsámbék Basin, Part I: Litho-, bio- and chronostratigraphic subdivision. Acta Geologica Hungarica, 39, 1–31.

Góczán, F. & Oravecz–Scheffer, A. 1996b. Tuvalian sequences of the Balaton Highland and the Zsámbék Basin, Part II: Characterization of sporomorph and foraminifer assemblages, biostratigraphic, palaeogeographic and geohistoric conclusions. Acta Geologica Hungarica 39, 33–101.

Haas, J., Budai, T. & Raucsik, B. 2012. Climatic controls on sedimentary environments in the Triassic of the Transdanubian Range (Western Hungary). Palaeogeography Palaeoclimatology Palaeoecology, 353–355, 31–44, https://doi.org/10.1016/j.palaeo.2012.06.031

Hounslow,M.W., Posen, P.E.,Warrington, G., 2004.Magnetostratigraphy and biostratigraphy of the Upper Triassic and lowermost Jurassic succession, St. Audrie's Bay, UK. Palaeogeogr. Palaeoclimatol. Palaeoecol. 213, 331–358.

Hounslow, M.W., Muttoni, G., 2010. The geomagnetic polarity timescale for the Triassic: linkage to stage boundary definitions. Geol. Soc. Lond. Spec. Publ. 334, 61–102.

Hounslow, M. W., & McIntosh, G. 2003. Magnetostratigraphy of the Sherwood Sandstone Group (Lower and Middle Triassic), south Devon, UK: detailed correlation of the marine and non-marine Anisian. Palaeogeography, Palaeoclimatology, Palaeoecology, 193(2), 325-348.

Howard, A.S., Warrington, G., Ambrose, K & Rees, J.G. 2008. A formational framework for the Mercia Mudstone Group (Triassic) of England and Wales. British Geological Survey, Keyworth, Nottingham, Research Report RR/08/04.

Jeans, C V. 1978. The origin of the Triassic clay assemblages of Europe with special reference to the Keuper Marl and Rhaetic of parts of England. Philosophical Transactions of the Royal Society of London, Series A, Vol. 289, 549–639.

Kustatscher, E., Heunisch, C & Van Konijnenburg-Van Cittert, J.H.A. 2012. Taphonomical implications of the Ladinian megaflora ans and palynoflora of Thale (Germany). Palaios, 27, 753–764, https://doi.10.2110/palo.2011.p11-090r

Lindström, S., Irmis, R.B., Whiteside, J.H., Smith, N.S., Nesbitt, S.J. & Turner, A.H. 2016. Palynology of the upper Chinle Formation in northern New Mexico, U.S.A.: implications for biostratigraphy and terrestrial ecosystem change during the Late Triassic (Norian–Rhaetian): Review of Palaeobotany and Palynology, 225, 106–131, https://doi.10.1016/j.revpalbo.2015.11.006

López-Gómez, J., Escudero-Mozo, M.J., Martín-Chivelet, J., Arche, A., Lago, M. & Galé, C. 2017. Western Tethys continental-marine responses to the Carnian Humid Episode: Palaeoclimatic and palaeogeographic implications. Global and Planetary Change, 148, 79–95, https://doi.org/10.1016/j.gloplacha.2016.11.016

Miller, C.S., Peterse, F., da Silva, A-C., Baranyi, V., Reichart, G.J. & Kürschner, W.M. 2017. Astronomical age constraints and extinction mechanisms of the Late Triassic Carnian crisis. Scientific Reports, 7:2557, https://doi.10.1038/s41598-017-02817-7

Mueller, S., Hounslow, M.W. & Kürschner, W.M. 2016a. Integrated stratigraphy and palaeoclimate history of the Carnian Pluvial Event in the Boreal realm; new data from the Upper Triassic Kapp Toscana Group in central Spitsbergen (Norway). Journal of the Geological Society, 173, 186–202, https://doi.10.1144/jgs2015-028

Mueller, S., Krystyn, L. & Kürschner, W.M. 2016b. Climate variability during the Carnian Pluvial Phase — A quantitative palynological study of the Carnian sedimentary succession at Lunz am See, Northern Calcareous Alps, Austria. Palaeogeography, Palaeoclimatology, Palaeoecology, 441, 198–211, http://dx.doi.org/10.1016/j.palaeo.2015.06.008

Paterson, N.W., Mangerud, G. & Mørk, A. 2016. Late Triassic (early Carnian) palynology of shallow stratigraphical core 7830/5-U-1, offshore Kong Karls Land, Norwegian Arctic. Palynology, 41, 230–254, http://dx.doi.org/10.1080/01916122.2016.1163295

Raine, J.I., Mildenhall, D.C. & Kennedy, E.M. 2011. New Zealand fossil spores and pollen: anillustrated catalogue. 4th edition. GNS Science miscellaneous series, 4. (available at http://data.gns.cri.nz/sporepollen/index.htm)

Roghi, G. 2004. Palynological investigations in the Carnian of the Cave del Prdil area (Julian Alps, NE Italy). Review of Palaeobotany and Palynology, 132, 1–35, https://doi.org/10.1016/j.revpalbo.2004.03.001

Roghi, G., Gianolla, P., Minarelli, L., Pilati, C. & Preto, N. 2010. Palynological correlation of Carnian humid pulses throughout western Tethys. Palaeogeography, Palaeoclimatology, Palaeoecology, 290, 89–106, https://doi.org/10.1016/j.palaeo.2009.11.006

Visscher, H., Van Houte, M., Brugman, W.A. & Poort, R.J. 1994. Rejection of a Carnian (Late Triassic) "pluvial event" in Europe. Review of Palaeobotany and Palynology, 83, 217–226, https://doi.org/10.1016/0034-6667(94)90070-1

Visscher, H. & Van der Zwan, C.J. 1981. Palynology of the circum-Mediterranean Triassic phytogeographical and palaeoclimatological implications. Geologische Rundschau, 70, 625–636.

Warrington, G, & Whittaker, A. 1984. The Blue Anchor Formation (late Triassic) in Somerset. Proceedings of the Ussher Society, Vol. 6, 100–107